Development of a Real-time Optical Sensor for Detecting Wheat Growth Status

(小麦生育診断のためのリアルタイム光学センサに関する研究)

北海道大学　大学院農学院

環境資源学専攻　博士後期課程

VALI RASOOLI SHARABIAN

Development of a Real-time Optical Sensor for Detecting Wheat Growth Status

BY

Vali Rasooli Sharabian

Master of Science in Agricultural Engineering – Agricultural Mechanization,
Shahid Chamran University of Ahvaz, IRAN

Bachelor of Science in Agricultural Engineering – Agricultural Machinery,
University of Tabriz, IRAN

DISSERTATION

Submitted to Department of Environmental Resources in the Graduate School of Agriculture
Hokkaido University, Sapporo, Japan, 060-8589 in partial fulfillment of the requirements for the degree of

Doctor of Philosophy

September 2013

DEDICATION

To my parents;
to all of my teachers;
and to my family, my beloved wife and daughter

ACKNOWLEDGEMENTS

There are many I need to acknowledge without which this research would not have been possible. First I would like to express my deepest gratitude to my supervisor Dr. Noboru Noguchi, Professor of Laboratory of Vehicle Robotics (VeBots), for his motivation, enthusiasm, and immense knowledge. I thank him for the systematic guidance and great effort he put into training me in field of precision agriculture, remote sensing, and methodology for spectral data analyzing. I also acknowledge the valuable contributions of my other thesis committee member, Dr. Kazunobu Ishi provided the sensor platform and CANBUS communication, extensive in-field knowledge, and a great deal of the agronomic insight required to keep a realistic footing in this project. And give thanks to Dr. Hroshi Okamoto and secretaries of laboratory who have helped me a lot on the preparing of this thesis. Special thanks to Mr. Sato and his colleagues in the experimental farms of Hokkaido University for giving me the technical assistance in winter wheat cultivation and fertilizing. I acknowledge my gratitude to graduate school of agriculture of Hokkaido University for the support to the thesis. I also want to thank all of my colleagues in the Laboratory of Vehicle Robotics for support and help to investigate experimental field and taking data during of three years, and also their advices and kind friendship. They helped me to understand the Japanese culture and specially dealt with Japanese documents. My life and research in Sapporo would have never been the same without them. Finally, I would also like to thank my parents who have supported me throughout my life. I would also like to give special thanks to my wife, Roghayyeh, and my lovely daughter, Aysouda, for their patience, love and support that they have given me and for standing by me despite many difficult times. I would also like to thank all those who have contributed to the completion of the thesis and are not included here. They know who they are.

TABLE OF CONTENTS

LIST of FIGURES

LIST of TABLES

CHAPTER 1

INTRODUCTION

1.1 Introduction

In today's world, there is increasing concern with respect to the agriculture sector and the estimated longevity of a sufficient food production system. Environmental issues can hinder food production systems (e.g. soil erosion, water quality, climatic change), while socioeconomic issues can be equally as damaging. Concerns from both the consumer and the farm community stems from issues surrounding the volatility of the international agricultural marketplace, and the requirement of farmers to meet the food demands of an increasing population while maintaining quality. These factors coupled with increasing production costs have resulted in a substantial decrease in the farms and public concern surrounds the subsequent increase in industrial and corporate farms (Brklacich *et al.,* 1991). The adoption of sustainable agriculture practices by farmers involves daily management strategies that strive to protect the land resources required to grow food. A sustainable food production system has been defined as an agri-food sector that over the long term can simultaneously maintain environmental quality, provide economic and social rewards for all individuals involved in the system, and produce an adequate and accessible food supply (Brklacich *et al.,* 1991). Essentially, if the food production system cannot meet these criteria then the system is deemed unsustainable. Site-specific agriculture is one approach to farm management that can promote sustainable agriculture. Site-specific agriculture, also known as precision agriculture, can be defined as the application of technologies and principles to manage spatial and temporal variability associated with all aspects of agricultural production to improve crop performance and environmental quality (Pierce and Nowak, 1999). This style of agriculture practice refers to a "knowledge-based system" that allows farmers to manage variability at scales that are within a defined farm unit (e.g. section, quarter section) and to specific spatial regions of the farm unit where required (Lu *et al.,* 1997). Spatially variable crop yield can exist due to many factors such as soil nutrient and moisture content, topography, as well as insect and weed infestations that change over time. Site specific agriculture requires both spatial and temporal management, which in the case of farming can require highly time-sensitive information over large agricultural fields. In the past this type of real-time information has not been easily accessible and

farmers have treated fields as homogenous units applying average rates of crop inputs over the entire field. As a result of this practice, farmers tend to over or under-apply crop inputs (e.g. fertilizer) which can result in both economic loss and environmental contamination (Lu *et al.,* 1997). More recently, the increased availability of remote sensing imagery accompanied by comprehensive site-specific crop management plans has offered farmers a more definitive means of implementing sustainable agricultural practices in large agricultural areas. Remote sensing can play a unique role in agriculture because it is a non-invasive, time-specific method of acquiring information about seasonally variable crop and soil conditions. Remote sensing is a geospatial tool often incorporated into a management strategy for the whole farm operation that together with the benefits of global navigation satellite system (GNSS) and Geographic Information Systems (GIS) can be used to develop Variable Rate Application (VRA) maps for crop inputs (Lu *et al.,* 1997; Pierce and Nowak, 1999; Batte, 2000). Launched commercial Earth Observation (EO) satellites can provide the spatial resolution, timeliness, and high quality imagery that site-specific agriculture requires (Moran *et al.,* 1997). Remote sensing as part of a site-specific agriculture management strategy can provide the farm enterprise with the ability to satisfy increasing environmental, economic, and market demands (Stafford, 2000)

1.2 Research objectives

In this study, for development of a real-time optical sensor for detecting wheat growth status, in first step, the potential of the plant nutrition active remote sensing instrument was evaluated by comparison with the passive sensor for predicting spatial variation of the crop growth condition in winter wheat (Triticum aestivum L.). Specific objectives in this step were (a) to install and introduce a ground-based remote sensing system for monitoring winter wheat growth status and (b) to evaluate and verify the performance of installed system by regression models that estimate crop characteristics.

Significant wavelengths related to the winter wheat growth characteristics as a preliminary step toward developing a real-time spectral-based crop sensor are necessary. Therefore in the second step of this research, the objectives were I) to present a

step-by- step multivariate analysis method to determine important wavelengths in the spectral reflectance data for assessing the N status, protein content and grain yield of winter wheat, II) to develop prediction models in terms of the N status, protein content and grain yield using partial least squares regression (PLSR), III) to select individual significant wavelengths using stepwise multiple linear regression (SMLR) analysis.

The third step on this study was selection and evaluation of optimal vegetation indices for prediction of crop growth status. In this step, the performance of various types of hyper-spectral vegetation indices for characterizing agricultural crop physiological variables was evaluated with the goal of determining the optimal number of hyper-spectral bands, their centers and widths, in the visible and infrared portion of the spectrum (400~1350 nm), thus reducing redundancy in hyper-spectral data.

1.3 Organization of thesis

This thesis is organized into seven chapters. In the chapter 1, the thesis has been introduced and the research objectives have been stated.

In Chapter 2, the literature is reviewed, starting with the broader context of this research in agriculture and site-specific management. The role of remote sensing in site-specific agriculture is defined in terms of how spatial management tools contribute to the practice of sustainable agriculture. Environmental factors that influence leaf and canopy spectral reflectance are outlined, and crop biophysical parameters are described. Moreover, some fundamental information on crop growth prediction and vegetation indices is given.

In Chapter 3, field experiments and materials including the study area, work history and specifications of used devices are described.

In Chapter 4, the usefulness of a ground-based sensor embedded on tractor for monitoring the growth of winter wheat using a two plant nutrition active sensors and RTK-GPS are presented and discussed.

In chapter 5, a step-by-step multivariate analysis to select significant wavelengths related to the winter wheat growth characteristics is described and results of regression coefficients and variable importance for projection (VIP) in partial least squares

regression (PLSR) and a stepwise multiple linear regression (SMLR) procedures are discussed.

Chapter 6 is presenting both calculation and selection methodology to determine optimal vegetation indices with two-waveband and three waveband combination.

Chapter 7 summarizes the main topic of the research and draws an abstract for whole thesis.

CHAPTER 2

RESEARCH BACKGROUND

2.1 Precision agriculture

The use of innovative technologies collectively named "Precision Agriculture" is a promising approach to optimize agricultural production of crops. In field crop production precision agriculture methodologies are applied to site-specific application of fertilizer or pesticides, automatic guidance of agricultural vehicles, product traceability, on-farm research or management of production systems (Gebbers and Adamchuk, 2010). Recently precision agriculture also enhances management decisions in livestock production, pasture management, viticulture, and horticulture (Gebbers and Adamchuk, 2010; Schellberg *et al.,* 2008). Precision crop production aims to match agricultural input and practices to the spatial and temporal variability within a field, instead of managing an entire field based on a hypothetical average. Small-scale site-specific differences can lead to great differences in yield and quality, thus a better use of resources to preserve the quality and quantity of agricultural products with respect on environmental resources is essential (Gebbers and Adamchuk, 2010). The philosophy behind precision agriculture is not only including a direct economical optimization of agricultural production, it also stands for a reduction of harmful outputs into environment and non-target organisms. In particular a contamination of water, soil, and food resources with pesticides has to be minimized in crop production (Bongiovanni and Lowenberg-Deboer, 2004). With this aim, site-specific fertilizer application was the first successfully implementation in 1988, soil sampling, yield mapping, and site specific herbicide application succeeded (Adamchuk *et al.,* 2004; Gerhards and Oebel, 2006; Stafford, 2000). Against the background of food security and sustainable production, adequate technologies are fundamental for this agricultural practice (Zhang *et al.,* 2002). The implementation of information-based management systems into crop production since the mid 1980s implies a huge potential to modernize the agricultural practice. Since then different techniques for the characterization of soils and crops have been engineered and included into decision making systems. To name the most important ones, precision agriculture integrates different technologies like global positioning systems (GPS), geographic information systems (GIS), as well as different kind of sensors and therefore it demands a high level of expertise (Stafford, 2000). For the future an information-driven crop production as a combination of geospatial and

agricultural data management will encourage the actual utilization of precision agriculture applications (Nash *et al.,* 2009; Reichardt *et al.,* 2009). Current research on precision agriculture for crop production focuses on the development of sensors for remote detection of crops and soil in real time. Relevant field parameters like soil properties, topography, water status, crop micro-climate, nutritional status, weeds, and pests and diseases as well as yield can be monitored and estimated. Integration of different remote sensing techniques and image analysis in combination with a global positioning system will be an essential step towards online application. Still one limiting factor of a successful use of precision agriculture is the interpretation of properties derived from sensor data, rather than the collection of relevant data (Schellberg *et al.,* 2008). The interpretation of information and its implementation into robust decision support systems will improve the acceptance and implementation of precision agriculture techniques.

2.2 Need for an agricultural monitoring

The economic and social importance of the agricultural sector in many regions of the world, together with the concern about world population increase, economic development and the uncertainty in the changes of production caused by climate change, made necessary the development of procedures and techniques to monitor the conditions of crops, to improve the crop field management and also to be able to make early prediction of crop production. This need for an efficient crop monitoring and management, as well as, the prediction of crop production is thus enhanced by climate change issues and by the changes in agriculture related to human activities.

Regarding to human activities, the Food and Agricultural Organization of the United Nations (FAO) states that the world population will increase at a rate of 43 million per year in the period 2045-2050 (Bruinsma, 2003). This rise of human beings in the world will be a consequence of the population growth in developing countries (45 million), and prognosis is that half of this accruement will occur in the sub-Saharan Africa (23 millions). In those developing countries, especially in Africa, the increase of population will aggravate even more the current world undernourished state. It is expected that industrial countries will have some reactions for increasing food production in

concordance to this population growth. Thus, there is a matter of fact that it exists a general concern about increasing agricultural production.

Furthermore in the frame of what is also known as food security strategies, there is an interest in predicting problems like pest infections and drought periods than can damage the crop production. In the large arid and semiarid regions of the world droughts are frequent and they commonly cause a decrease or a total failure of crop production, important economic losses in developed countries, and famine in undeveloped countries. An increase of some of these problems is expected with climate change, mainly in the Mediterranean region, which might be one of the most vulnerable regions to global change in Europe. Climate change projections for the Mediterranean region show a reduction of agricultural areas and losses of agricultural potential during the twentieth century (Schröter *et al.,* 2005) due to the pronounced decrease in precipitation that is predicted (Giorgi and Lionello, 2008).

The current change of alimentary habits in some important emerging countries, like India and China is increasing the demand for agricultural products. In these countries, a growing sector of the population is becoming wealthy enough to change from a mostly vegetarian diet, based on rice and other cereals, to a diet that includes more meat. Livestock needs to be fed with cereals, which increases the demand and, therefore, market prices. Furthermore, some developed countries are increasing their production of biofuels, which diminishes the quantity of crops used for human consumption. This is also helping to increase the prices of cereals. Last, but not least, the upward trend of prices is attracting speculators to the markets. This increase of prices is causing political tensions, as happened during the spring of 2008 in countries like Haiti, where the prime minister had to resign, Cameroon, Senegal, but also Egypt or Thailand. A means for limiting price increases would be to increase production, which would need an increase of agricultural productivity. In fact, during the FAO summit of June 2008, it was stated that more investments should be done to increase agricultural productivity.

The need for an increase of production has induced important changes in the agricultural practises during the last decades. For example the use of fertilizers has been extended worldwide and genetically modified crops are used as a solution for a "sustainable" production increase (Qaim and Zilberman, 2003). There is also a concern about the impacts associated with these new agricultural practises. The expansion of

agriculture needs to be done in a sustainable way as the generalized use of fertilizers or over exploitation of water resources represents environmental risks and can even have consequences for human health. The increase intensive processes like irrigation and/or the abuse of fertilizers also might produce some negative consequences on water quality and the degradation of irrigated lands for instance as a consequence of salinisation.

Finally, another noticeable change in modern agriculture is that more and more frequently crop rotations are decided by market fluctuations and policy regulations. This introduces an additional dynamics in crop distribution, which make necessary to update crop maps with a high temporal frequency.

The other important issue that requires a system for crop monitoring is the impacts of climate change in agriculture. Studies conducted over the last decades have provided evidence about the modifications of several climatic parameters (Solomon *et al.,* 2007). For instance, noticeable trends in surface temperatures have been recorded during the twentieth century at the global scale (Jones and Moberg, 2003). Satellite observations using AVHRR and ATSR data confirmed an increase in global sea temperature (+0.13ºC in a decade). An increase of extreme events such as hot waves, droughts and extreme precipitation events has also been recorded in different regions (Karl and Easterling, 1999). The existing models of climate agree on the increase of global surface temperatures for the second half of the 21st century. For instance, after a doubling of the concentration of CO_2, the increase in temperature is likely to be in a range that goes from 2 to 4.5°C, with a best estimate of about 3°C. Nevertheless, although this is the general pattern predicted at the global scale, models indicate an important spatial diversity in the manifestation of the effects of climate (Räisänen, 2007).

The feedback effect of climate change on agriculture is complex. The increase in temperature and the increase in the concentration of atmospheric CO_2 could affect the plant biological processes (photosynthesis, respiration, growth, etc) (Barnes *et al.,* 1995; Booker *et al.,* 2005). The fertilizing effect of the atmospheric carbon could produce a general increase of the vegetation activity and production (Long *et al.,* 2005). Nevertheless, the positive response of vegetation activity and production to climate change is only expected in areas with an adequate availability of water, on the contrary, the areas affected by an increase of temperatures and evapotranspiration together with a

decrease of precipitation will suffer from a higher water stress in vegetation, which, in turn, would cause a decrease of the production (Vicente-Serrano *et al.,* 2006). Finally, extreme events (hot waves, droughts, extreme rainfalls) have a negative effect in crop production (Vicente-Serrano, 2007). The undesirable impacts that climatic change can have in crop production show the strong requirement for the monitoring of crops at present and to be maintained in the future.

2.3 Crop monitoring

In the previous section it was highlighted that the relationship between agriculture and climate and the important changes in agriculture practises during the last part of the 20th century shows that agricultural monitoring systems are necessary. To be efficient, such systems should satisfy at least the three requirements listed hereafter: they should be able to provide a map of crops timely, to survey the growth of crops and if possible to predict the yields. Below, each of these requirements is discussed in more detail.

2.3.1 Crop investigation

The substantial increase of intensive agriculture together with the influence of the policy regulations and market demands leads to frequent changes in the surface meant to agriculture and in the distribution of crops within the land devoted to agriculture. Therefore, the timely identification, inventory and cartography of crops becomes necessary for estimations of crop yield. In addition to the crop production assessment, crop mapping is also useful for the management of water resources or the estimations of sequestration of carbon by the soil, among others.

2.3.2 Crop growth survey

Crop growth survey consists in the monitoring during the growth period of several crop and soil parameters, which are indicators of the plant condition, together with the actual plant phenological stage. Those parameters are for example plant height, LAI (Leaf Area Index), biomass or nitrogen content. Typically, the survey of crop growth is focused in the following issues, which are in-turn interconnected:

1) Phenology development: That is the succession of biological events during the plant life. The survey of phenology implies, for example, the observation of the exact moment in which certain crop organs appear (ex. wheat ears). Phenology is often simulated in terms of the sum of degree-days and crop specific characteristics, for instance vernalisation factors.
2) Canopy development: it can be quantified by the measurement of the LAI, the plant biomass of the plant height. In terms of biological processes, canopy development is the result of photosynthesis, respiration and biomass allocation. The amount of energy received and the capacity of the plant to use this energy will determine the biomass production. The amount of intercepted radiation is a function of the LAI. Only a part of the intercepted radiation, denoted as fPAR, is efficiently used by the crop and will be used for biomass accumulation. The way in which biomass partitioning is performed is specific to each cultivar type. In the modelling of canopy development the high vegetative structural diversity is controlled by genetic variables that intervene in this partitioning.
3) Roots growth and uptake ability: the function of plant roots is to uptake water and nutrients from the soil. This is closely related to the soil chemical and physical properties as well as the soil moisture conditions. Any lack of nutrients, especially nitrogen, or any water deficiencies would negatively impact the plant development. The shortages in mineral content or basic nutrients in the soil can be detected with periodical analysis of soil samplings and compensate with fertilization. The monitoring of moisture conditions is also necessary. Regarding biological aspects, there is a big difference between the root system of annual crops (ex. wheat, corn, potatoes…) and perennial crops (ex. vineyards).
4) Water balance among the plant, the soil and the atmosphere. The water requirements of a crop in a particular moment depend on the environmental variables (ex. air temperature), the soil conditions and the crop phenology. The processes involved in the water balance include evaporation and transpiration, both in the soil and in the plant. The list of variables that take part in the water balance, mainly describing the soil status and soil water behaviour, can be very extensive (soil albedo, drainage coefficients, etc….) but the most important is soil moisture.

5) Nitrogen balance in the soil and in the plant. The content of nitrogen in the soil can change as a result of organic decompositions, fertilisation, etc. Crops absorb nitrogen through the roots system and fix it in their elements. The nitrogen content in the leaves is related to the chlorophyll content, which is easier to measure than nitrogen content.

The information obtained from the survey of the previous points through the quantification of several parameters is of great valuable for the management of fields and are the basis of the human interventions like the use of fertilizers or a particular irrigation schedule. However, the monitoring of the parameters of crops along a growing season is expensive and time consuming, and therefore, there is a need for developing remote sensing techniques that will be useful in this context.

2.3.3 Prediction of crop yield

Several techniques have been used to obtain an early prediction of crop production, most of them based on previous climate conditions summarised by means of drought indices, vegetation indices obtained from remote sensing data (e.g., Mkhabela *et al.,* 2005; Kalularme *et al.,* 2003; Royo *et al.,* 2003) and both of them (Vicente-Serrano *et al.,* 2006). These methods are based on regression models between the final crop yields, the climate data and vegetation indices. Although these methods are widely used, they have the problem that predictions are site specific from local measurements and sometimes the spatial extrapolation is difficult, as a consequence of the geographic and topographic diversity and the different crop types. To solve these problems, more complex models, based on biophysical processes, can also be used. These are likely to be more general than the statistical methods based on local regressions. A model of crop growth describes how a plant grows, that is, how the carbon is allocated in the plant. These models require daily meteorological data: incoming solar radiation, temperature and precipitation. Many models have been developed or adapted to a unique cultivar, a reduced number of them or to particular crop conditions like water stress, nitrogen stress, salinity conditions, etc. and make use of many parameters. Thus, the benefits of using a monitoring system that provides crop parameters describing canopy development, for instance LAI would be very important for model calibration, forcing, etc.

A huge diversity of crop growth models exists in the scientific literature. Some well-known models and their related 'families' are SUCROS (Simple and Universal Crop Growth Simulator) (Spitters *et al.,* 1989), CERES (Crop Environment Resource Synthesis) (Jones and Kiriny, 1986; Ritchie *et al.,* 1985) that was developed for cereals, CROPGRO (Hoogenboom, 1992) is a family of grain legumes models and STICS (Simulateur mulTIdisciplinaire pour les Cultures Standard) (Brisson *et al.,* 1998) developed at the INRA, France. There are also software "packages" like DDSAT (Decision Support System for Agrotechnology Transfer) (Jones *et al.,* 2003) and APSIM (Agricultural Production Systems sIMulator) (McCown, 1986) that integrate several of the previously cited models.

Nevertheless, despite the great usefulness of these models, there are noticeable limitations concerning its calibration. Crop parameters describing canopy development and dynamic are commonly needed for the calibration of the models. This involves time and cost consuming field samplings and very often there is a lack of spatial representation, mainly in areas in which spatial diversity of crops, soil characteristics and climates are important.

Therefore, due to these limitations, there is a need to develop methods based on remote sensing data, which allow the monitoring of crop parameters over large areas, to improve the yield prediction.

2.4. The role of remote sensing in crop monitoring

The monitoring of crops can be done by means of ground survey at the local scale. However, at a regional scale, remote sensing appears appropriate booth in terms of spatial and temporal coverage.

2.4.1 Crop mapping

As it was said before, crop mapping is necessary in land change studies, climate change, hydrological studies and other applications like yield prediction and the efficient management of water resources, the later usually based in the estimates of evapotranspiration (Simonneaux *et al.,* 2008). Crop maps are usually used in combination with crop growth models for yield prediction or to model for example soil carbon sequestration (Doraiswamy *et al.,* 2007).

Because of the amount of applications, the classification of crops using remote sensing images is an important topic in remote sensing research. The advantages of using remote sensing techniques, instead of field survey, are the lower cost and the possibility of covering large areas. Another important reason is that it is easier to update the classifications, due to the possibility of repeated time frequency of the data. The use of optical remote sensing data is well established for crop mapping and the methodologies have been proved to be quasi operational. Crop classification using optical data is often performed with data with a spatial resolution compatible with the field size: in general Landsat-TM or SPOT-HRV data at regional scale are used. Medium-resolution data (200 Km – 1 Km) and coarse resolution data (> 1 Km) are often considered as insufficient with regard to the size of the fields. Those data (AVHRR, MODIS, MERIS, SPOT-VGT) are mostly used for multi-year temporal surveys, and to obtain land use/land cover maps at continental or global scales (Loveland *et al.,* 2000; Strahler *et al.,* 1999; Bartholomé and Belward, 2005). A well-known limitation of optical data is the presence of the cloud cover that prevents the acquisition of images at the desiderate time. Radar data, in contrast, has the advantage of being independent from cloud cover and thus show a high potential for crop classification. It may also happen that vegetation needs to be monitored at a specific phenology stage. This is the case, for example, when two crops have similar behaviour during the growing season except for a specific development stage. However, satellite radar data have not often been used for this purpose, (Saich and Borgeaud, 2000; Schotten *et al.,* 1995; Tso and Mather, 1999) mainly because, until very recently, satellites were only able to measure single linear polarisations at a single frequency: ERS-1 and ERS-2 operate at C Band at VV polarisation, RADARSAT operated at C band and HH polarisation, JERS operated at L Band, HH polarisation. Future missions will measure the complete scattering matrix at a single frequency and there is a need for developing adequate classification methods.

Several algorithms use radar data for the classification of crops. In a general way, they can be classified into knowledge-based approaches, classification by scattering mechanism and statistical data-driven methods (Oliver and Quegan, 1998). Knowledge-based approaches are based on the analysis of the physics that determines the measured

backscattering for each crop type. Those classifiers have the advantage of being more robust and easier to adapt to the specific conditions of the area to classify.

2.4.2 Crop condition and growth monitoring using remote sensing data

Remote sensing data can be used to estimate biophysical parameters, which are indicators of the crop condition along the growing season. Multi-temporal estimations of these parameters contribute to the growth survey. Biophysical variables like LAI, fraction of photosynthetically active radiation (fPAR), biomass or nitrogen content are important because they contribute to the understanding of the crops dynamics and environmental dynamic at any spatial scale. In spite of the availability of radar data under any weather conditions, the retrieval of biophysical parameters is more frequently done using optical data, mainly because the interaction between the radar signal and the vegetation is more complex than with the optical signal and it is more difficult to establish the biophysical relationships. Generally they can only be established for one type of crop, because it has a particular structure. In addition it is complex to handle radar data compared with optical data. A large amount of papers were published on the derivation of biophysical parameters at leaf and canopy level from optical data. Many examples can also be found for LAI (Turner *et al.,* 1999; Weiss *et al.,* 2000; Combal *et al.,* 2002a), Duchemin *et al.,* 2006), fPAR, canopy water content and leaf chlorophyll content. For agricultural crops, for which temporal changes are more rapid than for instance forest surfaces, multi-temporal observations are very important. Few papers have addressed the effective inversion of multi-temporal and high-resolution satellite images for various crop types. Thus, more work needs to be done on the retrieval of biophysical parameters using multi-temporal data. In the radar domain, multi-angular, polarimetric and interferometric data have been shown to be of interest for the retrieval of biogeophysical parameters like crop height, plant water content, LAI and biomass (Le Toan *et al.,* 1984). Those studies were mainly conducted with the X and C Bands. It has been demonstrated that if the vegetation cover has components with specific orientations, the penetration depth, the volume scattering, and the attenuation may be different at different polarisation states (Ferrazzoli *et al.,* 1999; Picard *et al.,* 2003, and Mattia *et al.,* 2003). This phenomenon was the base used to develop an algorithm to map rice fields (Le Toan *et al.,* 1989).

As with crop mapping the retrieval of biophysical parameters using radar satellite data have been limited by type of data. The ASAR sensor onboard ENVISAT allowed, for the first time, to measure two simultaneous polarisations HH/VV, HH/HV and VV/HV at different non-simultaneous incidence angles in Band-C. This motivated studies on the use of polarimetry for biomass retrieval of wheat (Mattia *et al.,* 2003). This work studies the potential of polarized radar data in the derivation of biomass for small grain cereals using ENVISAT-ASAR data.

2.4.3 The role of remote sensing in combination with crop growth models for crop yield prediction

It is difficult for the models to account for the spatial heterogeneity in vegetation and soil conditions as well as the inherent difficulties of phenology modelling. Crop growth depends on many factors (weather, species, soil status, soil characteristics and management strategies) and, as a result, models need many parameters. For instance STICS v3.0 depends on 132 parameters (Ruget *et al.,* 2002). It is frequent that some of these parameters, like the sowing date, are unknown, or need to be adjusted for each crop type or geographical location. One solution consists in calibrating the models using measurements of biophysical parameters (e.g. Brisson *et al.,* 1998; Spitters *et al.,* 1989; Bondeau *et al.,* 1999; Launay and Guerif; 2005). LAI, which accounts for the leaf surface intercepting in-coming radiation, and biomass are key variables to calibrate crop growth models.

The calibration can be done with in-situ measurement of biophysical parameters. However, in-situ measurements are expensive and time consuming and generally can only be done at a limited number of fields. Thus, calibration has the risk of becoming site and cultivar-specific. In this context satellite remote sensing is useful when integrated in the models of crop growth as it provides spatial information on actual vegetation status. Remote sensing can be used to estimate key variables in the models: LAI, aboveground biomass and other crop characteristics like chlorophyll or nitrogen content. This information can be integrated in the calibration process using for example forcing methodologies (Clevers and van Leeuwen, 1996; Moulin *et al.,* 1998).

2.5 Sustainability and site-specific agriculture

2.5.1 Sustainable agriculture

The implementation of sustainable farm practices is closely related to the way the agricultural sector has historically evolved. In the 1950s through to the 1980s, the emphasis in farming was placed on the modernization and industrialization of agriculture to increase farm output (Ilbery and Bowler, 1998). This time period is also referred to as the "green revolution" that was conceptually adopted on the farm due to the introduction of higher yielding grain varieties, an increased number of irrigation facilities, and increased access to inorganic fertilizers, and changes to redundant government policies (Khush, 1999). A key factor in this era of agricultural intensification was global consideration for the food-balance equation that focused on meeting higher demands for food due to population growth in underdeveloped countries (Khush, 2001). Higher demand for production led to intensified agricultural land use which resulted in environmental degradation (e.g. over use of chemicals, soil erosion). These environmental consequences were realized through an international movement that focused on sustainable development and conscious use of the world's limited natural resources. It was through this paradigm shift that both the public and the farm community became aware of the environmental damage which occurred due to intensive agriculture practices. By the 1990's, the focus changed from increasing food output to concern over food quality and sustainable food production (Ilbery and Bowler, 1998). The 1990's were not only characterized by reduced output of food, but also progressive withdrawal of subsidies, resulting in an increasingly competitive market, and growing environmental regulation of agriculture (Ilbery and Bowler, 1998). During this time period there were vast advances in biotechnology which also affected how farmers implemented sustainable agriculture practices (Mannion, 1998). Overall, farmers became more aware of alternative sustainable practices (e.g. organic farming, improved crop rotation, no-till practices, site-specific agriculture) and the implementation of these practices became more common (Sivakumar *et al.,* 2000; Rigby *et al.,* 2001). As farmers began to recognize the importance of sustainable agriculture, the adoption of alternative practices on the farm involved a transition from substituting capital for labor, to substituting management for capital (Petrzelka *et al.,*

1997). Measuring management as capital can be quite difficult to quantify, and the literature describes the issues surrounding the development of an adequate definition for sustainable agriculture (Brklacich *et al.,* 1991). Ilbery and Bowler (1998) summarized the work of Brklacich *et al.,* (1991) by defining a sustainable agriculture system in terms of simultaneously satisfying three types of sustainability:

• *Environmental sustainability* - the capacity of an agricultural system to be projected into the future without unacceptable pollution, depletion or physical destruction of its natural resources such as soil, water, air, and natural or semi natural habitats.

• *Socio-economic sustainability* - the capacity of an agricultural system to provide an acceptable economic return to those employed in the productive system.

• *Productive sustainability* - the capacity of an agricultural system to supply sufficient food and support the non-farm population.

2.5.2 Site-specific agriculture

Site-specific agriculture is a knowledge-based system that enables farmers to apply precise amounts of fertilizers, pesticides, water, seeds or other inputs to specific areas where and when they are needed for optimal crop growth (Lu *et al.,* 1997). Successful site-specific agricultural management systems are well documented in the literature (Stafford, 2000; Macy *et al.,* 1994; Mulla, 1991, Stafford *et al.,* 1991; Wollenhaupt and Buchholz, 1992). Schilfgaarde (1999) emphasized that this type of management is very information intensive, and is not based solely on spatial technology but also on rapidly evolving information technologies that contribute to the site-specific modification of land management as conditions change spatially and temporally. One of the most important factors in farm practices is managing more static natural field variability (i.e. soil type, topography) and variability that is in flux due to environmental stressors (i.e. weather induced, pests). Managing crop variability successfully considers two domains: (1) the spatial variability of the land under production (e.g. soil sampling to establish the amount of phosphorus in the soil), and (2) how that variability changes over time with improved management practices (e.g. applying more phosphorus to those regions of the field that require more for optimal crop production). Successful sitespecific farming is dependent on how well practices can be used to assess, manage, and evaluate the 'space-time continuum' in crop production (Pierce and Nowak, 1999). A quality food

production system requires optimal yield performance from the land, and farmers employ site-specific management practices to reduce production costs and increase crop yields (Mulla, 1991). Other reasons for employing site-specific farming practices are not just economic in nature, but include environmental benefits (Hammond, 1992). However, the environmental benefits are not widely documented in the literature (Pierce and Nowak, 1999) and are not easily quantified (Perez-Munoz and Colvin, 1996). Site-specific farming has been primarily 'technology-driven' (Stafford, 2000) and involves the use of four primary enabling technologies: (a) Geographic Information Systems (GIS), (b) Global Positioning Systems (GPS), (c) Sensors and (d) Variable Rate Technology (VRT). A GIS is an organized collection of computer hardware, software, geographic data, and personnel designed to efficiently capture, store, update, manipulate, analyze, and display all forms of geographically referenced information (ESRI, 1995). A GIS is a key tool in extracting and quantifying crop variability within agricultural fields (Pierce and Nowak, 1999). A GIS not only establishes where the variability is, but can address the variability through the application of crop inputs using maps (e.g. variable rate fertilizer maps). Over time, the GIS is a record keeping tool that can provide a costbenefit analysis for the farmer (e.g. assess if adding more fertilizer to a specific region of the field resulted in more crop yield and more economic return). The second enabling technology, GPS, became widely accessible in the early 1990s and was originally a constellation of military satellites known as the NAVSTAR (NAVigation System with Time and Ranging) system. In 1994, NAVSTAR became available for general civilian use, including agriculture (Pierce and Nowak, 1999). In 1995, a Russian constellation of satellites was also launched for civilian use and is known as the GLObal Navigation Satellite System or GLONASS (Stafford, 2000). GPS provides location control in site—specific agriculture and is essential to delineate within field spatial variability and to deliver site-specific applications using variable rate technology (VRT) (Tyler *et al.,* 1997). The third enabling technology involves the use of sensors that can be defined as devices that transmit or receive an impulse in response to physical stimulus such as heat, light, magnetism, motion, pressure and sound (Pierce and Nowak, 1999). The sensors include yield monitors, remote sensing, and soil sensors that measure surface and subsurface features. Remote sensing and visual image interpretation of individual fields has been used in agricultural research and

development for the last 25 years (Bullock *et al.,* 2000). Remote sensing has been used in agriculture in the laboratory, in the field, and from the sky. The advantages of remote sensing in agriculture are its nondestructive, non-intrusive measurement capabilities and its flexibility of scale. The fourth enabling technology, VRT, involves the controlled application of crop inputs. Variable Rate Technology (VRT) is a remediation tool that ingests the 'map' results derived from the GIS, remote sensing and GPS technologies and is available with farm equipment. Examples of a VRT tool are fertilizer or pesticide applicators, and yield monitors, both of which have evolved rapidly and have resulted in the growth of site-specific agriculture significantly (Brisco *et al.,* 1998). The degree to which a farmer will invest in "high technology" or expensive VRT equipment is not only dependent on the size of operation but also on the type of crop and the current market value of that crop (Batte, 2000). It is important to recognize that all of the technology components listed above work together to form a viable site-specific farm management system. GPS is used to spatially record the location of field activities, sensors are used to spatially characterize the physiological properties of the crop, a GIS ingests the GPS and sensor derived information to create management maps, and VRT is used to implement the management strategies back in the field. As described next, remote sensing in agriculture is an important component of this comprehensive approach to site-specific management.

2.6 Remote sensing of crop information

Remote sensing is the practice of deriving information about the earth's land and water surfaces using images acquired from an overhead perspective, using electromagnetic radiation in one or more regions of the electromagnetic spectrum, reflected or emitted from the earth's surface (Campbell, 1996). Optical remote sensing provides an indirect method of observing the physical processes in plant canopies. Radar and other remote sensing methods can provide structural information about the crop but are not as successful in identifying the physiological processes of the crop canopy. Recognition of the value of remote sensing by the agriculture community provides additional motivation for further research within the context of site-specific agriculture (Moran *et al.,* 1997; Brisco *et al.,* 1998; McNairn and Brown, 1999;

McNairn *et al.,* 2001a). It wasn't until the mid 1970's to early 1980's when the first Earth Observing (EO) satellites were launched that a significant research effort was initiated to investigate the use of multispectral images for crop inventory and crop production (Moran *et al.,* 1997). In site-specific agriculture, three types of information can be obtained: (1) information on seasonally stable conditions, (2) information on seasonally variable conditions, and (3) information required to diagnose the cause of the crop yield variability and develop a management strategy (Moran *et al.,* 1997). This research primarily focuses on the use of remote sensing to derive the third type of information. Remote sensing can be used as a diagnostic management strategy to estimate crop yield variability, aid in the creation of field management zones based on crop vigour and soil variability, and in turn guide in-field soil sampling to derive zone-based variable application maps (Bullock *et al.,* 2000). Remote sensing is also an efficient method of spatially characterizing both site-specific crop biophysical parameters as well as broader ecological information and for modelling (Wiegand and Richardson, 1990; Mack *et al.,* 1990; Wiegand *et al.,* 1991; Thenkabail *et al.,* 1994; Cihlar *et al.,* 1991). The advantage of remote sensing is that it allows the farmer access to information about the health of the crop at more mature growth stages and much later in the growing season. Other ground-based technologies (e.g. plant tissue sampling) may be too impractical and labor intensive in mature crop stages. Using remote sensing throughout the growing season to define crop variability potentially provides farmers with a pro-active method of remedying crop stress prior to actual yield loss.

2.6.1 Factors affecting the spectral properties of crops

The focus of this research is to better analyse crop conditions that are important in farm management, such as biophysical parameters (e.g. LAI) that can aid in the identification of poorer yielding regions of the farm. All plants, both native and cultivated, respond to environmental stresses in the same way: through a decline in growth rate and in the rate of acquisition of all resources (Chapin, 1991). Many studies have been conducted on the ability of remote sensing to detect stresses in crops such as nutrient deficiencies (Milton *et al.,* 1991; Yoder and Pettigrew-Crosby, 1995; Masoni *et al.,* 1996; Marrioti *et al.,* 1996). To fully understand canopy level reflectance in airborne agricultural applications of remote sensing, one must first understand leaf spectral

properties and how the leaf is linked to morphological and physiological conditions (Mariotti *et al.,* 1996).

1) Leaf spectral properties

The leaf of a plant is the primary photosynthesizing organ. Photosynthesis occurs in the chloroplasts where the chlorophyll pigment is located. When examining the spectral properties of a single leaf, only part of the incident energy is reflected with the balance either absorbed or transmitted. Figure 2.1 demonstrates how these components are closely related and it is necessary to consider the interplay among all three to evaluate the physical and physiological basis for leaf reflectance (Knipling, 1970). A plant leaf typically has low reflectance in the visible (except in the green region) because of strong chlorophyll absorption, relatively high reflectance in the near infrared because of internal leaf scattering and no absorption, and relatively low reflectance in the infrared beyond 1.3 um because of strong absorption by water (Knipling, 1970). This strong absorption beyond 1.3 um due to water as a function of dehydration of a bean leaf. Water content in the leaf is a dynamic feature because cell structure scatters light as it passes through air and water interfaces of the leaf (Yoder and Pettigrew-Crosby, 1995). Leaf photosynthetic rate is linked to the amount of absorbed radiation, which depends on incident radiation and leaf absorptance.

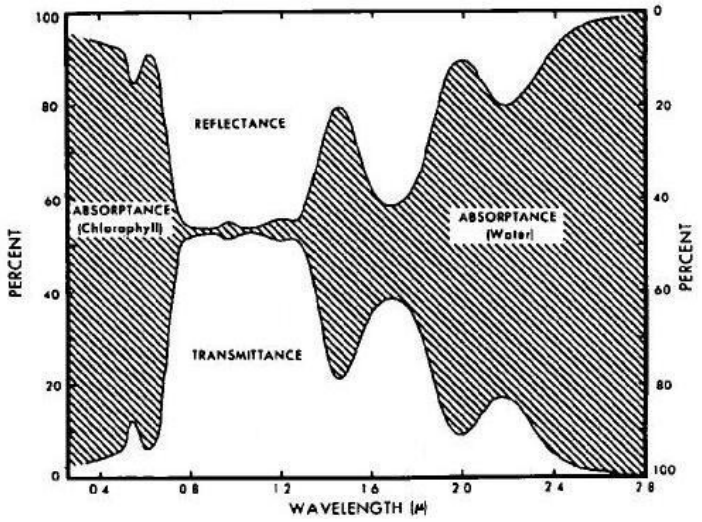

Fig. 2.1 Reflectance, absorptance, and transmittance spectra of plant leaf (Knipling, 1970)

Leaf absorptance is affected by external and internal reflectance and by leaf pigment content that is essentially represented by chlorophyll content (Masoni *et al.,* 1996). The distribution of chemical constituents within the leaf is not uniform because proteins and chlorophylls are packed into chloroplasts that migrate and clump as the light environment changes, and due to the distribution of lignin in the cell walls (Yoder and Pettigrew-Crosby, 1995). There have been many studies that have examined the relationship between regions of the electromagnetic spectrum, crop leaf structure, and chemical constituents (Wolley, 1971; Thomas and Gausman, 1977; Wiegand and Richardson, 1984; Maas and Dunlap, 1989; Walter-Shea *et al.,* 1991; Horler *et al.,* 1983; Buschmann and Nagel, 1993). Leaf reflectance responses to environmental conditions that inhibit growth (i.e. plant stress) usually involve increased reflectance in the visible region of the electromagnetic spectrum and in the infrared regions if the stress is severe enough to cause dehydration (Carter, 1992). Remote sensing, and the ability to analyze specific regions of the electromagnetic spectrum, provides a method to examine crop stress at the leaf level, and at the canopy level as described next.

2) Canopy spectral properties

The dynamic spectral nature of individual crop leaves contributes to the nonuniformity of the canopy, and furthermore the spectral characteristics of a crop canopy change due to variation in landscape (e.g. topography, soil fertility and texture). Under varying conditions, the reflectance of a plant canopy is modified by the non-uniformity of incident solar radiation, plant structure, leaf area, shadow, and background reflectivities (Knipling, 1970). One significant difference between the amounts of infrared energy reflected from a leaf versus a canopy is that a portion of the incident infrared energy is transmitted through the uppermost leaves, reflected from lower leaves, and retransmitted up through the upper leaves to enhance their reflectance (Knipling, 1970). In agricultural applications of remote sensing, it is important to understand how the canopy structure and crop geometry (i.e. size, shape and orientation of the plants and their leaves) plays a role in what is being sensed from the target. The size, shape and orientation of plants are also heavily influenced by human management practices and seasonal growing conditions. All of these factors contribute to the optical

properties of crop leaves, and in turn the canopy with respect to the remotely sensed reflection patterns (Knipling, 1970).

2.7 Biophysical parameters

In the case of agricultural remote sensing applications, biophysical parameters are measured either directly or indirectly from the field of interest during the growing season to evaluate how the crop is performing. The information collected by an optical sensor (e.g. reflected and transmitted solar energy) must be related to the ground based biophysical parameters of the crop. If biophysical parameters are strongly correlated with remote sensed data, then these data can be used to predict those biophysical characteristics for variable scene and sensor characteristics over large areas (Treitz and Howarth, 1999). Empirical relationships established in the literature has led to the development of indirect methods for quantifying crop biophysical parameters using remote sensing imagery.

2.7.1 Ground based biophysical parameters

In remote sensing studies, ground based biophysical sample site locations are typically mapped using GPS to enable a direct comparison of the biophysical parameter with the imagery. Sampling methods may be designed based on the size of the study area, and more importantly the spatial resolution of the imagery or pixel size. Ground based biophysical parameters commonly reviewed in the literature for agricultural studies are; percent crop cover, leaf area index (LAI), biomass, and yield (post-harvest).

1) Percent crop cover

Vegetation cover can be defined as the vertical projection of the shoot area of vegetation to the ground surface and is expressed as fraction or percent of the reference area (Purevdorj *et al.,* 1998). In remote sensing applications, this definition can be elaborated to include all "green vegetated areas that are directly detected by the sensor from any view direction" (Purevdorj *et al.,* 1998). Percent crop cover during the growing season can be measured using in-field photographs taken directly above the crop. The photographs are imported into an image analysis software and classified to obtain the percent ground cover for each cover type (McNairn *et al.,* 2001b). Percent

crop cover is measured to deduce the percentage of each ground cover component in the image (i.e. percent crop, percent shadow, percent crop residue or dead matter, percent bare soil). This tool is a method of spatial validation for both traditional and new remote sensing image processing methods.

2) Leaf area index (LAI)

In assessing the health of the crop, it is very important to understand not only health but also how much plant is present. LAI is defined as the leaf area per unit area of soil surface (Daughtry, 1990). Norman and Campbell (1989) defined both direct and indirect methods of collecting LAI of a vegetation canopy. Compared to direct methods, the indirect methods are less labour intensive. Predicting LAI from remotely sensed imagery or physically measuring LAI is important in characterizing how the field is producing site-specifically. LAI prediction can aid in defining within field variability and if done early enough in the growing season could allow the farmer to remedy problems before actual yield loss results. In remote sensing studies, LAI field measurements are typically acquired at a limited number of representative sites and used for remote sensing input and/or validation over large areas.

(1) Direct measurements of LAI

One of the earliest direct methods of collecting LAI was leaf tracing. A sample of leaves would be harvested and their contours traced onto graph paper and the area measured by counting the squares within the leaf outline (Daughtry, 1990). The leaf tracing may be weighed and area calculated based on the area to weight ratio for the paper tracing. This method was very accurate, but not time efficient. Other similar methods involved matching leaf shapes and sizes to standard sets of leaves by species, and calculations were based on linear measurements (Daughtry, 1990). In the interest of time efficiency, direct LAI measurements have been developed in recent years to include the use of laboratory instruments that measure leaf area such as the LAI-3100. With the LAI-3100, a sub-sample of the crop is harvested and the leaves are placed through the optical planimetric instrument. This instrument measures the leaf area of the sub-sample in cm^2. This direct method requires additional calculations to determine the leaf area index of the entire canopy from the sub-sample measurements. Daughtry

(1990) defines LAI as a function of the leaf area to leaf mass relationship, according to the following equation:

Eq. 2.1 Leaf Area to Leaf Mass Relationship for deriving LAI:

$$A_L = (A_s / M_S) M_L \quad (2.1)$$

Where:

A_L = Leaf Area Index

A_s = Leaf Area of sub-sample of leaves

M_s = Leaf Mass of sub-sample of leaves

M_L = Total leaf mass for a larger sample of leaves

(2) Indirect measurements of LAI

There are many methods and instruments used in measuring LAI indirectly such as hemispherical photography, crown meters, and line quantum sensors all of which are described in Welles (1990). In this review only the indirect methods that are pertinent to agricultural studies will be discussed. A common indirect field instrument used in agricultural applications is the LAI-2000. The LAI-2000 measures the gap fraction in foliage and is an optical instrument that does not involve destructive sampling. The LAI-2000 instrument measures all light blocking objects simultaneously in five equal zenith angles from 0 to 75 degrees and therefore is considered to provide a "foliage area index". The units of this instrument are dimensionless, but can in theory be thought of as (m^2 foliage area/m^2 ground area). This instrument makes the assumption that the canopy has random foliage distribution, and the clumping properties of the canopy are not considered (Leblanc and Chen, 1998). Not accommodating for a clumping index results in a measure of effective LAI *(eLAl)* and not absolute LAI. In the field, the LAI-2000 measurements are generally collected in overcast conditions to minimize the effect of scattering within the canopy. Other factors to consider in the measurement of LAI in an agricultural setting is the orientation of the foliage, foliage size, and gaps in the foliage (Welles and Norman, 1991). The Tracing Radiation and Architecture of Canopies (TRAC) instrument (Chen and Chilar, 1995) is an optical instrument that measures the gap fraction, however it considers clumping properties (e.g. boreal forests have a non-random and 'clumped' leaf architecture). Unlike the LAI-2000, the TRAC

foliage clumping index allows for the calculation of absolute LAI values. Pacheco *et al.,* (2001) compared the LAI-2000 and TRAC iastruments for three crop types in southern Ontario and found that the LAI-2000 and eLAI values correlated more strongly with the percent crop cover derived from photographs than the TRAC instrument.

3) Biomass

Biomass is the total dry-matter production of a crop, the net result from photosynthesis, respiration, and mineral uptake (Stoskopf, 1981). Quantifying crop biomass can help a farmer to locate inadequately producing regions, and aid in developing crop input management strategies (e.g. fertilizer and pesticide application). In remote sensing agricultural applications above ground biomass measurements should be taken within a day of acquiring the remote sensing image to ensure that the derived empirical relationships are valid. The collection of biomass data involves harvesting plants from the field within a specified sampling area that adequately represents the corresponding pixel size in the imagery. Plants are weighed wet (fresh weight), dried and then reweighed (dry weight). The plant water content is calculated from the wet minus the dry weight (Staenz *et al.,* 1999; Deguise *et al.,* 1999). Timely pre-harvest biomass prediction from remote sensing imagery could help to quantify marketable yield and give the farmer an international competitive advantage that could lead to economic benefits for the farm operation.

4) Yield

In remote sensing agricultural applications, the most spatially accurate yield data available today is obtained using a yield monitor coupled with a Differential Global Positioning System (DGPS). A DGPS yield monitor is placed on the combine at the time of harvest and captures position as well as crop volume and moisture readings on a per second basis. The DGPS receiver allows the yield data to be "stamped" with a geographic coordinate and enables the yield across the field to be mapped. Most DGPS receivers used in agriculture today are 12 channel and use phase smoothed pseudo-range positioning to permit sub-metre accuracy (Stafford, 2000). A typical example is the Trimble AgGPS 106 differential GPS antenna and receiver (Linco Equipment Inc., 2003). The yield monitor units used to represent yield data can vary by both the yield

monitor and the manufacturers software used for data post-processing. In the North Amercian marketplace yield is represented as bushels per acre (bu/ac), kilograms per hectare (kg/ha), or tonnes per hectare (t/ha). Generally, yield monitors provide an accurate and reliable source of information for farmers over time (Perez-Munoz and Colvin, 1996; DeHaan *et al.,* 1999). Yield maps can be visualized in a raw format represented by a set of yield points, or points can be interpolated into a continuous map surface. The goal of yield map interpretation is enhanced profitability through better control of natural and management induced sources of yield variation (Doerge, 1999). Successful yield mapping is heavily dependent on the auxiliary information from the farmer such as field history (e.g. soil type, perennial weed regions, and crop rotation), the analysts' geostatistical knowledge (e.g. appropriate data interpolation methods) and the available GIS tools (Doerge, 1999). Sources of yield variation are not always easily identifiable and can be a result of weather, soil-water relationships, soil physical and chemical properties, slope and aspect of a region, pest infestation, crop inputs, field history, and cultural practices and errors (Doerge, 1999). The yield map can be used as a seasonal "report card" whereby farmers can evaluate how well the crop performed due to the implementation of new site-specific management strategies.

2.7.2 Conventional remote sensing methods for biophysical information extraction

1) Band ratios and vegetation indices

Remote sensing has extended the usefulness of the Geographic Information System (GIS) in site-specific agriculture by incorporating non-intrusive image analysis tools for assessing crop health during the growing season. Vegetation indices, based on the differential reflectance in the red and near-infrared wavelengths, are widely used to assess vegetation amount and/or health. Compared to non-vegetated surfaces, vegetated surfaces show a sharp contrast in the red and near infrared wavelengths (Bannari *et al.,* 1995; Chen, 1996). Chen (1996) described the earliest form of the vegetation index which was the Simple Ratio (SR) (Eq. 2.2).

$$SR = (\lambda_{NIR})/ (\lambda_{Red}) \quad (2.2)$$

An issue with the SR occurs when λ_{Red} values are close to zero the index values increase with no bounds (Chen, 1996). Recognizing this led to the development of the Normalized Difference Vegetation Index (NDVI). The NDVI (Eq. 2.3) resolves the issue by normalizing the difference between λ_{NIR} and λ_{Red} using the sum and the difference of both values.

$$NDVI = (\lambda_{NIR} - \lambda_{Red})/ (\lambda_{NIR} + \lambda_{Red}) \quad (2.3)$$

The NDVI is not an inherent physical quantity of vegetation but is correlated to the physical properties of the vegetation canopy, the LAI, percent crop cover, vegetation condition, and biomass. However, the sensitivity of the NDVI to crop biophysical parameters such as LAI becomes weak in conditions beyond a threshold value of LAI, typically 2 or 3 (Carlson and Ripley, 1997). A common variation of the NDVI used in agricultural studies is the Green Normalized Difference Vegetation Index (GNDVI) in which reflectance in the green band is substituted for reflectance in the red band (Smith *et al.,* 1999; Peddle *et al.,* 2001; Bannari *et al.,* 1995) (Eq. 2.4).

$$GNDVI = (\lambda_{g} - \lambda_{Red})/ (\lambda_{g} + \lambda_{Red}) \quad (2.4)$$

where λ_g is green reflectance.

A common disadvantage of the SR, NDVI and GDVI is the influence of soil background. Huete (1988) reported that for a given amount of vegetation, darker soil substrates resulted in higher vegetation index values for the SR and the NDVI. To accommodate for soil background influences in incomplete vegetation land cover Richardson and Wiegand (1977) created the Perpendicular Vegetation Index (PVI) (Eq. 2.5).

$$PVI = (\lambda_{soil} - \lambda_{veg})^2_{Red}/(\lambda_{soil} - \lambda_{veg})^2_{NIR} \quad (2.5)$$

where $(\lambda_{soil} - \lambda_{veg})$ is the difference between the "bare soil-vegetation" reflectance in the corresponding spectral band (NIR = near infrared).

Similar to darker soil substrates, Huete (1988) found that brighter drier soils with sparser vegetation also resulted in higher PVI values. Several improvements have been made to the PVI, and better methods of accommodating for background soil have been implemented (Eq. 2.6) in the Soil Adjusted Vegetation Index (SAVI) (Huete, 1988).

$$SAVI = (\lambda_{NIR} - \lambda_{Red})(1+L)/ (\lambda_{NIR} + \lambda_{Red} +L) \quad (2.6)$$

where L is a soil adjustment factor.

Based on a simplified radiative transfer model, Huete (1988) showed that a value L= 0.16~0.5 permits the best adjustment to minimize the secondary backscattering effect of canopy transmitted soil background reflected radiation (Bannari *et al.,* 1995). Three versions of the SAVI were developed by Major *et al.,* (1990) to accommodate for wet and dry soils, and varying solar inclination angles. As a result of these improvements, and other modifications by Baret and Guyot (1991), the Transformed Soil Adjusted Vegetation Index (TSAVI) (Eq. 2.7) is now believed to be a better indicator than the NDVI for low vegetative covers, and is more sensitive to senescent vegetation than the NDVI (Bannari *et al.,* 1995).

$$TSAVI = [a(\lambda_{NIR} - a\,\lambda_{Red} - b)]/[(a\,\lambda_{NIR} + \lambda_{Red} - ab + X(1+a^2)] \quad (2.7)$$

where *a* and *b* are calculated by the "soil line" or "soil brightness vector" which is $\lambda_{NIR} = a\,\lambda_{Red} + b$, where *a* is the slope of the bare soil line, *b* is the ordinate at the origin of the bare soil line, and X=0.08 a soil effect minimization constant.

The equation of the soil line can be determined from a remote sensing image if there are enough bare soil pixels with sufficient dynamic range. If the current image being used cannot adequately provide a distinct soil line then it can be determined from a previous image of the same region with sufficient dynamic range (Bannari *et al.,* 1995). One of the main drawbacks in the "SAVI family" of indices is that a soil line must be established for each remote sensing acquisition (Rondeaux *et al.,* 1996). In an effort to create an index that was more universal, Rondeaux (1995) created the Optimized Soil Adjusted Vegetation Index (OSAVI) (Eq. 2.8). In the SAVI indices, minimization of soil background noise is done by the adjustment of parameters *X,* whereas with OSAVI,

X has been re-examined to optimize the index over a variety of soils, and for high and low vegetation cover. OSAVI also incorporates bi-directional reflectance in the NIR and red bands.

$$OSAVI = (\lambda_{NIR} - \lambda_{Red}) / (\lambda_{NIR} + \lambda_{Red} + 0.16) \quad (2.8)$$

In equation 2.8, 0.16 is a static soil adjustment coefficient that is used to minimize background noise due to soil type variation. It is quite similar with respect to performance as the TSAVI and other indices of the SAVI class. The advantage to this index is that it is a simplified formula that does not require *a priori* knowledge of the soil type. The residual variation in OSAVI due to soil is evenly spread across the range (0-1) of crop ground cover, and is therefore promoted as being an optimal vegetation index for agricultural applications (Steven, 1998). They evaluated both traditional and soil-adjusted vegetation indices using hyper-spectral remote sensing imagery. Vegetation indices have been related to several biophysical parameters such as LAI (Turner *et al.,* 1999; Wiegand and Richardson, 1990); photosynthetic activity (Mack *et al.,* 1990; Wiegand *et al.,* 1991); canopy chlorophyll content (Broge and Leblanc, 2000), biomass and yield (Thenkabail *et al.,* 1994). However, in most vegetation studies there are limitations surrounding the relationship between vegetation indices, LAI, photosynthetic activity, and yield in high LAI conditions (Wiegand and Richardson, 1990). The ratio of red to NIR approaches limiting values asymptotically as LAI increases (Wiegand and Richardson, 1984). The relationship between Vis and LAI can vary with crop stage and leaf water content (Carlson and Ripley, 1997). Hatfield *et al.,* (1985) performed a ground based remote sensing experiment on different planting dates of wheat and found that Vis saturated at a LAI above 4.0 and did not return to the pre-emergence bare soil value at senescense. Therefore, the VI to LAI relationship is not absolutely reliable later in the growing season in mature crop stages. In remote sensing agricultural applications, Vis calculated too early in the growing season do not relate well to actual crop yield because measurements do not represent the canopies' photosynthetic capacity (Wiegand and Richardson, 1990). There are also issues with Vis because the algorithms are performed on the entire pixel and do not discriminate for mixtures at sub-pixel scales (e.g. volunteer crops, weeds). Components of a pixel in

agricultural remote sensing scene may include the crop vegetation, but also shadow, background soil and residue, and other types of vegetation (e.g. weeds), all of which contribute to the overall remote sensing signal (Peddle *et al.,* 2001).

2.8 Remote sensing platforms for agricultural investigations

Remote sensing has been identified as a cost-effective technology for site specific management. This technology offers geographically extensive and continuous assessment of plants, soil and water resources, and other land surface phenomena. Selection of the best available remote sensing technology is determined in most cases by platform and sensor attributes.

Moran *et al.,* (1997) reported limitations of satellite data include restricted spectral range, coarse spatial resolution, slow turn-around time, and the inadequate repeat coverage. Satellite-based sensors have fixed spectral bands that are not applicable to project objectives and the spatial resolution too coarse to detect in-field variability. Satellite imagery varies in spectral, spatial, and temporal resolutions and is available from numerous providers. Regardless of the satellite platform/model, the spectral and spatial resolutions are set (i.e., no modifications can be made with respect to changing band or band widths). In comparison to other available satellites, AVHRR and MODIS are available at no cost, pass every 1-2 days, and have set spectral bands with coarse spatial resolutions ranging from 0.25 km to 1 km. These datasets are useful for monitoring at global, continental, and biome scales as they generate continuous seasonal and year-to-year data. In contrast, high resolution imagery from the Quickbird satellite developed and operated by Digital-Globe provides 61-cm panchromatic and 2.44-m multi-spectral images at nadir. Finally, satellite imagery requires extensive training in image acquisition, analysis, and interpretation.

Moran (1994) reported numerous disadvantages associated with SPOT, HRV, and Landsat TM satellite data for day-to-day irrigation management decisions. The study made an effort to acquire every possible SPOT and Landsat image for an entire growing season. Only 31% of the forecasted satellite data acquisition opportunities were realized. A majority of failures were due to weather conditions (i.e., cloud, cirrus, cumulus, and haze) or technical difficulties (i.e., conflicts at the receiving station, the sensor view

angle was of opposite sign with a view angle of +12º, programming errors, failure to order satellite data, sensor calibration, and atmospheric interference). Advantages of satellite imagery are repeat coverage over the same location at the same altitude, time, and orbital inclination. Another advantage is the availability of highly processed images that have been orthorectified to correct distortions resulting from the earth's curvature and rotation, satellite motion, viewing perspective, and relief displacement.

Airplanes and helicopters have the ability to collect data more frequently, which is particularly important during periods when close monitoring of pending stress (i.e., infestations and drought) is critical (Thomson *et al.,* 2005) or when disaster strikes (i.e., fires and floods). Although the type of aircraft used depends on the requirement of the data collected, fixed winged aircraft is the usual platform of choice. Many projects that require large-scale imagery over relatively small areas can be accomplished in a day with a single-engine aircraft (Falkner and Morgan 2002). Historically, the expense of data collection from manned aircraft and/or satellites has led to limited implementation, especially for real time management in natural resources and agriculture. Although the cost of satellite imagery is declining, the cost of aircraft is still prohibitive for many research projects, particularly those requiring repetitive monitoring.

A disadvantage of using airplanes is the instability of the platform that affects the exterior orientation (i.e., position and angular orientation) of the image (X_o, Y_o, and Z_o), making image rectification difficult (Laliberte *et al.,* 2008). The camera's angular rotation is expressed as omega (ω), phi (φ), and kappa (κ). This describes the relationship between the ground space coordinate system (X, Y, and Z) and the image space coordinate system (x, y, and z) (Leica Geosystems 2005). Rotation about the camera axis results in distortions in the image
and image coordinates (Laliberte *et al.,* 2008). These distortions increase from the center and out towards the image perimeter (Laliberte *et al.,* 2008). In addition, the orthorectification and mosaicing of multiple aircraft images requires an overlap of 60% along the flight line and a 20%-30% sidelap along parallel strips or flight lines (Laliberte *et al.,* 2008). The required distance between flight lines is dependent on the camera view angle and the altitude above ground level (Jensen 1996). Flying at lower altitudes produces higher resolution images but this requires more flight lines and

processing in comparison to operations flown at higher altitudes and this can be a disadvantage (Jensen 1996).

RPVs and UAVs are increasing popular alternatives to satellite and manned aircraft. Other terms that have been used to describe remotely controlled platforms include, Unmanned Vehicle Systems (UVS), Automatically Piloted Vehicles (APV), Remotely Operated Aircrafts (ROA), pilotless airplanes, Remote Controlled airplanes (RC-airplanes), model airplanes, and drones (Eisenbeiss 2004). The name UAV covers all vehicles capable of programmable flight patterns and operated without human intervention (Eisenbeiss 2004).

RPVs and UAVs provide an effective, low cost alternative to traditional platforms for acquiring high-resolution images (5 cm – 30 cm pixel size) at relatively low costs (Laliberte *et al.,* 2008). Unlike satellite and high altitude photography (4,000 m – 6,000 m above ground level), high spatial resolution imagery from RPVs and UAVs provide differentiation of vegetation and landscape features necessary to classify, map, and monitor ecosystem changes at the local and regional levels. These systems share the same orientation challenge as airplanes, to a greater extent, because they are considerably smaller in size and are more susceptible to wind effects (Laliberte *et al.,* 2008).

Low-cost, high-resolution digital photography from RPVs and UAVs have been used in identifying root-rot fungus infection in Douglas fir (Pseduotsuga menziessi) to evaluate vineyard health (Johnson *et al.,* 2002), coffee bean ripeness (Johnson *et al.,* 2002), nutrient status of corn and crop biomass of corn, alfalfa, and soybeans, yield estimation in citrus (MacArthur *et al.,* 2005), and for weed mapping.

Hand-held sensors are the easiest type of sensor to deploy. These sensors can be held with the hand (Roanhorse *et al.,* 2009) or fixed to a handheld mast. Disadvantages of hand-held sensors include time consuming data collection; site accessibility limitations (i.e., dense vegetation, lack of roads, and flooded areas) (Rango *et al.,* 2006); and disturbances to the study area.

Over the past four decades, scientists have developed various motorized ground-based sensor systems and booms (Rundquist *et al.,* 2004). These technologies provide very high spatial and taxonomic resolutions on small spatial scales and are commonly used to ground truth aerial data (Rango *et al.,* 2006). Booms were developed and

utilized in several recent studies (El-Shikha *et al.,* 2007) that measured reflectance at specific bands with the sensors carried through the field by tractors and center pivot or linear move irrigation systems. Spectral data collection with motorized booms is more systematic than hand-held sensors because they maintain constant elevation and sensor orientation (Rundquist *et al.,* 2004).

Selection of the remote sensing technologies is determined, in most cases, by platform and sensor attributes (i.e., cost, efficiency, flexibility, payload capacity, spatial coverage, and spatial, spectral, and temporal resolutions). If these attributes can be quantified, then a multi-objective analysis may be performed to assess quantitatively the tradeoffs between different sensor and platform attributes, identifying the best overall technology. We present pioneering work by applying multi-objective analyses to remote sensing technology selection. Experts were surveyed to identify the best overall technology at three different pixel sizes: very fine (<5 cm), fine to moderate (0.5 m – 1.0 m), and moderate to coarse resolutions (0.1 km – 1.0 km). Platform/sensor technologies (Table 2.1) included hand held sensors and booms in Group 1; RPVs, UAVs, and manned aircraft in Group 2; and Quickbird, Landsat, AVHRR, MODIS, ASTER, and SPOT in Group 3. The platform attributes considered in identifying the best overall technology were system and data costs, efficiency, flexibility, payload capacity, spatial coverage, and spatial, spectral, and temporal resolutions (Roanhorse *et al.,* 2009). Fig 2.2 shows several types of remote sensing platforms in agriculture.

Table 2.1 List of remote sensing technologies

Group 1	Group 2	Group 3
A_1 = automated booms	A_4 = RPVs	A_7 = Quickbird
A_2 = hand held sensors	A_5 = UAVs	A_8 = Landsat
A_3 = embedded on vehicles (Tractors, Combines and Implements)	A_6 = manned aircraft	A_9 = AVHRR
		A_{10} = MODIS
		A_{11} = ASTER
		A_{12} = SPOT

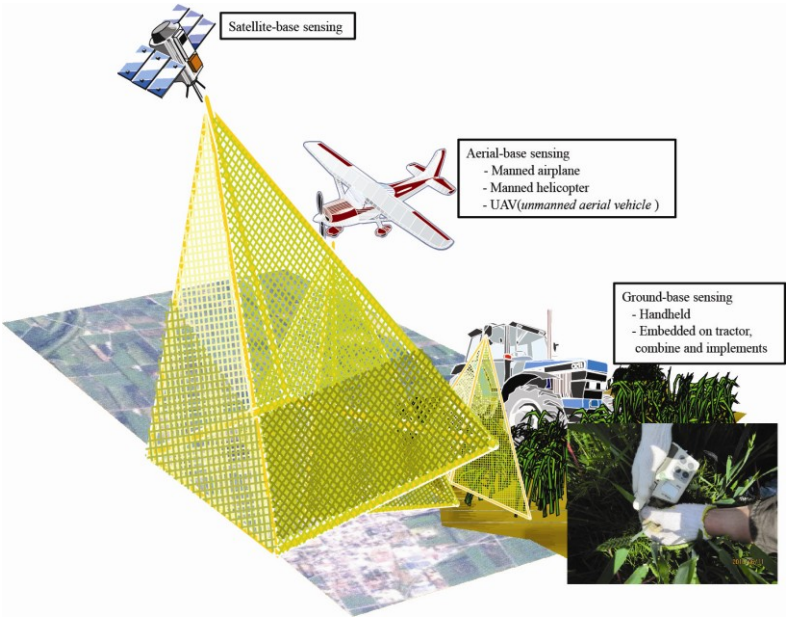

Fig. 2.2 Remote sensing platforms in agriculture

2.9 N-sensors

There are many commercial types of N-sensor in the market. These N-sensors can be classified in two groups; Contact-type such as SPAD meter and Remote-type such as passive N-sensor. On the other hand the Remote-types included passive and active sensor, which passive type works based on natural light reflectance while the active-type uses Laser diodes light source, which can be available even in the night with very little effect by sunlight intensity and direction.

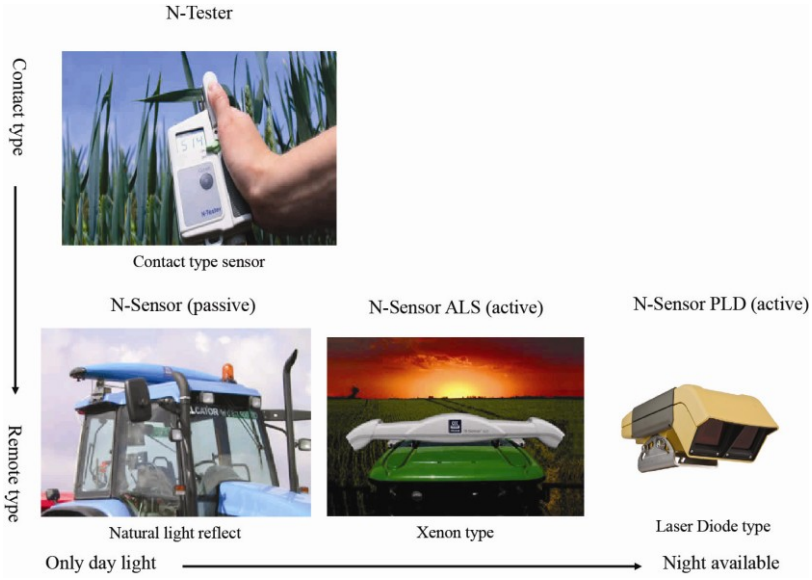

Fig. 2.3 N-sensors for crop monitoring

CHAPTER 3

FIELD EXPERIMENTS AND MEASURMENTS

3.1 Experimental field

An experimental winter wheat field (Fig. 3.1) was conducted in the farming area of Hokkaido University (43° 4' N 141° 20' E). A conventional variety "Kitahonami" of winter wheat in Hokkaido was cultivated in three consecutive years. According to the map (Fig 3.1) in 2010 and 2012 the field was in south side but in 2011 it shifted to the north part as a rotation. Dimensions of this field were 40 m x 120 m. The field was divided into 8 areas (blocks) and 0, 30, 60, and 90 kg ha^{-1} fertilizer (ammonium nitrate) was applied with two repetitions at the regrowing stage, so that the difference of the growth condition can be appeared (Fig. 3.2). After the bloom stage, growth investigation was done. Reflectance data by using a Spectroradiometer (Field Spec 3), SPAD value, and height of crop, number of stem, nitrogen content and protein content of wheat ear was taken from target points as reference area which was randomly set in the field.

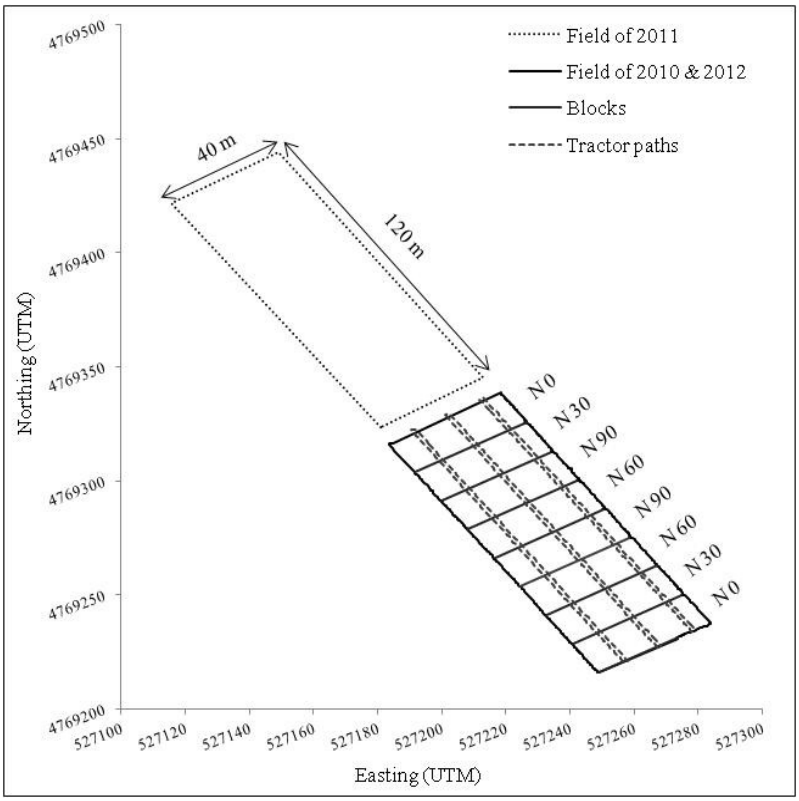

Fig. 3.1 Map of experimental field including blocks (different fertilizer), tractor paths for using remote sensing and two different places in three years

Fig. 3.2 A photo of experimental field on 2011 that difference of growth condition after additional fertilizer can be recognized

3.2 SPAD value measurments

Chlorophyll content of the leaf is an important parameter for plant physiologists and agriculturists; it is used as an indicator of leaf senescence and nitrogen status of plants and can be altered in response to environmental stresses. There are methods now that are able to determine approximate chlorophyll content in the leaf non-destructively, using a measurement of the leaf transmittance (T) at certain suitable wavelength(s). Several instruments based on this principle are now available including a SPAD-502 chlorophyll meter (Konica Minolta Sensing, Japan). This chlorophyll meter measures intensity of light transmitted through the leaf sample at two wavelengths (650 and 940 nm) using light emitting diodes with approximate halfwidth of the emission spectrum of

15 and 50 nm, respectively. The display shows a value M in relative SPAD units (Jan Naus 2010).

The quantity M is defined as (Eq. 3.1):

$$M=k.[log(I'(949)/I(940))-log(I'(650)/I(650))]+C= k.[log\ T(940)-log\ T(650)]+C \quad (3.1)$$

where $I(650)$ and $I(940)$ are signals without the sample and $I'(650)$ and $I'(940)$ signals with the sample and log is a common logarithm. The quantity k (a confidential proportionality coefficient) defines the relative SPAD units, and C is the compensation value adjustable in the instrument software. For practical usage it is supposed that the negative common logarithm of the transmittance T at 650 nm related to that at 940 nm is proportional to the chlorophyll content. In each individual experiment, the reading of the SPAD- 502 chlorophyll meter should be calibrated for the real chlorophyll content in the leaf as their relationship can differ among species or cultivars as well as among plants grown under different conditions. Also the producer declares that SPAD reading can vary in dependence on the leaf type.

Fig. 3.3 SPAD merer that measures SPAD value

3.3 Plant nutrition sensor

CropSpec (commercialized by TopCon) is a real-time integrated plant nutrient monitoring and application system for agricultural equipment. CropSpec is a powerful crop canopy sensor system utilizing two sensors that allow an operator to monitor plant conditions and apply fertilizer and other inputs only as needed. This system will help revolutionize and simplify variable rate applications. CropSpec sensors measure spectral reflectance using light from pulsing laser diodes (PLD) focused on the plants. The reading can be correlated to measure chlorophyll content, which is closely linked to nitrogen in the plants. Scanning the crop creates a map to indicate relative canopy vigor. The information can then be analyzed to determine crop areas that need treatment, construct prescription maps for later application, or immediately provide variable rate applications in real-time. CropSpec allows farmers to perform real-time analysis of crop needs and meet those deficiencies immediately as they are traveling through the field. The sensors measure nitrogen levels and controller executes that prescription immediate controlling the output of fertilizer in one pass. This provides the benefits of a variable-rate application in a simple one-step process, reducing the complications. And can reduce both cost and waste associated with blanket fertilizer applications. The compact system mounts on the tractor roof out of harm's way, eliminating the need for a boom mounted sensor, reducing the potential for sensor damage as the machine is operating within the field.

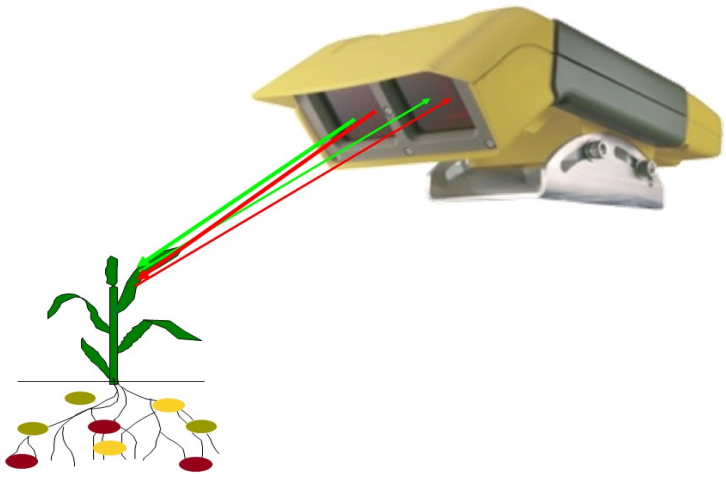

Fig. 3.4 CropSpec as a N-sensor can measure nitrogen content using PLD

3.4 Spectroradiometer

In this study a high-resolution spectroradiometer, FieldSpec3 (FS3) was used to take the spectral data. FS3 is a hyper spectral sensor designed to collect data on solar radiance, irradiance, and reflectance. It can measure the spectral reflectivity within the range of 350 nm to 2500 nm with sampling intervals of 1.4 nm and 2 nm in the ranges of 350-1050 nm and 1000-2500 nm, respectively (2150 wavelengths in total). The wireless connection allows for remote control of data collection up to 50m away. It is designed for field environment remote sensing to collect solar reflectance, radiance and irradiance measurements. A notebook computer was used to acquire data for the control of FS3 in which special software was installed. In addition, the fiber cable 1.5m measurements from various angles are possible. Viewing angle is a 25° standard, by mounting the lens can be adjusted 1°, 3°, 8°, to 10°. In this study, the viewing angle was set to 25 degrees. When the height of sensor was 150 cm above from the ground, the detection area is about 0.4 m^2. In addition, for providing the reference data of the background light data a solar sensor were used. The calibration was done using a standard white board immediately before measuring reflectance value. Figure 3.5 shows the appearance of the FieldSpec3 (Su, 2013).

Fig. 3.5 Spectroradiometer 3 (field spec 3) (Analytical Spectral Devices, Inc., USA)

3.5 Solar sensor

Due to high spectral resolution of the spectraradiometer is sensitive to the light changes, even the slight changes of the background light would result in great change of the measured result. Therefore, it is necessary to know the amount of ambient light at the time of getting radiation data for correcting the radiation data. PCM-01, a sensor for measuring the total amount of solar radiation with high accuracy, reliability, sensitivity, was used in this study. Solar radiation sensor was used to detect solar radiation data corresponding with FS3. It has a high sensitivity to the wave length range of 305 nm to 2800 nm. Light intensity was output using analog signal. In this study, it was connected to the computer using an analog-to-digital converter and RS232/USB converter (Fig 3.6) (Su, 2013).

Fig. 3.6 solar sensor

3.5 Positioning data

Position information of the sampling data is significant for the spatial change analysis. In this study, a dual-frequency RTK-GPS receiver system, Trimble's MS750™ was equipped in the sensor system to provide the location information for the corresponding radiation data. The MS750 sets a new standard for dynamic positioning by providing 20 mm (1") accuracies, 20 times per second with a latency of less than 20

milliseconds. At higher latencies, the MS750 provides positions of 10 mm (0.5") 5 times per second (Fig. 3.7). To provide the reference signal to the MS750TM, a PDA using DOCOMO net was used in this study. The longitude and latitude data is converted to the UTM (Universal Transverse Mercator) coordinate system and then assigned to the spectral data; finally, the spatial data was processed through ArcGIS (Su, 2013).

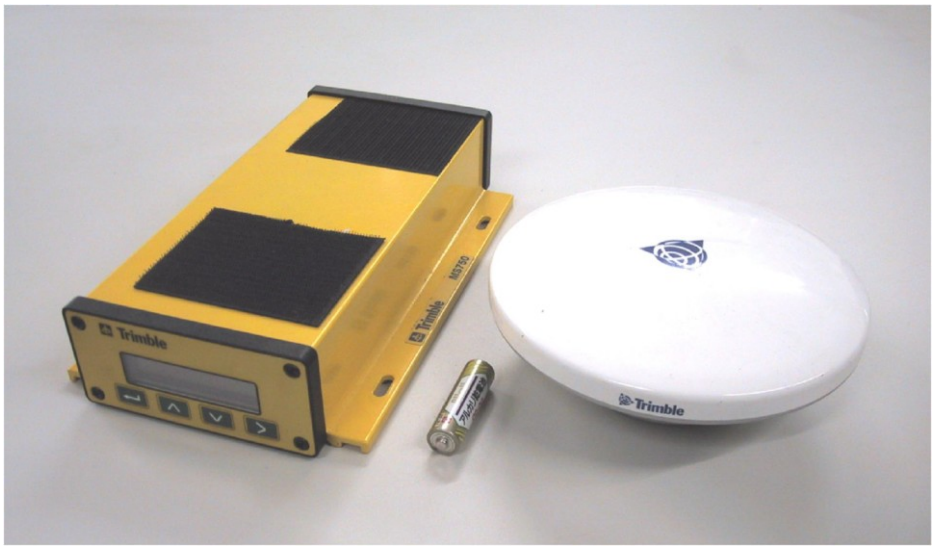

Fig. 3.7 GPS Receiver (MS750 Trimble) and Antenna

CHAPTER 4

PERFORMANCE EVALUATION OF PLANT NUTRITION SENSOR

4.1 Introduction

Remote sensing, using passive sensor systems (imagery or spectral radiometers), has long been advocated as a way to characterize spatial variability in fields. Passive sensors detect irradiance (incoming radiation) and canopy radiance (reflected radiation) through self-calibration using sensors facing upwards and downwards (Stamatiadis *et al.,* 2010-a). Recent advances in precision agriculture technology have led to the development of ground-based active remote sensors (or crop canopy sensors) that calculate normalized difference vegetation index (NDVI) readings. Previously, this index was determined using passive sensors via airborne or satellite imagery, which had several limitations, including expense and weather-related issues such as cloud cover, narrow time window for operation (around solar noon), and bidirectional reflection issues associated with solar angle, that could greatly limit the effectiveness of these sensing techniques, while active sensors have their own source of light energy and allow for the determination of NDVI at specific times and locations throughout the growing season without the need for ambient illumination or flight concerns (Shaver *et al.,* 2011). Plant reflectance is affected by leaf surface properties, internal structure, plant stress, and the concentration and distribution of biochemical components; therefore, analysis of reflected light may be used to assess plant biomass and the physiological status of a plant (Penuelas and Filella 1998). Wavelengths in the red (*R*) and near-infrared (NIR) wavebands are frequently used for indirect measurements of plant characteristics (Wood *et al.,* 2003). In a study by Raun *et al.,* (2001), a vegetation index ratio (NIR/R) was most sensitive to high crop biomass production in corn (Zea Mays L.) and soybean (Glycine max L.), but during early vegetative growth (e.g., Zadoks scale in winter wheat growth stages (Zadoks *et al.,* 1974): growth stage (GS) 25 in winter wheat), an NDVI, Eq. 4.1, has been shown to provide more accurate estimates of biomass.

$$NDVI = (NIR - Red) / (NIR + Red) \tag{4.1}$$

Research has shown that expected yield determined from NDVI had a strong relation with actual grain yield in winter wheat ($R^2 = 0.83$) and that NDVI is useful for estimating grain yield in certain crops (Inman *et al.,* 2008). The sensor-determined

green-NDVI [= (NIR – Green)/ (NIR + Green)] could potentially be used to direct in-season N applications. However, because passive sensor systems rely on natural sunlight, their effectiveness for assessing canopy N status is limited by numerous factors mentioned previously (Solari *et al.,* 2008).

Recently, commercialized active ground-based sensors have eliminated the need for frequent calibration and have overcome the problems of cloud cover and limitations of the time of day when measurements can be made (i.e., natural illumination and shadows). This is achieved by generating modulated (pulsed) light from an auxiliary light source so that the active sensors can operate equally well under all lighting conditions (Stamatiadis *et al.,* 2010-a; 2010-b). Active remote sensing has shown some potential for improving nitrogen-use efficiency (NUE) in winter wheat. The grain yield potential could be estimated using an active remote sensor by calculation of NDVI from mid-season (Feekes growth stages 4-6 in winter wheat). Use of the number of growing-degree days (GDD) from the day of planting to the day of sensing as a standardizing factor for NDVI resulted in regression models that could be applied for crop measurements across the growth season. However, these models could not account for conditions arising after sensing because the reflectance was measured in the middle of the growth season (Inman *et al.,* 2007). On the other hand, Solari *et al.,* (2008) reported that canopy assessments using the GreenSeeker (NTech Industries, Ukiah, CA) active sensor, which generates its own source of modulated light in the red (~650 nm) and NIR (~770 nm) bands to calculate NDVI, could be used to direct variable rate N applications to wheat and improve fertilizer NUE. Despite the positive results obtained using the GreenSeeker for wheat, little work has been conducted to date using active sensors to assess corn N requirement during the in-season application window, beginning at early vegetative growth (V8) and proceeding through silking (R1). Shanahan *et al.,* (2008) used GreenSeeker to assess canopy N status during this window is problematic because of the high vegetation fraction (i. e., area ratio of vegetation and the defined area, such as a pixel) normally present during this time and the associated problems of using red light to assess canopy N status. For this reason, Solari *et al.,* (2008) chose to work with the Crop Circle ACS-210 active sensor manufactured by Holland Scientific (Lincoln, NE) as a tool for assessing corn N status. The Crop Circle sensor measures canopy reflectance in the NIR band (centered at 880 nm) and the VIS band (centered at 590 nm,

near the green reflectance peak). In this study, the potential of the plant nutrition active remote sensing instrument was evaluated by comparison with the passive sensor for predicting spatial variation of the crop growth condition in winter wheat (Triticum aestivum L.). Specific objectives of this study were (a) to install and introduce a ground-based remote sensing system for monitoring winter wheat growth status and (b) to evaluate and verify the performance of installed system by regression models that estimate crop characteristics.

4.2 Material and Methods

4.2.1 *Field Experiments*

Field experiments were conducted in June-July 2010 in the farmland of Hokkaido University (43° 4' N 141° 20' E), Sapporo, Japan with annual average precipitation of 1106.5 mm and with minimum temperature (-7 ºC) in January and maximum temperature (26.4 ºC) in August. The field dimension was 40 m × 120 m and the field was divided into eight areas as blocks. Four levels of fertilizer (N as ammonium nitrate) 0, 30, 60 and 90 kg ha^{-1} with two repetitions, were applied at the reviving growth stage (GS 30) (Zadoks *et al.,* 1974) to create a range of crop growth conditions. Twenty random target points in the field with at least two target points in each block were set as ground reference areas with three lines for tractor travel. A map of the field including the eight blocks and different amounts of fertilizer is shown in Fig. 4.3-a.

4.2.2 *System Platform*

A tractor was used as a platform for the sensors (Fig. 4.1). This system included an RTK-GPS, a solar sensor, two plant nutrition sensors (CropSpec^{TM}) and a laptop PC. The RTK-GPS consists of a GPS device and a cellular phone to compensate the GPS signal. The RTK-GPS acquired Universal Transverse Mercator (UTM) coordinates with an error of +/-2 cm. As shown in the schematic diagram of the system in Fig. 4.1, the positioning data from the GPS device and the cellular phone via a GPS convertor as well as the reflectance data from the CropSpec sensors in both sides of the cabin are transmitted to the PC via a CAN BUS communication. An algorithm was programmed

to receive and save both GPS data and reflectance data of the CropSpec. Data from the solar sensor were used to correct reflectance data from the passive sensor.

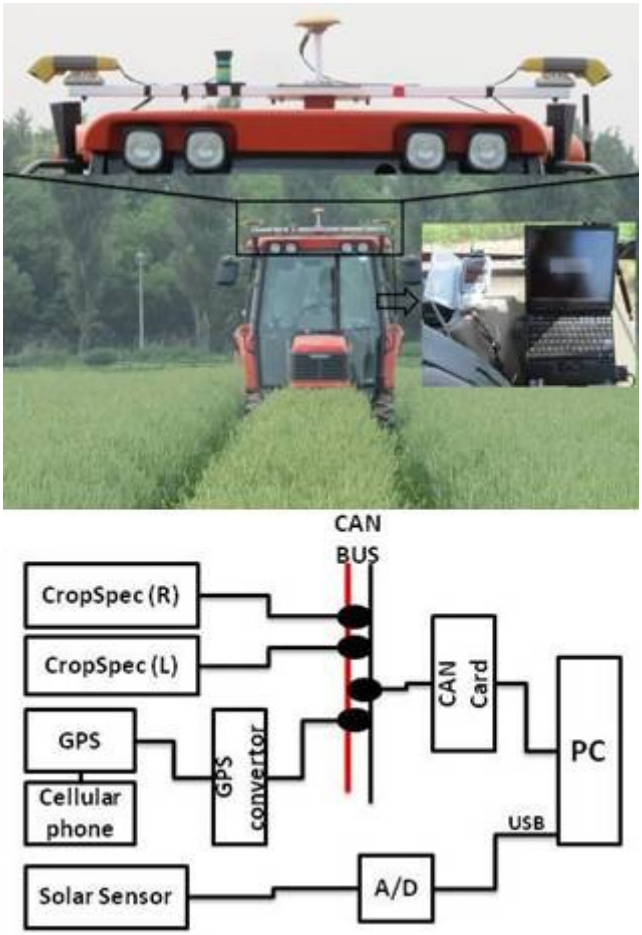

Fig. 4.1 Photograph showing the tractor in the field which two CropSpec, solar sensor, and GPS antenna were mounted top of cabin. PC, CAN BUS and cellular phone were put in inside of cabin. The schematic diagram shows the communication in developed system.

4.2.3 *Data Collection and* devices

CropSpec as explained in section 3.3 is an active sensor monitoring and application system for agricultural equipment that was developed in cooperation with Yara International. The sensors were mounted on the cabin roof (Fig. 4.1) at a height of 230 cm from the ground and with a 1 m × 3 m footprint for crop scanning. The specifications of CropSpec are shown in Table 4.1. CropSpec uses pulsing laser diodes (PLD) for sensing by using two different wavelengths on red edge (735 nm) and

infrared (808 nm) bands. The sensor measures plant reflectance to determine the chlorophyll content based on reflectance, which is closely related to the nitrogen

Table 4.1 Specification of CropSpec

Environment	IP 67 compliant
Laser safety	Class 1 or Class 1M
Physical Dimensions	200 mm x 80 mm x 80 mm
Viewing angle	45°~ 55°
Operating Temperature	0 ~ 60 °C
Operational wavelength	Red (730 ~740 nm) and NIR (800 ~ 810) nm
Supply voltage	10 - 32 VDC
Supply current	5A

concentration in leaves. It measures the nitrogen levels and, through a variable rate control (VRC) program, controls the output of fertilizer in one pass over the crop.

Canopy spectral reflectance was measured using a portable spectroradiometer, FieldSpec®3 (FS3) (Analytical Spectral Devices, Inc., USA), from 10 am to 2 pm under cloudless conditions (as described in 3.4). A PC was used to acquire data for the control of FS3 in which special software was installed. The viewing angle of FS3 was set at 25 degrees and the height was 150 cm from the ground. In each target point, an area of 1 m × 3 m in size was covered with five repetitions. Calibration was done using a standard white board immediately before measuring the reflectance value.

A soil plant analysis development (SPAD) meter (MINOLTA Co. LTD.) determines the relative amount of chlorophyll present in plant leaves by measuring the absorbance of the leaf in two wavelength regions of red and near-infrared. According to the catalogue of the SPAD-502 meter (www.konicaminolta.eu 2011), there is a close relationship ($R^2 > 0.9$) between SPAD value and leaf nitrogen concentration, and it has therefore been widely used for detecting crop chlorophyll and nitrogen content and for the guidance of plant health and use of additional fertilizer (Zhang *et al.,* 2003).

After the flag leaf stage (GS 37), growth investigations including measurements of SPAD values and heights of crops at four growth stages (GS 37, GS 39, GS 45, and GS 60) across the growth season were performed, and values were averaged in the same target points (1 m × 3 m area) from leaves of ten different plants. Reflectance data obtained both from CropSpec and the spectroradiometer (FS3) were collected from the same target points. Crop samples from the target points were taken and dried in an oven

at 75 ºC for 48 h, and the nitrogen content of wheat was measured using 50 g of powdered samples including leaves and stems. Protein content and yield of grain were also measured after harvesting and threshing a 1 m × 3 m area in each reference point.

4.2.4 *Data Analysis*

Reflectance data from CropSpec were used to calculate the Nitrogen Sufficiency Index (S1 value, Eq. 4.2). The average of S1 values obtained from both the right side sensor (C_r) and the left side sensor (C_l) in the round passing was used.

$$S1\ value = (NIR/Red - 1) \times 100 \tag{4.2}$$

In order to compute green-NDVI (GNDVI), amber-NDVI and red-NDVI, four wave bands, 550 nm, 590 nm, 660 nm and 800 nm (Solar *et al.,* 2008; Li *et al.,* 2010; Thomason *et al.,* 2010; Shaver *et al.,* 2011), were used for green, amber, red and NIR, respectively. Fig. 4.2 shows averaged spectral measurements at four different times during the growth season. As shown in the Fig. 4.2, the trends of variations in spectral data in the four measurements were similar, though the amount of reflectance in two last stages (GS 45 and GS 60) was generally higher than the first two measurements. In the visible wavelengths, reflectance was less than 20%, but it increased dramatically in the NIR region until about 70%. This means that the absorbance of spectra in the visible region was higher than that in the NIR region. In other words, the crop has reflected most parts of NIR wavelengths and it can be a criterion for investigation of crop conditions. In the calculation, those reflectance data acquired by FS3 that were more than 100 percentage of reflection, because of noises or absorption by the atmosphere, were removed (Fig. 4.2).

The in-season estimation (INSE) for reflectance measurements, height of crop, and SPAD value were calculated by dividing each measured parameter by the number of days from early April to the sensing date, when the growing degree days (GDD) were greater than zero (Stone *et al.,* 1996). GDD were calculated by the method described by Dwyer *et al.,* (1999). According to weather and climate information obtained from the Japan Meteorological Agency (www.jma.go.jp 2011), average daily temperature in

early April in Sapporo was around 4-6 ºC, and GDD were therefore calculated from the first day of April to the sensing day. They were 72, 83, 91 and 106 days for GS 37,

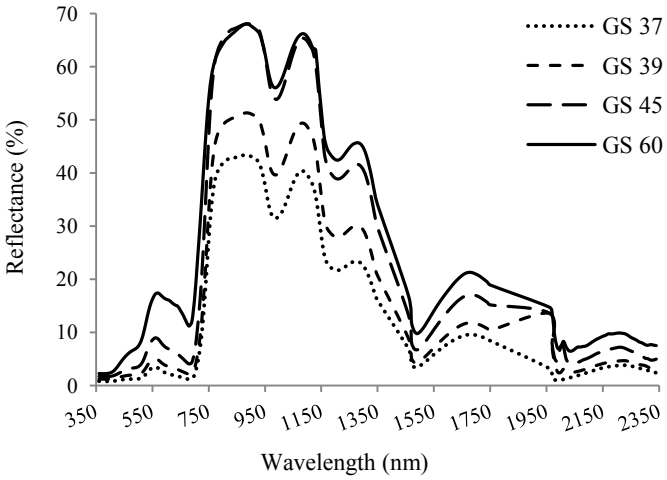

Fig. 4.2 Reflectance measurments in four different growth stages use of spectroradiometer (FS3).

GS 39, GS 45 and GS 60, respectively. The in-season estimated yield (INSEY) is an estimation of the rate of accumulated biomass from the day of crop planting to the day of active remote sensing (Stone *et al.,* 1996), and limiting the denominator to days on which GDD were greater than zero (GDD>0) ensures that only days in which plant growth was possible are used.

Using the mean reflectance of a well-fertilized area with a higher level of nitrogen, the NDVI ratio (Inman *et al.,* 2007; Thomason *et al.,* 2010) was calculated by Eq. 4.3. This ratio is similar in concept to the nitrogen reflectance index (NRI) proposed by Bausch and Diker (2001).

$$\text{S1 value ratio} = \frac{\text{S1 value of an interest area}}{\text{S1 value of the rich nitrogen strip}} \tag{4.3}$$

S1 values of the nitrogen-rich strip were 64.3, 58.7, 47 and 11.8 for GS 37, GS 39, GS 45 and GS 60, respectively.

The performance of the model was evaluated by comparing the differences in the coefficient of determination (R^2) and root mean squared error (RMSE) of prediction. Larger R^2 and smaller RMSE indicate greater precision and accuracy of the model for predicting plant nitrogen concentration (PNC) (Li *et al.,* 2010). RMSE was calculated using Eq. 4.4:

$$RMSE = \sqrt{\frac{1}{n}\sum_{i=1}^{n}(y_i - \hat{y})^2} \tag{4.4}$$

where y_i, $\hat{y}$ and n are the measured values, predicted values and number of samples, respectively. For investigation of variations in the field, Arc Map 9.3 (ESRI, CA, USA. 2008) was used to make a map for several measured parameters.

4.3 Results and Discussion

An overview of the measured crop biophysical parameters in the twenty points of the field is shown in maps that were interpolated using kriging by ArcMap9.3 software (Fig. 4.3). Kriging is an advanced geostatistical procedure that generates an estimated surface from a scattered set of points with z-values. Unlike other interpolation methods supported by ArcGIS Spatial Analyst, kriging involves an interactive investigation of the spatial behavior of the phenomenon represented by the z-values before selecting the best estimation method for generating the output surface (Oliver 1990). In this study, the ordinary method of kriging with several models was examined during the processing, and an exponential model was finally fitted for all of measured crop biophysical parameters with 95% of probability and 0.5 of lag size. The maps clearly show that the aggregation of each factor was almost in the middle of the field. Indeed, this area was subjected to application of the largest amount of fertilizer (Fig. 4.3-a). Fig. 4.3-a and Fig. 4.3-d indicate that the S1 value and nitrogen content varied similarly across the field, and there was a high correlation (R^2>0.77) between these factors that also presented in Table 1. Also, a comparison shows a high level of similarity in Figs. 4.3-b, 3-c and 3-e, and there was a close relationship between SPAD value and height of the crop

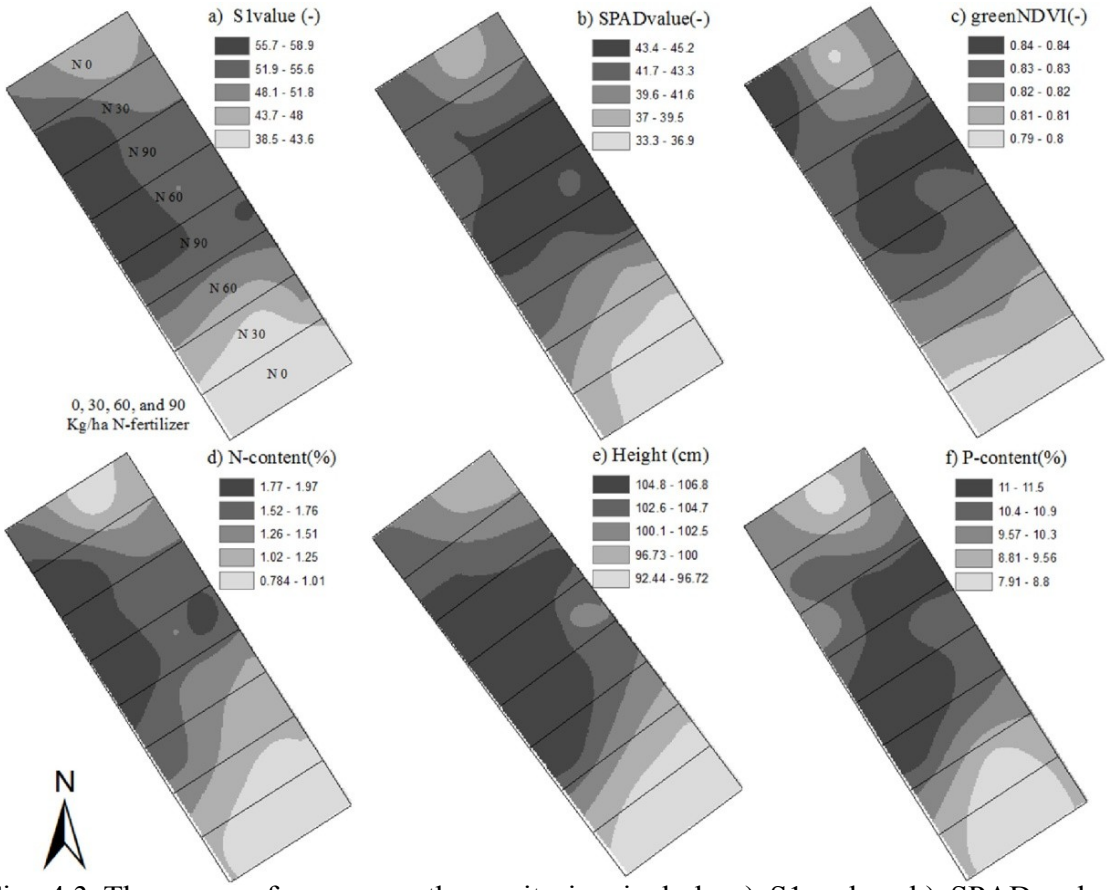

Fig. 4.3 The maps of crop growth monitoring include a) S1 value, b) SPAD value, c) green NDVI, d) Nitrogen content e) Height of crop, and f) Protein content which maps of S1 value, height of crop, and SPAD value were made according to data of second measuring stage (GS 39).

(R^2=0.82) in the second stage of measurement. Moreover, SPAD values at the four measurement times (GS 37, GS 39, GS 45 and GS 60) and nitrogen content measured at the first time (GS 37) indicated correlation of 0.76, 0.91, 0.68 and 0.63, respectively. Hence, because of a) these high relationships, b) lack of other measurements of nitrogen content and also c) close relationship ($R^2 > 0.9$) between SPAD value and leaf nitrogen concentration (according to the SPAD meter technical catalogue mentioned above), the SPAD value was used for comparison with the S1 value instead of nitrogen content in four different measurement period of crop growth. Fig. 4.3-c shows that green-NDVI use of passive sensor (spectroradiometer in this study) has the potential to predict nitrogen content, though a comparison with Fig. 4.3-d shows that it is not as good as S1 value (Fig. 3-a) prediction. Fig. 4.3-f shows that the quality of grain yield was directly related to distribution of N fertilizer and areas rich in N fertilizer, therefore had higher

quality than that of areas with little N fertilizer. However, a large area in the southern side of the field and some parts in the northern side had low values of nitrogen content and other parameters. According to the amount of additional fertilizer, it is understandable that there was a strong relationship with amount of fertilizer in each block (Fig. 4.3-a), although the maps pointed out that there was some impact of other factors that modified the patterns due to application N rates.

The means and standard deviations of the investigated crop variables including S1 value, SPAD value, height of the crop (H), nitrogen content (N), protein content (P), and grain yield are shown in Table 4.2. A linear regression model [$Y= \beta_0 + \beta_1$ (S1 value)] was used to investigate and estimate the relationship between field measurements (ground truth data) and crop scanning with CropSpec (S1 value). The results indicated that the coefficients of the linear regression model to estimate crop variables by the S1 value were mostly significant at the 0.01 probability level (Table 4.2). This included the SPAD value and height of the crop, which were measured four times during the growth stages, and the nitrogen content of wheat measured in the first stage (GS 37) of data collection, as well as protein content and yield of grain measured after harvesting. Higher correlations (R^2>0.70) were generally observed in the second stage (GS 39), although yield had a stronger relationship at GS 45 (Table 4.2). The generally high R^2 and low RMSE for predicted values such as SPAD value (0.74 and 1.81, respectively), height of the crop (0.75 and 2.3), and especially nitrogen content (0.77 and 0.2) revealed that spectral measurements by CropSpec can be used to monitor crop status. Accordingly, information on the crop condition is necessary to make a decision about additional fertilizer. Because, SPAD value is a strong detection of chlorophyll content and nitrogen concentration present in leaves. It also is a primary indication for plant health and decision about the use of additional fertilizer (Zhang *et al.,* 2003).

Therefore, the existence of a strong correlation (R^2=0.74) between S1 value and SPAD value, which verifies the goodness of the nitrogen content and crop health situation, will be a guideline for use of appropriate plant nutrition and protection. Weak relationships were observed at GS 60, possibly because, the developing grain obscured the leaves and some of the leaf N content moved to the grain.

With the development of precision farming and use of remote sensing systems in the field, the quality of production has been considered in the most studies simultaneously. One of the main parameters for evaluating the quality of wheat is amount of protein in the grain after harvesting, which can be increased by additional N applied during the growth season. Consequently, a strong relationship between S1 value and grain protein will help us to make a decision for improving crop quality during the growth season.

Table 4.2 Mean and standard deviation of S1 value , SPAD value, height of crop (H), nitrogen content (N), protein content, and yield with coefficients of linear regression model, coefficient of determination (R^2), root mean squared error (RMSE) for predicted values and significant situation in linear regression

	Mean	Std. Deviation	Linear Model		R^2	RMSE	Sig.
			β_0	β_1			
S1-GS 37	55.15	7.89	-	-	-	-	-
SPAD-GS 37	41.89	3.24	25.77	0.29	0.51	2.33	**
H-GS 37	83.68	4.13	61.07	0.41	0.61	2.65	**
N-GS 37	1.37	0.41	-1.04	0.04	0.70	0.23	**
Protein	9.99	1.16	3.33	0.12	0.68	0.68	**
Yield	7510	837	4862	48	0.21	767	*
S1-GS 39	50.18	6.37	-	-	-	-	-
SPAD-GS 39	40.97	3.46	17.48	0.47	0.74	1.81	**
H-GS 39	100.3	4.48	70.98	0.61	0.75	2.30	**
N-GS 37	1.37	0.41	-1.47	0.06	0.77	0.20	**
Protein	9.99	1.16	2.31	0.15	0.71	0.64	**
Yield	7510	837	4792	54.2	0.17	783	ns
S1-GS 45	41.58	4.69	-	-	-	-	-
SPAD-GS 45	36.94	3.70	17.25	0.47	0.36	3.03	**
H-GS 45	102.6	4.39	75.51	0.64	0.72	2.38	**
N-GS 37	1.37	0.41	-1.12	0.06	0.47	0.30	**
Protein	9.99	1.16	2.97	0.17	0.47	0.87	**
Yield	7510	837	2791	113.5	0.41	663	**
S1-GS 60	11.54	1.35	-	-	-	-	-
SPAD-GS 60	11.37	1.59	13.33	-0.17	0.02	1.62	ns
H-GS 60	102.8	4.33	7.44	0.64	0.28	3.77	*
N-GS 37	1.37	0.41	2.17	-0.07	0.05	0.41	ns
Protein	9.99	1.16	14.17	-0.36	0.18	1.08	ns
Yield	7510	837	8530	-88.8	0.02	851	ns

ns. Not significantly different at the 0.05 probability level for coefficients of linear regression model

* Significantly different at the 0.05 probability level for coefficients of linear regression model

** Significantly different at the 0.01 probability level for coefficients of linear regression model

S1 value rate is another parameter to describe relationship between ground truth data (crop variables) and CropSpec measurements (Eq. 4.3). By fitting linear functions (Table 4.3), the S1 value ratio explained 66% and 53% of the variation in nitrogen content and grain protein, respectively. The exponential fitting had the greatest (R^2 =0.7, Table 4.3) explanation for variation in nitrogen content. In general, nitrogen content and protein content increased steadily with increase in the S1 value ratio up to 1. Similarly, Bausch and Diker (2001) found that the nitrogen ratio index (NRI) was an excellent predictor of nitrogen sufficiency in irrigated maize. According to Table 4.3 non-linear regression work well to predict crop variables compare than linear regression. However, because of interference from soil background (i.e., NIR scattering by the soil surface), the ability to use NRI to estimate N sufficiency was restricted to growth stages later than the GS 37 crop growth stage. Therefore, our aim was to acquire canopy reflectance measurements in this study between crop growth stages (GS 37 to GS 60) in winter

Table 4.3 Regression model, regression function, coefficient of determination (R^2), root mean squared error (RMSE) for predicted values (nitrogen content ($\hat{N}$) protein content ($\hat{P}$) grain yield ($\hat{Y}$)) and significant situation of model coefficients

Model	Regression function	R^2	RMSE	Sig.
Linear	$\hat{N}$ (%) = -1.05 + 2.82 x*	0.66	0.23	**
	$\hat{P}$ (%) = 4.14 + 6.83 x	0.53	0.71	**
	$\hat{Y}$ (Mg ha^{-1}) = 4139.65 + 3887.01 x	0.27	665.3	**
Quadratic	$\hat{N}$ (%) = -0.11 + 0.53 x + 1.37 x^2	0.66	0.23	**
	$\hat{P}$ (%) = -10.08 + 41.58 x – 20.78 x^2	0.61	0.68	**
	$\hat{Y}$ (Mg ha^{-1}) = -14102.57 + 47087.07 x – 25159.36 x^2	0.43	607	**
Exponential	$\hat{N}$ (%) = 0.197 e$^{2.2x}$	0.70	0.17	**
	$\hat{P}$ (%) = 5.4 e$^{2.04x}$	0.55	0.69	**
	$\hat{Y}$ (Mg ha^{-1}) = 4552.4 e$^{0.57x}$	0.30	651	**

* x: S1 value Ratio = S1 value of an area of interest / S1 value of the nitrogen-rich strip

** Significantly different at the 0.01 probability level

wheat. However, according to the results, the best stage was GS 39 because the effect of crop leaves covering the soil background becomes less in this stage. There is also a need for a better understanding of the S1 value ratio used in this study and for establishing a threshold of critical level for N responsiveness. Although not conclusive, the results suggest that the S1 value ratio has the potential to infer grain yield responsiveness to N

fertilizer applications across the fields. However, in case of grain yield in both regression analyses and using ArcMap (not shown), the relationships of S1 value and S1 value ratio with yield were not strong. The highest relations (i.e., R^2=0.41 with RMSE=663 (Mg ha^{-1}) and R^2=0.43 with RMSE=607 (Mg ha^{-1})) were obtained in a linear model (Table 4.2) and quadratic model (Table 4.3), respectively. This was probably because of the existence of crop lodging areas in some of the target points at end of the growth season that affected grain yield or because the wavelengths used in CropSpec were not appropriate for early estimation of grain yield. There have been many studies on the use of multi spectral characteristics to monitor and measure crop conditions in the field. In all cases, one or more kinds of vegetation index were used. The normalized difference vegetation index (NDVI) has been mostly applied to estimate crop growth status by using two different wavelengths in NIR and VIS bands, which would increase with increasing green cover; however, this only holds true until canopy

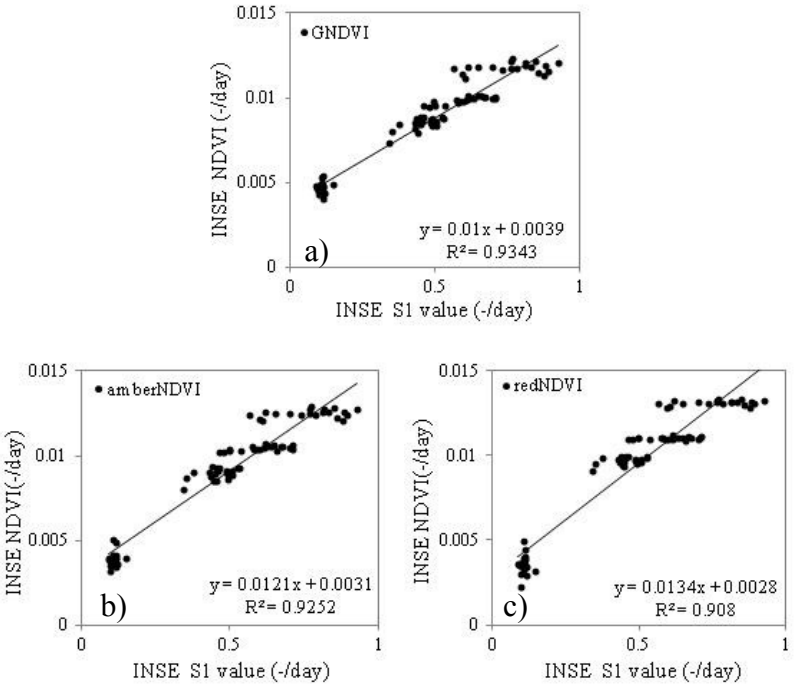

Fig. 4.4 In-season estimation (INSE) of a) green NDVI (GNDVI), b) amberNDVI, and c) redNDVI versus INSE S1 value for all four growth stages combined. Linear equation and coefficient determination (R^2) are presented.

closure when the crop has a leaf area index (LAI) of up to three (Dampney *et al.,* 1998), where LAI is defined as the ratio between total leaf area, on one side only, per unit area of ground. In this study, in order to evaluate the performance of CropSpec, a comparison was made between S1 value (acquired by CropSpec as an active sensor) and NDVIs (acquired from FS3 as a passive sensor). Therefore, green-NDVI (GNDVI), amber-NDVI, and red- NDVI were calculated across four growth stages.

In order to incorporate the age of the crop at the time of sensing, S1 value, NDVIs, SPAD value, and height of the crop, which were measured in four growth stages, were divided by the number of calendar days from the first of April and were called the in-season estimation (INSE). This is similar to the calculation used by Lukina *et al.,* (2001) and Inman *et al.,* (2007) to determine the in-season estimated yield (INSEY) as well as that used by Thomason *et al.,* (2010) to determine the yield prediction index (YPI). The relationships (R^2) between S1 value and three NDVIs (GNDVI, amber- NDVI and red-NDVI) were 0.93, 0.92 and 0.90, respectively (Fig. 4.4).

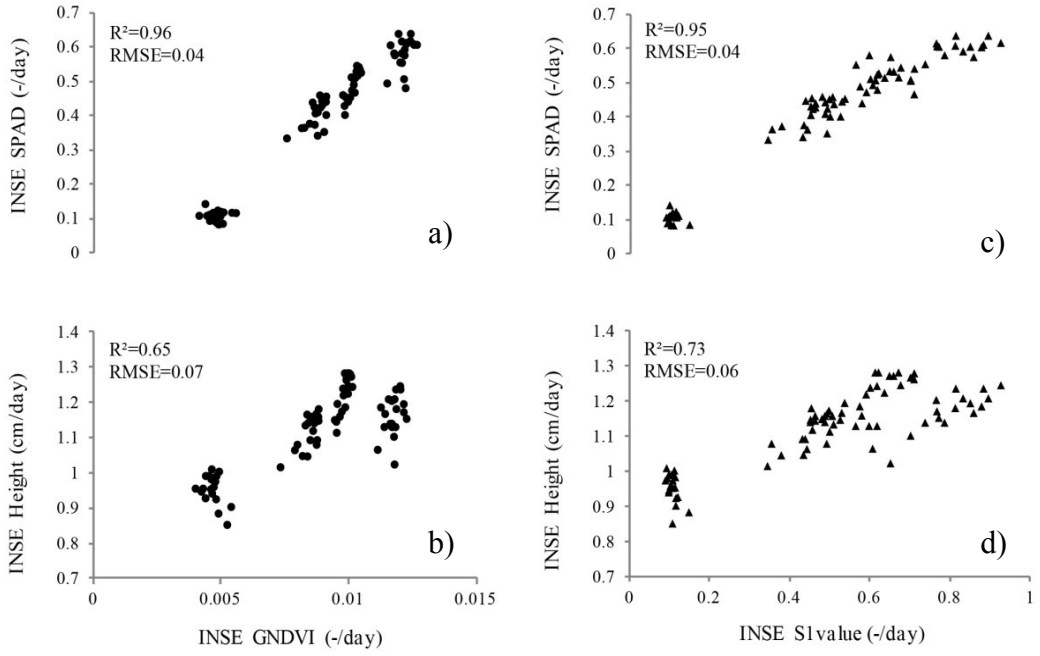

Fig. 4.5 Scatter plots of calculated: a) INSE GNDVI (-/day) and INSE SPAD (-/day), b) INSE GNDVI (-/day) and INSE Height (cm/day), c) INSE S1 value (-/day) and INSE SPAD (-/day), and d) INSE S1 value (-/day) and INSE Height (cm/day)

On the other hand, scatter plots of INSE-S1 value and INSE-GNDVI versus INSE-SPAD and INSE-Height with linear regression results (R^2 and RMSE) are shown in Fig. 4.5. In all cases, INSE-S1 and INSE-GNDVI increased with increase in crop height and SPAD. Thenkabail *et al.,* (2000) reported that non-linear exponential models were better in most cases for explaining variability between spectral vegetation indices and crop biophysical parameters across several agricultural crops. However, based on the data obtained in this study, the relationship appears to be linear.

The coefficients of determination of the linear regression models for INSE-S1 and INSE-SPAD, INSE-S1 and INSE-GNDVI and INSE-SPAD, and INSE-GNDVI and INSE-Height were 0.95, 0.73, 0.96, and 0.65, respectively. Consequently, according to the results, the performance of CropSpec was verified to be an appropriate ground-based active remote sensing system for winter wheat during the growth season by comparison; (a) the strong relationship (R^2>0.90) between NDVIs calculated by FS3 as a passive sensor and S1 value obtained by CropSpec (Fig. 4.4) and (b) similar trends for S1 value and GNDVI in cases of SPAD and height of the crop (Fig. 4.5).

Both Fig. 4.5-a and Fig. 4.5-c show that FS3 and CropSpec can be used to estimate the SPAD value with a high level of prediction (R^2>0.95), which is closely related to nitrogen concentration in the leaf as well as crop greenness and health (Bullock and Anderson, 1998).

However, use of the INSE S1 value was an appropriate method to eliminate the effect of different measurement times, but it just can distinguish the difference of the growth stage. In the other words, the difference in crop health status cannot be distinguished in the same growth stage consequently for the diagnostics for variable rate application measured S1 value in each growth stage should be used. Although this high coefficient of correlation is not equivalent to a high level of accuracy of CropSpec, the results show that use of this sensor can give us an opportunity for prediction and assessment of parameters for growth status in the field. Therefore, CropSpec can be used as an on-the-go, easy and fast crop sensor instead of the SPAD meter for diagnosis of N deficiency and color changes in leaves that can be caused by nutrition shortage in crops. In general, the use of CropSpec as a non-destructive and non-contact method provides accurate, stable readings and repeatable values. The output of CropSpec is used directly in a PC program to control fertilizer as a variable rate application (VRA).

However, the results cannot completely confirm the optical performance and accuracy of the new active sensor (CropSpec) because further standard optical experiments are needed to calibrate the instrument, because CropSpec integrated from many optical parts and performance of each part should be considered. On the other hand, it should be noted that N application is sometimes not the main factor that affects yield or other field characteristics, and farmers should be aware of this fact and carefully make a decision regarding the use of these technologies in fields with spatially and temporally stable yield-limiting factors. Causes for spectral variability within the field must be adequately understood before sensor-based variable rate fertilization can be safely used to reduce or optimize N side-dressings in winter wheat (Zillmann *et al.,* 2006). A superior strategy for variable-rate N application would be consideration of the history of production of the field, yield maps, and precipitation during the growth season and by the farmer's experience regarding yield-limiting attributes when implementing any N management scheme and then combining this information with sensor measurements.

4.4 Conclusion

A ground-based remote sensing system to measure wheat growth parameters was evaluated. According to the results, CropSpec has the potential to estimate growth status in winter wheat. We observed high linear relationships between CropSpec and SPAD value, height of the crop, nitrogen content, and protein content of grain. The results indicated that CropSpec can be used to determine crop health status and make an appropriate topdressing decision. CropSpec allowed better relationships for SPAD, nitrogen, and protein at the GS 39 growth stage. This suggests that the optimum time to take S1 value readings in Sapporo may be the GS 39 to GS 45 growth stages. Green NDVI had the best correlations with INSE S1 value and other measured parameters, indicating that use of other optimal wavelengths may improve the capability of CropSpec for prediction of crop conditions rather than the present wavelengths. However, for diagnosis of crop condition in each growth stage for variable rate application, it is better to use S1 value without elimination of different measurement times. The advantage of the on-the-go, fast, easy and non-destructive sensor for a variable rate application system is that no crop sampling or laboratory tissue analysis is

required. This time and labor saving should result in more accurate and appropriate rates of top-dress N being applied and application to a greater proportion of the crop.

CHAPTER 5

WAVELENGTHS SELECTION

BY MULTIVARIATE ANALYSIS

5.1 Introduction

Remote sensing has great potential for several applications because it enables wide-area, non-destructive, and real-time acquisition of information on ecophysiological plant conditions (Inoue, 2003). Remotely sensed data, obtained either by satellite or aircraft, can provide a set of detailed and spatially distributed data on plant growth and development (Plant *et al*., 2000).

Measurement of various crop canopy variables during the growing season provides an opportunity for improving grain yields and quality by site-specific application of fertilizers (Hansen *et al.*, 2003). Plant reflectance is affected by leaf surface properties, internal structure, plant stress, and the concentration and distribution of biochemical components; therefore, analysis of remote reflected light may be used to assess plant biomass and the physiological status of a plant (Penuelas and Filella, 1998). Wavelengths in the red and near infrared (NIR) wavebands are frequently used for indirect measurements of plant characteristics (Wood *et al*., 2003). The majority of agricultural studies use measurements in the visible (400–700nm wavelength) and near infra red (700–2500nm wavelength) region of the electromagnetic spectrum. The principle is that the majority of the red light is absorbed by the chlorophyll in the canopy and therefore little is reflected, in contrast a high proportion of the near infra red light is reflected. As canopy green area increases, either due to increasing crop density or chlorophyll content, the percentage of red reflectance decreases whilst the near infra red reflectance increases. Depending on the canopy and soil type the position of the red edge can also change, this spectral shift is exploited in some research (Boochs *et al*., 1990).

Various mathematical and statistical analysis methods have been used in setting up linear and non-linear models. Hansen *et al*. (2002), applied a Multi-way partial least squares regression (N-PLS) to predict grain yield and protein content, and they showed that the relation between reflectance measurements and protein content was slightly better in wheat, where especially N-PLS improved the prediction of grain protein content. Also they fund that data from repeated measurements of reflectance used in multi-way partial least squares regression before heading improved the prediction of grain yield and protein content in wheat and barley. Card *et al*. (1988) found that N in

dried and ground tree leaves could be determined accurately from reflectance with a laboratory spectrometer. Stepwise multiple linear regressions (SMLR) were used to select 580 nm and 480 nm for total nitrogen prediction, and R^2 was 0.90. Lee *et al*. (1999) found that SPAD (Soil and Plant Analyzer Development, Minolta, Inc.) readings, based on transmittance at 659 and 940 nm, were well correlated with N content in corn ear leaves (R^2 = 0.962). They developed prediction models by partial least squares (PLS) regression, principal component regression (PCR), and multiple linear regression (MLR). The results showed that models built by PLS and PCR were better than models from MLR, and that the standard errors of prediction (SEP) for ear leaf N were 0.16%, 0.15%, and 0.20% for PLS, PCR, and MLR, respectively. Tumbo *et al*. (2002) used a back-propagation neural network model for corn nitrogen prediction in field conditions. The model used 201 spectral bands as input, covering the range from 407 to 940 nm, and results proved that the neural network model could considerably reduce interfering effects of cloud cover and solar angle. The model showed good correlation between predicted and actual chlorophyll meter readings of the training set (R^2 = 0.91). A good relationship was also found in the validation dataset (R^2 = 0.74). There has been little research reported regarding spectral characteristics and nutrient assessment in citrus.

Yield and protein content are two important key factors for bread wheat production and marketing (Jenner *et al*., 1991). Protein concentration is known to influence the bread-making quality of wheat (Johansson *et al*., 2001). The protein concentration is determined in wheat by the genetic background, but also, to a large extent, by environmental factors such as nitrogen, water access and temperature conditions (Johansson *et al*., 2001). In barley used for malt, the grain protein content should be lower than 11.5% (Bertholdsson, 1999). This may be difficult as the protein content is influenced by cultivation practices and by environmental factors such as availability of nitrogen and stress situations caused by drought (Birch *et al*., 1997). Prediction of grain protein for the prospective wheat and barley harvest would, therefore, be of value to farmers when deciding if the field should be divided into different management zones in order to harvest and deliver the targeted qualities. Grain yield and quality can however be influenced by late season fertilizer and fungicide application (Bertholdsson, 1999), but the net profit for the farmer depends on application costs, yield response and crop value. There is therefore a need to predict grain quality during the growing season to

improve decision-making concerning management practice. The objectives of this research were I) to present a step by step multivariate analysis method to determine important wavelengths in the spectral reflectance data for assessing the N status, protein content and grain yield of winter wheat, II) to develop prediction models in terms of the N status, protein content and grain yield using partial least squares regression (PLSR), III) to select individual significant wavelengths using stepwise multiple linear regression (SMLR) analysis.

5.2 Materials and Methods

5.2.1 Field experiments

The test winter wheat fields were conducted for three years in the farming area of Hokkaido University (43° 4' N 141° 20' E), Japan, with annual average precipitation of 1106.5 mm and minimum temperature (-7 c^o) in January and maximum temperature (26.4 c^o) in August. The fields dimension was 40m × 120m divided into 8 areas and four levels of fertilizer (ammonium nitrate) 0, 30, 60, and 90 kg ha^{-1} with two repetitions, were applied at the reviving stage (growth stage GS 26), (Zadoks *et al*., 1974), to create a range of crop growth variations. Field in-season measurements included SPAD value (soil plant analysis development) and canopy reflectance data in the 2010 at the flag leaf stage (GS 37) and anthesis stage (GS 60) were done in 20 target points as well as in the 2011 (56 target points) and in the 2012 (40 target points) after the stem elongation (GS 36) and anthesis stage (GS 60) growth investigations were performed. The protein content and grain yield were measured after harvesting and threshing 1 m × 3 m area in each target point in three years.

The SPAD value use of a SPAD meter (MINOLTA Co. LTD.) was determined the relative amount of chlorophyll presence by measuring the absorbance of the leaf in two wavelength regions of red and near-infrared. It can provide an indication of chlorophyll content present in plant leaves. According to the catalogue of SPAD 502 (www.konicaminolta.eu, 2011) there is high relationship (R^2 > 0.9) between SPAD value and leaf nitrogen concentration, therefore it has been widely used in detecting crop chlorophyll and nitrogen content and the guidance of plant healthy and topdressing

(Zhang *et al*., 2003). In this study data of SPAD value was dealt as an index of actual nitrogen content in crop leaves.

5.2.2 Reflectance measurement

Wheat canopy reflectance measurements in the 350 to 2500 nm wavebands (1 nm in width) were made using a portable spectroradiometer Field Spec FR (350~2500 nm) held above the wheat canopy at a distance of 150 cm from the ground, under cloudless conditions, and as close to solar noon as possible (Rasooli *et al*., 2013a). The calibration was done using a standard white board immediately before measuring reflectance value. Five canopy spectral reflectance measurements were obtained from a 2 m radius centered on the geo-referenced point. These measurements were then averaged for the particular location. Reflectance data were preprocessed to remove erroneous measurements and improve stability of the regression. Owing to observed noise problems because of absorption by the atmosphere, the first 50 readings (from 350 nm to 400nm) at the lower visible wavelengths and last 1150 readings (from 1350nm to 2500nm) at the shortwave infrared (SWIR) were deleted due to their low signal-to-noise ratio; thus, the revised spectra began at 400 nm (Fig. 5.1).

5.2.3 Dataset arrangement

The three years datasets were separated into modelling and validation datasets. The modelling dataset included a combination of 2010 and 2011 samples (20 samples from each year) to make a calibration model. The 2012 samples (40 samples) were used as the validation dataset. Three methods; correlation coefficient spectrum, Partial least squares regression (PLSR) and step-wise multiple linear regressions (SMLR) were used for wavelength selection.

5.2.4 Statistical analysis

1) Correlation coefficient spectrum

The simplest method was to compute correlation coefficients between reflectance at each wavelength and the actual crop variables. The correlation coefficient spectrum provided a picture of the relationship between reflectance and crop variables.

Wavelength regions showing high correlation are regions that should be selected, and regions showing low or no correlation should be ignored. The SPSS version 18 (SPSS Inc., Chicago, USA) was used to calculate correlation coefficients (*r*).

2) Pre-processing for reflectance data

A large amount of spectral data is usually obtained from spectral instruments and yields useful analytical information (Blanco and Villarroya, 2002). However, the data acquired from spectrometer contains back- ground information and noise besides sample information. In order to obtain reliable, accurate and stable calibration models, it is very necessary to pre-process spectral data before modelling with Partial Least Square (PLS) (Cen and He, 2007). Spectral pre-processing techniques are required to remove any irrelevant information including noise, uncertainties, variability, interactions and unrecognized features. A lot of pre-processing techniques for spectral data have been developed recently (Moghimi *et al.*, 2010). In this study, original spectral dataset with four types of pre-processing methods were used such as Gaussian filter, Savitzky-Golay smoothing, differentiation (first derivative) and Maximum normalization.

3) Regression analysis

Partial least squares regression (PLSR) implemented in Unscrambler version 10.2 (CAMO, Inc., Oslo, Norway) and step-wise multiple linear regression (SMLR) in SPSS version 18 were used to develop calibrations between crop variables and reflectance spectra. Both PLSR and SMLR have been widely used in chemometrics, remote sensing, and spectral data processing to deal with large datasets containing highly correlated variables. Although PLS has been more widely used in recent years, successful SMLR applications to soil spectral analysis have also been reported (e.g., Nanni and Dematte, 2006; Vasques *et al*., 2009).

(1) Partial least squares regression

PLS is a full-spectrum method, in that it uses information from all wavelengths in the original spectrum to develop a calibration algorithm. The PLS calibration creates a new set of variables, called factors, that are uncorrelated and that explain variation in both response and predictor variables (Beebe and Kowalski, 1987). A key step in PLS

regression is selecting the optimal number of factors to best represent the calibration data without overfitting. This requires a validation step that is generally done either by through a leave out one (LOO) cross-validation procedure or splitting the dataset into independent calibration and validation sets. Therefore we applied several combination of independent and validation dataset, then we selected the best combination model regarding to the coefficient of determination (R^2), and root mean square error (RMSE, eq. 1). Based on these statistics, the Unscrambler software determined a recommended number of factors to minimize estimation error. The final calibration model was then obtained from the full dataset using this number of factors. The basic PLS algorithm was described in Ehsani *et al.* (1999).

In the PLS, the wavelengths strongly contributing to the model were identified using the B-matrix computed by the Unscrambler PLS software. The B-matrix contains coefficients relating the original independent variables (reflectance values) to the dependent variable (crop variables), and independent variables with larger B-coefficients can be viewed as contributing more to the overall regression model, but should not be used alone for wavelength selection (Brenchley *et al*., 1997). However, since the regression coefficients represent the importance, each predictor has in the prediction of just the response. The variable importance for projection (VIP) represents the contribution of each predictor in fitting the PLS model for both predictors and response. It summarizes the contribution a variable makes to the model. If a predictor has a relatively small coefficient (in absolute value) and a small value of VIP (VIP< 0.8), then it is a prime candidate for deletion (Wold, 1994).

(2) Stepwise multiple linear regression (SMLR)

Stepwise multiple linear regressions (SMLR) are an improved version of forward regression that permits re-examination at every step of the variables incorporated in the model in previous steps. Each forward selection step, with a significance level (α) of 0.5, can be followed by one or more backward elimination steps with a significance level (α) of 0.1. The stepwise selection process terminates if no further variable can be added to the model or if the variable just entered into the model is the only variable removed in the subsequent backward elimination. SMLR was reported to have a good ability for wavelength selection by Card *et al*. (1988).

5.2.5 Significant wavelengths selection

The following six wavelength selection steps were proposed to develop calibration models and were tested for their prediction performance;

1) Considering that wavelengths having high correlation coefficients (| r | > 0.6) with crop variables may contribute more to calibration models.

2) The PLSR procedure with each type of mentioned pre-processing methods was applied to the entire spectral reflectance (400 to 1350 nm) of modeling dataset (samples of 2010 and 2011), with the maximum number of PLS factors up to 15 and two cross validation (leave one out and 8 points validation set) were set, and the optimum number of factors was defined based on CVTEST in PLS.

3) According to the results of step 2, the best PLS model (whit higher R^2 and lower RMSE) was determined.

4) The determined PLS model was validated use of validation dataset (samples of 2012) and also plots of B-coefficients and VIPs were drawn.

5) To avoid from high collinearity because of existence large number of spectral data could make the stepwise procedure unstable, the new dataset was generated using validated wave ranges of 2012 data regarding to plots of B-coefficients and VIP. In an approach similar to that used by Thomasson *et al*. (2001) to reduce collinearity, reflectance values of every 5 wavelengths were averaged into one variable.

6) SMLR was applied to new reflectance dataset of 2012 samples and among of results, the best wavelengths to predict SPAD value, protein content and grain yield were selected.

The precision of the models were quantified with the coefficient of determination (R^2) and the root mean squared error (RMSE) and the relative error (RE), as shown in Eq. (5.1) and (5.2) (Yi *et al*., 2007).

$$RMSE = \sqrt{\frac{1}{n}\sum_{i=1}^{n}(y_i - \hat{y}_i)^2} \tag{5.1}$$

$$RE = \frac{100}{\bar{y}}\sqrt{\frac{1}{n}\sum_{i=1}^{n}(y_i - \hat{y}_i)^2} \tag{5.2}$$

where $\hat{y}_i$ and y_i are the estimated and measured value of the ith sample; n is the number of samples; $\overline{y}$ is the average of measured value.

5.3 Results and Discussion

The experimental treatments, including different years, nitrogen application, and strategies together with the temporal timing of plant sampling, caused a wide range of variation within the investigated crop variables (Table 5.1). This wide range of variation in the investigated crop variables was planned in order to make the relationship between plant performance and reflectance measurements (Fig. 5.1) as realistic and universal as possible.

Table 5.1 Selected properties of the investigated crop

Crop Variables	Year	Mean	S.D.	Min	Max	Range
SPAD (-)	2010	43.4	1.29	41	45.8	4.8
	2011	43.1	1.38	39.4	45.3	5.9
	2012	42.6	1.62	38.2	46	7.8
Yield (Kg/ha)	2010	7490	819	5669	8533	2864
	2011	6864	966	5516	8549	3033
	2012	6708	615	5450	8154	2704
Protein (%)	2010	9.88	0.75	8.59	10.9	2.35
	2011	11.4	0.99	8.86	12.1	3.24
	2012	11.6	1.55	9.62	14.0	4.39

The reflectance was at all wavelengths on average higher in 2010 in green and red visible (VIS) and middle infrared wavebands (MIR) regions compared to 2011 and 2012 (Fig. 1-a), but lower than 2011 in near infrared (NIR) regions. One of the reasons that the reflectance in visible region in 2010 increased comparing with the other years might be influenced by the difference in the soil background (Kimura *et al*., 2004). The other reason might be due to the higher SPAD value (hence, nitrogen concentration of leaves and stems) in 2010, as shown in Table 1, as the increase of chlorophyll concentration causes increased reflectance in the visible regions and the movement of the red edge to longer wavelengths (Demetriades-shah *et al*., 1990), the position of the

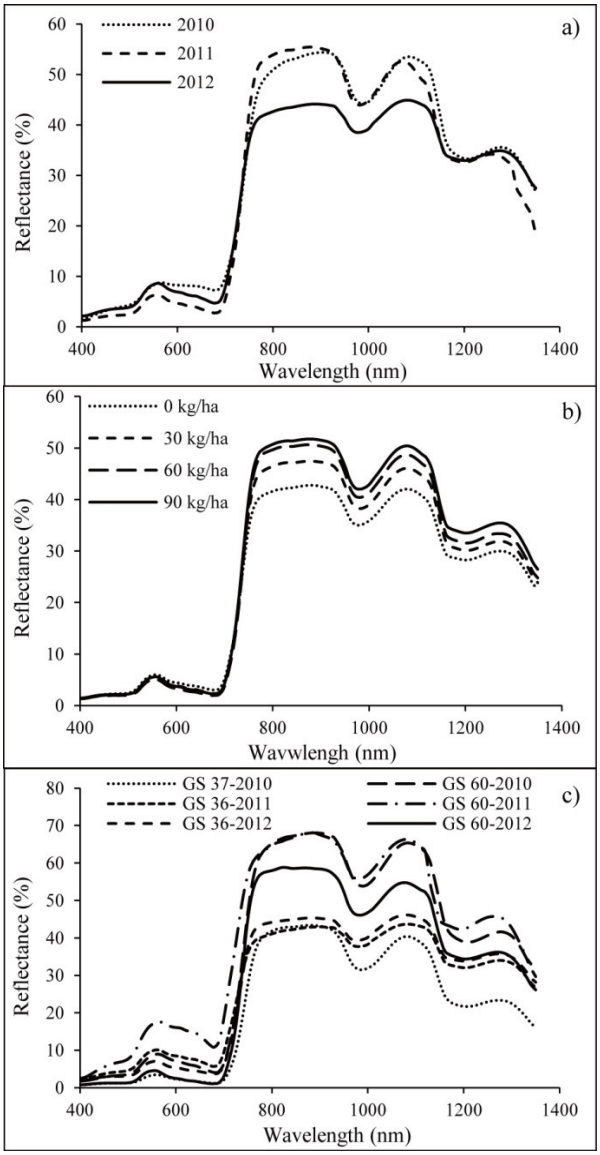

Fig. 5.1 Average of reflectance spectrum of the different experimental treatments; years (n = 20+56+40), nitrogen application (n = 20+56+40), and date of measurement (n = 20 +56+40).

red edge in 2010 (around 720) was different from that in others (around 700 nm). Increasing nitrogen supply caused on average lower reflectance in the VIS spectral range (400 ~700 nm), while the reflectance was higher in the NIR and SW spectral range (700 ~ 900 nm and 900 ~1350 nm, Fig. 5.1-b). The canopy reflection in the near infrared spectral range increased with growth stage from the stem elongation (GS 36) to

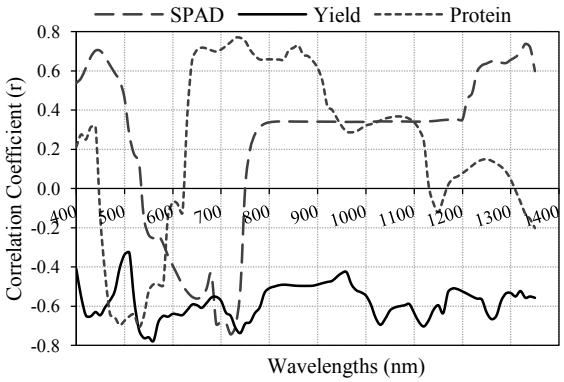

Fig. 5.2 Correlation coefficients between reflectance at each wavelength and three crop variables (SPAD, yield and protein) of the modelling dataset

heading stage (anthesis stage (GS 60)) (Fig. 5.1-c) and the increased pattern of reflectance in theheading stage was similar to that in the stem elongation (GS 36) (Ryu *et al*., 2009).

Fig. 5.2 shows the correlation coefficient spectrum between reflectance and actual crop variables (SPAD, grain yield and protein content) of the modelling samples. Reflectance in some regions was highly correlated with the crop variables.

Wavelengths 440, 690, 720 and 1330 nm for SPAD, 420, 440, 550, 730, 1030, 1110 and 1260 nm for yield and 490, 530, 650, 730 and 860 nm showed a peak correlation coefficient of $| r |>0.6$. The highest correlation coefficients were seen at 720nm (r = -0.74), 550nm (r = -0.77) and 730nm (r = +0.76) for SPAD, grain yield and protein content, respectively. The “hot spot” wavelength in case of SPAD was similar to results by Carter and Knapp (2001). They reported that wavelengths near 700 nm were significant for detecting chlorophyll, which is also closely correlated with N concentration in green leaves.

Various calibration models were developed by using different pre-processing techniques on the spectral data (Table 5.2). Each calibration model was used to predict SPAD value, grain yield and protein content of modelling dataset in order to verify the improved ability of models based on different pre-processing techniques. A proper model should have a low root mean squares error (RMSE) and relative error (RE) with a high coefficient of determination (R^2) between the predicted and actual value of each

Table 5.2 the prediction results of SPAD, grain yield and protein content with different pre-processing techniques and appropriate number of PLS factors based on CVTEST in two calibration methods

Crop variables	Pre-processing	Calibration Method							
		Cross Validation (LOO)				Cross Validation (20% of samples)			
		Factor	R^2	RMSE	RE (%)	Factor	R^2	RMSE	RE (%)
SPAD	Original Data	7	0.665	1.98	4.65	7	0.727	1.61	3.78
	Smoothing (Savitzky-Golay)	6	0.675	1.91	4.49	6	0.738	1.53	3.59
	Smoothing (Gaussian Filter)	6	0.701	1.71	4.02	6	0.771	1.30	3.05
	First Derivative	6	0. 690	1.73	4.06	5	0.754	1.42	3.34
	Maximum normalization	5	0.714	1.68	3.95	5	**0.774**	**1.28**	**3.01**
Yield	Original Data	6	0.664	789	10.9	6	0.737	719	9.89
	Smoothing (Savitzky-Golay)	6	0.668	782	10.8	6	0.741	713	9.80
	Smoothing (Gaussian Filter)	6	0.717	739	10.2	5	0.759	682	9.38
	First Derivative	6	0.687	758	10.4	6	0.748	704	9.68
	Maximum normalization	5	0.725	732	10.1	5	**0.763**	**677**	**9.31**
Protein	Original Data	7	0.658	0.747	7.02	7	0.729	0.671	6.30
	Smoothing (Savitzky-Golay)	7	0.661	0.745	7.00	6	0.731	0.666	6.26
	Smoothing (Gaussian Filter)	6	0.703	0.798	7.50	5	0.762	0.623	5.85
	First Derivative	6	0.682	0.723	6.79	6	0.755	0.639	6.00
	Maximum normalization	5	0.709	0.691	6.49	5	**0.767**	**0.620**	**5.82**

property. Moreover, a low number of PLS factors are desirable. Models have been developed using different appropriate number of PLS factors and different pre-processing techniques. However, only the most accurate models were presented in Table 5.2 with their R^2, RMSE and RE. If no pre-processing was applied, a minimum R^2 was observed in the 7, 6 and 7 factors of PLS model for prediction of SPAD, grain yield and protein content respectively in both LOO and 8 points in validation set cross validation methods. However, if pre-processing was applied, R^2 increases and the RMSE were reduced. In the meantime it was found that the number of PLS factors could be reduced by the use of data pre-processing. Maximum normalization reduced the number of PLS factors with increasing in R^2 and decreasing RMSE more than other methods (Table 5.2).

Wavelengths 440, 690, 720 and 1330 nm for SPAD, 420, 440, 550, 730, 1030, 1110 and 1260 nm for yield and 490, 530, 650, 730 and 860 nm showed a peak correlation coefficient of $| r |>0.6$. The highest correlation coefficients were seen at 720nm (r = -0.74), 550nm (r = -0.77) and 730 nm (r = +0.76) for SPAD, grain yield and protein content respectively. The "hot spot" wavelength in case of SPAD was similar to results by Carter and Knapp (2001). They reported that wavelengths near 700 nm were significant for detecting chlorophyll, which is also closely correlated with N concentration in green leaves.

Various calibration models were developed by using different pre-processing techniques on the spectral data (Table 5.2). Each calibration model was used to predict SPAD value, grain yield and protein content of modelling dataset in order to verify the improved ability of models based on different pre-processing techniques. A proper model should have a low root mean squares error (RMSE) and relative error (RE) with a high coefficient of determination (R^2) between the predicted and actual value of each property. Moreover, a low number of PLS factors are desirable. Models have been developed using different appropriate number of PLS factors and different pre-processing techniques. However, only the most accurate models were presented in Table 5.2 with their R^2, RMSE and RE. If no pre-processing was applied, a minimum R^2 was observed in the 7, 6 and 7 factors of PLS model for prediction of SPAD, grain yield and protein content respectively in both LOO and 8 points in validation set cross validation methods. However, if pre-processing was applied, R^2 increases and the RMSE were reduced. In the meantime it was found that the number of PLS factors could be reduced by the use of data pre-processing. Maximum normalization reduced the number of PLS factors with increasing in R^2 and decreasing RMSE more than other methods (Table 5.2).

This pre-processing method with using 8 selected samples of 40 samples as a cross validation set and 32 selected samples of 40 samples as a calibration set among of modelling dataset (2010 and 2011) increased R^2 from 0.665 to 0.774, from 0.664 to 0.763 and from 0.658 to 0.767 for prediction of SPAD, grain yield and protein content, respectively whilst the RMSE decreased from 1.98 to 1.28 for SPAD, from 789 to 677 for yield and from 0.798 to 0.62 for protein in the 5 number of PLS factors.

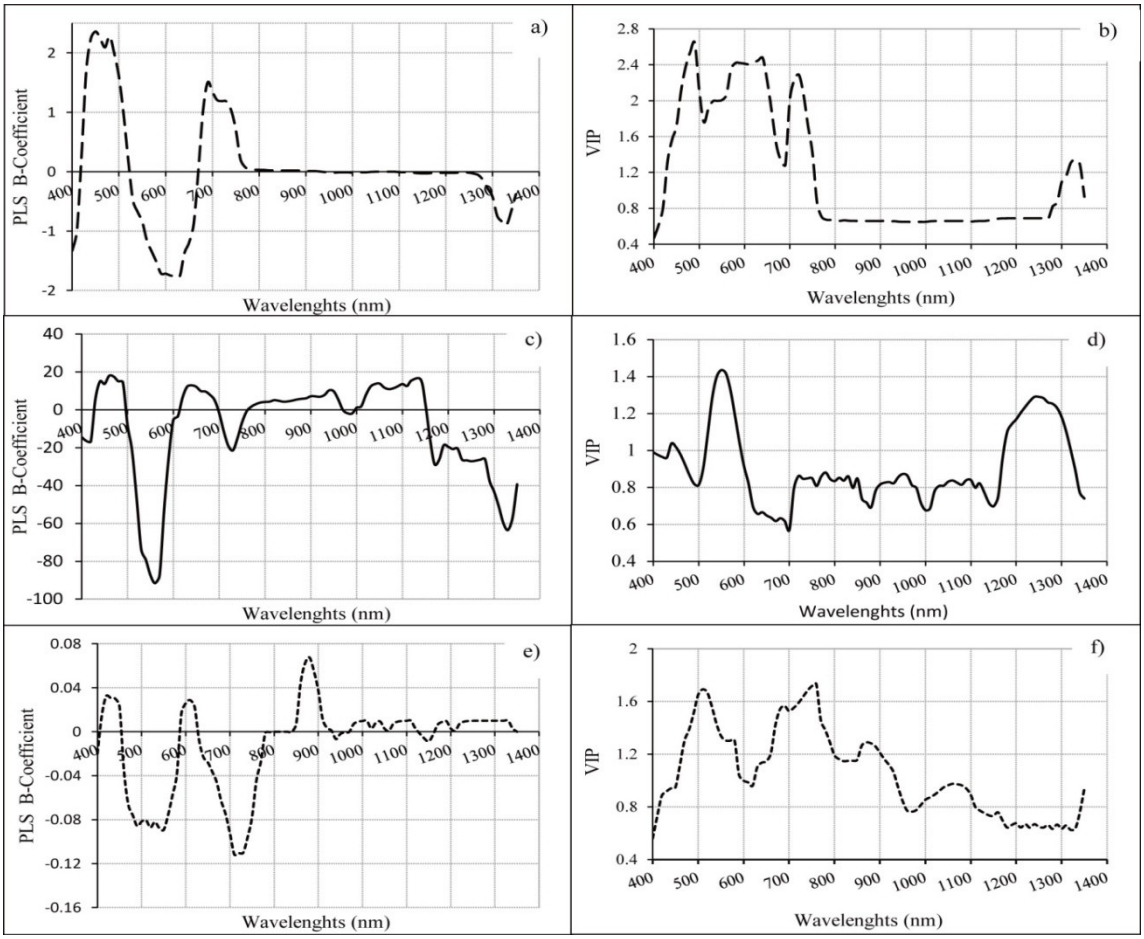

Fig. 5.3 PLS B-coefficients (a, c and e) and VIP (b, d and f) determined from validation dataset using maximum normalization pre-processing with 5 number of factors and 20% selected samples in cross validation for SPAD, grain yield and protein content.

Table 5.3 the best PLS regression model fitted to the modelling dataset including coefficient of determination (R^2), root mean squares error (RMSE) and relative error (RE) with the 5 number of factors and 20% selected samples in cross validation

Crop variables	Per-processing	Prediction with 5 Factors			The most important Factors	Efficacy of important factor %
		R^2	RMSE	RE (%)		
SPAD	Maximum normalization	0.774	1.28	3.01	2	45.6
Yield	Maximum normalization	0.763	677	9.31	3	39.9
Protein	Maximum normalization	0.767	0.620	5.82	1	41.5

The results of the best PLS model in modelling dataset have been shown in Table 5.3. On the other hand the most important PLS factors among of the 5 factors have been given in Table 5.3. The second factor with 45.6 %, the third factor with 39.9 % and the first factor with 41.5 % of selected model had highest efficacy in the PLS for SPAD, grain yield and protein content, respectively.

Table 5.4 The result of PLS regression with validation dataset (of 2012) using the best PLS model in modeling dataset, including coefficient of determination (R^2), root mean squares error (RMSE) and relative error (RE) and the ranges of important wavelengths according to the B-coefficient and VIP in Fig. 5.3

Crop variables	Per-processing	Prediction with 5 Factors			The most important Factors	Efficacy of important factor %	Ranges of important wavelengths	
		R^2	RMSE	RE (%)				
SPAD	Maximum normalization	0.841	1.94	4.50	2	51.7	Range 1	400~500
							Range 2	520~750
							Range 3	1300~1350
Yield	Maximum normalization	0.872	301	4.53	3	47.2	Range 1	405~480
							Range 2	520~750
							Range 3	1010~1350
Protein	Maximum normalization	0.803	0.786	6.77	1	43.8	Range 1	470~530
							Range 2	650~770
							Range 3	840~900

These results were improved in validation year (2012) so that R^2 was increased up to 0.84 for SPAD, 0.87 for yield and 0.8 for protein (Table 5.4). While RMSE for yield was decreased from 667 to 301 (RE was decreased up to 4.78 %), but in case of SPAD and protein were increased from 1.28 to 1.94 and 0.62 to 0.786 respectively. Maybe it was because of according to the Table 5.1 standard deviation (S. D.) of SPAD value (1.62) and protein content (1.55) in 2012 (validation dataset) was higher than these crop variables in 2010 and 2011 (modelling dataset). The different components can be defined by their respective PLS B-coefficients and VIP. The coefficients quantify the contribution of different wavelengths to the model. The coefficients allow the optimal fit to be achieved for the specific crop variable of interest. The B-coefficients and VIP

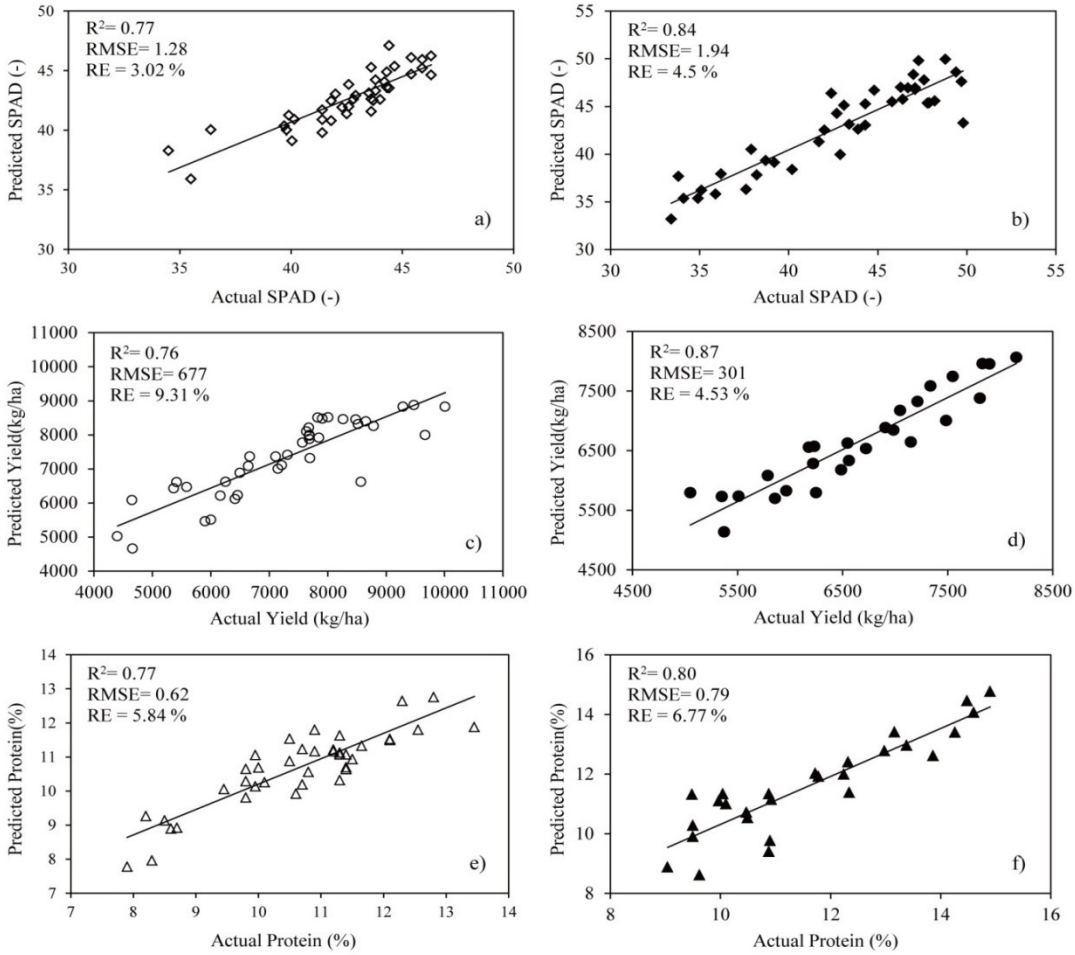

Fig. 5.4 Predicted crop variables (SPAD, grain yield and protein content) using PLS models, plots in left side are related to the PLS prediction result in modeling dataset and plots in right side are for predicted values in validation dataset, including R^2, RMSE and RE.

related to the three investigated crop variables are shown in Fig. 5.3. According to the figures there are some ranges of important reflecting (Table 5.4), with high relationship between the spectral data and the canopy. Three zones at approximately 400~500, 520~750 and 1300~1350 nm for SPAD, 405~480, 405~480, 520~750 and 1010~1350 nm for grain yield and 470~530, 650~770 and 840~900 nm for protein content of major importance for the PLS models could be identified.

Table 5.5 Results of stepwise multiple linear regression (SMLR) analysis using the verified wave ranges after application PLS for validation dataset.

Crop variables	Selected Wavelengths (nm) in Stepwise MLR	R^2	RMSE	RE (%)
SPAD	435, 550, 665, 705, 730, 1315, 1325	0.85	1.56	3.66
Yield	410, 520, 535, 1025, 1080, 1125, 1130, 1235, 1265, 1305	0.89	287	4.28
Protein	445, 505, 640, 665, 670, 700, 760, 890, 930	0.84	0.68	5.86

These zones showed either a shift or significant peaks. The VIP>0.8 was considered as an independent variable importance in projection, which was almost consistent of B-coefficients variation in each dependent variables. Based on PLS result of modelling dataset and validation dataset, the prediction of crop variables was plotted against the actual data in Fig. 5.4. After verification the selected PLS model using the validation dataset (Table 5.3 and 5.4), we applied SMLR for new spectral dataset generated by validation dataset use of specified wave ranges in Table 5.4 with actual crop variable in 2012. Table 5.5 lists the analysis results based on the SMLR procedures. The results show a good relationship between the actual crop variables and the predicted values for validation datasets. SMLR selected 7 wavelengths for SPAD, 10 wavelengths for yield and 9 wavelengths for protein. The R^2, RMSE and RE of SMLR results for the validation dataset, respectively was 0.85, 1.56 and 3.66 % for SPAD, 0.89, 287 and 4.28 % for yield and 0.84, 0.68 and 5.86 % for protein. SMLR showed the best R^2 because reflectance data were screened and reduced to the most effective dataset during of using previous three steps (correlation coefficients, PLSR with modelling dataset and PLSR with validation dataset) therefore the collinearity was reduced and made SMLR analysis more reliable. Comparing the SMLR and PLS procedures, both worked very well in this study. SMLR Models developed by using fewer (7 to 10) wavelengths than those developed by PLS. The most accurate prediction results, which were generated by SMLR, are shown in Table 5.5. The PLS procedure for full-spectrum analysis due to its ability to compress data appears superior to the SMLR. However, difficulties with the

PLS method include a complex algorithm, which could be difficult to understand, and the large number of wavelengths that were used for the calibration model. The results from this research could be used to help develop an in-field growth condition monitoring system such as N sensor and yield estimation sensor in the winter wheat. A possible sensing system consisting of a linear variable filter and a detector array could produce full-spectrum sensing in real time. The data collected could be combined with an SMLR or PLS algorithm to predict N concentration for fertilizer application, protein content and grain yield for crop quality and field performance as an on-the-go monitoring system.

5.4 Conclusion

Three years field measurements were conducted to select significant wavelengths related to the winter wheat growth characteristics as a preliminary step toward developing a real-time spectral-based crop sensor, for prediction of N status, grain yield and protein content. A correlation coefficient spectrum, PLSR, and SMLR procedures were used to determine important wavelengths. Both SMLR and PLS regression procedures yielded good results. The second dataset (validation dataset) was generated from 2012 spectral measurements using entire wavelengths. Three ranges of wavelengths selected by considering PLS B-coefficient and VIP plotted with validation dataset from 2012 spectral measurements in each crop variables (SPAD, grain yield and protein content). The accuracy of PLSR performance (R^2) was improved from 0.77 to 0.84, 0.76 to 0.87 and 0.76 to 0.8 in SPAD, grain yield and protein content respectively in validation results. The third dataset was made from 2012 spectral data use of selected wave ranges from validation PLS results and SMLR was applied to new dataset. Some wavelengths [(435, 550, 665, 705, 730, 1315 and 1325 nm), (410, 520, 535, 1025, 1080, 1125, 1130, 1235, 1265 and 1305nm) and (445, 505, 640, 665, 670, 700, 760, 890 and 930nm)] were identified by both PLSR and SMLR as significant wavelengths for SPAD, grain yield and protein content respectively which already have been recognized in two steps of modelling and validation PLSR. Due to the ability of PLS to reduce collinearity in datasets, models using PLS produced good wave ranges that used in SMLR procedure This result showed that SMLR was more suitable for datasets with lower

collinearity. Indeed these step by step methods worked such as data-screening procedure to discriminate the most effective wavelengths for prediction crop variables. The results from this research could be used to help develop an in-field growth condition monitoring system such as N sensor and yield estimation sensor in the winter wheat. However it is necessary to combine these individual wavelengths in appropriate vegetation indices related to crop growth properties.

CHAPTER 6

OPTIMAL VEGETATION INDICES

FOR WINTEAR WHEAT

6.1 Introduction

In winter wheat production, the farmer tries to optimize yield and protein quality with minimum usage of mineral fertilizer. For this purpose, it is necessary to know what amount of mineral-N should be given. The challenge for the farmer is determination of optimal N supply for the plants. Plant N concentration (PNC) has been commonly used as an effective indicator of N status, and different threshold values have been established for different crops (Fageria, 2009). A major advance was made with the observation that PNC declines with increase in biomass because of plant aging, phenology and dilution effect (Lemaire *et al.,* 2008).

Remote sensing technology has recently been used to estimate crop N status. Since leaf N concentration is linked to the amount of chlorophyll, many studies have focused on estimation of crop leaf chlorophyll concentration, which is easier to estimate, for an indirect assessment of crop N status (Haboudane *et al.,,* 2008). However, spectral absorption by chlorophyll is possibly confounded by other plant pigments (Hatfield *et al.,* 2008) that might affect the accuracy of crop N status estimation by remote sensing. Plant chlorophyll content is also affected by other stress factors such as water, light, disease and other nutrient deficiencies or toxification (Chaerle and Straeten, 2000). Therefore, it is more desirable to use remote sensing technologies to estimate crop N concentration directly for decision support in precision N management. Stroppiana *et al.,* (2009) reported that an optimal normalized difference index (NDI_{opt}) using reflectance at 503 (R_{503}) and 483 nm (R_{483}) was strongly correlated with PNC in rice (Oryza sativa) (R^2 = 0.65) but least correlated with leaf area index (LAI) (R^2 = 0.31) or above ground biomass (R^2 = 0.27). Fava *et al.,* (2009) found that pasture N concentration could be most accurately estimated by using simple ratio indices involving near infrared (NIR) (775~820 nm) and longer wavelengths of the red edge bands (740~770 nm). For winter wheat (Triticum aestivum L.), Li *et al.,* (2008) used a handheld spectrometer to simulate bands of the QuickBird satellite sensor, and they showed that none of the six broad band vegetation indices performed well for estimating PNC at Feekes (Feeks scale for measuring crop growth stages) growth stages 4–5 or 6–7 (Large, 1954), whereas all of the indices performed well at Feekes growth stages 9–10, with correlation coefficients (r) ranging from -0.48 to 0.57. Across years and growth stages, the red/green vegetation

index (RGVI) showed the highest correlation coefficient of 0.43. Hansen and Schjoerring (2003) achieved better results with hyper-spectral vegetation indices (VIs). They calculated all two-band combinations for the normalized difference vegetation index (NDVI) and found that the best indices for estimating leaf N concentration from early stem elongation to heading (Feekes growth stages 30–51) mainly used a blue band (440, 447 or 459 nm) paired with a green (573 or 509 nm) or red (692 nm) band (R^2 = 0.54~0.55). Most studies that have used remote sensing technology to estimate plant N status focused on leaf N concentration or accumulation (Oppelt and Mauser, 2004) and were conducted in a heated glasshouse (Yoder *et al.,* 1995), under controlled experimental conditions (Feng *et al.,* 2008), or used only broad band vegetation indices (Li *et al.,* 2008). In this chapter, the performance of various types of hyper-spectral vegetation indices for characterizing agricultural crop physiological variables was evaluated with the goal of determining the optimal number of hyper-spectral bands, their centers and widths, in the visible and infrared portion of the spectrum (400~1350 nm), thus reducing redundancy in hyper-spectral data.

6.2 Materials and Methods

6.2.1 Study site and data collection

A conventional variety “Kitahonami” of winter wheat in Hokkaido, Japan was cultivated in three consecutive years in the experimental field of Hokkaido University (40 m × 120 m in size). The field was divided into 8 areas, and four levels of fertilizer (ammonium nitrate), 0, 30, 60 and 90 kg ha^{-1} with two repetitions, were applied at the reviving stage (growth stage GS 26 (Zadoks scale for measuring crop growth stages such as Feeks scale)) (Zadoks *et al.,* 1974) to create a range of crop growth variations. Field in-season measurements including SPAD (Soil Plant Analysis Development) value and canopy reflectance data in 2010 at the flag leaf stage (GS 37) and anthesis stage (GS 60) were carried out at 20 target points, and growth was investigated in 2011 (56 target points) and 2012 (40 target points) after the stem elongation stage (GS 36) and anthesis stage (GS 60). The protein content and grain yield were measured after harvesting and threshing in a 1 m × 3 m area at each target point in the three-year period.

Methods of measuring SPAD value and spectral reflectance were described in 5.2.1 and 5.2.2 respectively.

6.2.2 Used vegetation indices

Among the various types of hyper-spectral vegetation indices (VIs) used in previous studies, seven VIs related to plant nitrogen content (N) and grain yield estimation were selected without their specific wavebands and only as equations to calculate all possible combinations of spectral datasets to find the most accurate combinations (Table 6.1). Two classes of indices were calculated with all possible two and three band combinations from 400 to 1350 nm with 5 nm intervals: simple ratio index (SR) and normalized difference index (NDI). To determine the effects of growth stages on the relationships and performance of different indices, we separated the growth stages into Zadoks scale 36–37 (when the canopy was not closed) and Zadoks scale 60 (when the

Table 6.1 Seven different equations that mentioned in prior literatures were used as vegetation indices to calculate all combination of two and three bands of reflectance data

Index	Equation	Original Vegetation Index	Reference
1	$(\lambda_2/ \lambda_1) -1$	Difference Vegetation Index (DVI)	Gitelson et al. (2005)
2	$(\lambda_2- \lambda_1)/ (\lambda_2+ \lambda_1)$	Normalized Difference Vegetation Index (NDVI)	Rouse et al. (1974)
3	$\sqrt{NDVI*DVI}$	Root Difference Vegetation Index (RDVI)	Roujean & Breon (1995)
4	$(1+0.16) (\lambda_2- \lambda_1)/ (\lambda_2+ \lambda_1+ 0.16)$	Optimal Soil Adjusted Vegetation Index (OSAVI)	Rondeax et al. (1996)
5	$(\lambda_2- \lambda_1)/ \lambda_3$	Plant Senescence Reflectance Index (PSRI)	Sime & Gamon (2002)
6	$(\lambda_2- \lambda_1)/ (\lambda_2- \lambda_3)$	Modified Simple Rate Index (MSRI)	Dash and Curan (2004)
7	$\lambda_2/ (\lambda_1* \lambda_3)$	Simple Rate (SR)	Datt (1998)

canopy was fully closed), in addition to combined analyses across all of these growth stages.

6.2.3 Calculation of vegetation indices

An algorithm was developed with MATLAB 7.1 software (The MathWorks, Inc., Natick, MA) to calculate all possible two or three wavelengths combinations of 190 wavelengths in seven equations (Table 6.1). Linear regression was performed in order to

determine each of the correlation coefficient (R^2) between generated indices and crop physiological variables (SPAD value, protein content and grain yield). Linear regression was preferred in the initial analysis in order to operate with linear relationships.

6.2.4 Selection of vegetation indices

In order to determine optimal vegetation indices with two-pair wavelengths, all R^2 values were plotted in a contour plot for each year dataset (2010 and 2011) separately in the ArcMap environment (ArcGIS 9, ESRI Inc, USA). To make a contour plot, we assumed λ_1 and λ_2 as coordinates (X and Y) and R^2 as a Z value for elevation, and then we interpolated (λ_1, λ_2 and R^2) using kriging. The contour plot was made use of appropriate contour interval regarding to Z value (R^2 in this case).To determine common areas (Z values) in two years, the contours from each year (2010 and 2011) were overlaid on each other as two layers and using intersect overlaying in the analysis tools could define the highest common R^2 (hot spots) in the two years. Hence, the best two-pair wavelengths were revealed.

On the other hand, for vegetation indices with three wavelengths (equations 5, 6 and 7 in Table 6.1), the use of intersect overlaying method in ArcMap environment because of three-dimensional coordinate was not possible, therefore we used a combination of dataset from 2010 and 2011 data and then we feed this dataset to the developed vegetation index calculation algorithm in MATLAB. All R^2 values resulted from calculation process were organized in a three-dimensional matrix including λ_1, λ_2, λ_3 and R^2 as X, Y, Z and elevation, respectively. Then a 3-D scatter plot was created by use of "scatter3" command in MATLAB. The plot revealed a characteristic pattern with a number of ''hot spots'' with relatively high correlation coefficients. These spots were selected by choosing the wavelength combinations that showed the highest R^2 between crop variables and indices in two-year's combined dataset. The center wavelength and bandwidth for each of the selected spots were determined by fitting a rectangle that could hold the spot of interest inside its limits.

6.2.5 Evaluation of the selected indices

To evaluate the performance of selected vegetation indices, two independent dataset were created as calibration dataset (a combination dataset from data for 2010 and 2011)

and validation dataset (data for 2012). Both linear ($y = ax+b$) and exponential ($y = ae^{bx}$) fitting procedures were applied using these new indices (generated by mentioned datasets) and crop physiological variables.

6.3 Results and Discussion

Fig. 1 shows an overview of reflectance data in the three years (2010, 2011 and 2012). The experimental treatments, including different years, nitrogen application, and strategies together with the temporal timing of plant sampling, caused a wide range of variation within the investigated crop variables (Table 6.2). This wide range of variation in the investigated crop variables was planned in order to make the relationship between plant performance and reflectance measurements as realistic and universal as possible. The reflectance at all wavelengths was on average higher in 2010 in visible (VIS) and moisture-sensitive near infrared (MS-NIR) regions than in 2011 and 2012 (Fig. 6. 1-a) but was lower in 2010 than in 2011 in the near infrared (NIR) region. One of the reasons for the increase in reflectance in the visible region in 2010 compared with that in the other years might be the difference in the soil background (Kimura *et al*., 2004). Another possible reason is the higher SPAD value (hence, nitrogen concentrations of leaves and stems) in 2010 (Table 6.2). An increase in chlorophyll concentration causes increased reflectance in the visible region and movement of the red edge to longer wavelengths, and the position of the red edge in 2010 (720 nm) was different from that in the other years (700 nm). Canopy reflection in the near infrared spectral range increased with growth stage from the stem elongation stage (GS 36) to the heading stage (anthesis stage (GS 60)) (Fig. 6. 1-b), and the increased pattern of reflectance in the heading stage was similar to that in the stem elongation stage (GS 36) (Rasooli *et al.,* 2013).

The availability of hyper-spectral data in n=190 discrete narrow bands (from 400 nm to 1350 nm with 5 nm intervals) allowed computation of n × n=36,100 narrow band vegetation indices (VIs) (Table 6.1). Regression coefficients (R^2) between all possible two-band vegetation indices and crop physiological variables were determined.

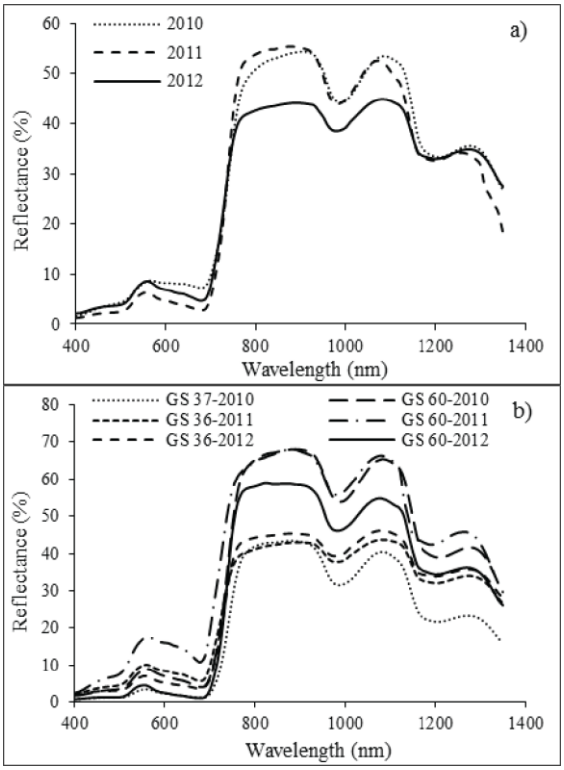

Fig. 6.1 Average of reflectance spectrum of the different years and measurement stages

The most effective results of this comprehensive analysis are illustrated in contour plots of the R^2 values, for each λ_1 and λ_2 pair, in Fig. 6.2 (a, b and c). For clarity, the higher R^2 values are shown by red contour lines for the 2010 dataset and by green contour lines for the 2011 dataset. Similar contour plots (too numerous to be presented here) were created for all of the other physiological crop variables. Based on the above results, band centers (λ_1 and λ_2) and bandwidths ($\Delta\lambda_1$ and $\Delta\lambda_2$) that combine to form the best seven indices (ranked on the basis of R^2 values) were determined for SPAD value, grain yield and protein content. The band centers and their widths are identified for the crop variables. This can be determined through λ_1 and λ_2 contour plots of R^2 values (Fig. 6.2).

We determined that a contour interval of 0.15 ~ 0.165 for R^2 values provided a reasonable and statistically sound approach for arriving at band centers and bandwidths. Smaller contour intervals result in several more gradients of R^2 values, providing other band centers and bandwidths.

Table 6.2 Selected properties of the investigated crop variables

Crop Variables	Year	n*	Mean	S.D.	Min	Max
SPAD (-)	2010	20	43.4	1.29	41	45.8
	2011	56	43.1	1.38	39.4	45.3
	2012	40	42.6	1.62	38.2	46
Yield (Kg/ha)	2010	20	7490	819	5669	8533
	2011	56	6864	966	5516	8549
	2012	40	6708	615	5450	8154
Protein (%)	2010	20	9.88	0.75	8.59	10.9
	2011	56	11.4	0.99	8.86	12.1
	2012	40	11.6	1.55	9.62	14.0

* n is the number of samples

These can be too numerous and often provide no significant statistical difference between two discrete contour intervals. For example, the index 1 that has the strongest correlation for SPAD value has band centers (λ_1 and λ_2) and bandwidths ($\Delta\lambda_1$ and $\Delta\lambda_2$) extracted from the contour plot range of 0.66 to 0.825 (highest R^2 value range) in the 2011 dataset in Fig. 6.1-a. The band centers and widths are tabulated in Table 6.3. The same range (0.66 to 0.825) of contour intervals can be split into distinctive groups of smaller intervals such as 0.66 to 0.72, 0.73 to 0.79, and >0.80. Then it is possible to derive band centers (λ_1 and λ_2) and bandwidths ($\Delta\lambda_1$ and $\Delta\lambda_2$) for each of these smaller intervals. However, the significance of the band centers and bandwidths from the small intervals of R^2 values, such as between 0.66 to 0.72 and 0.73 to 0.79, is limited since these R^2 values did not have significant statistical difference or were statistically different only at the 0.10 level or higher. Therefore, the λ_1 and λ_2 spectral band combinations obtained from the distinctive contour intervals of 0.15 ~ 0.165 were considered a reasonable and statistically sound approach.

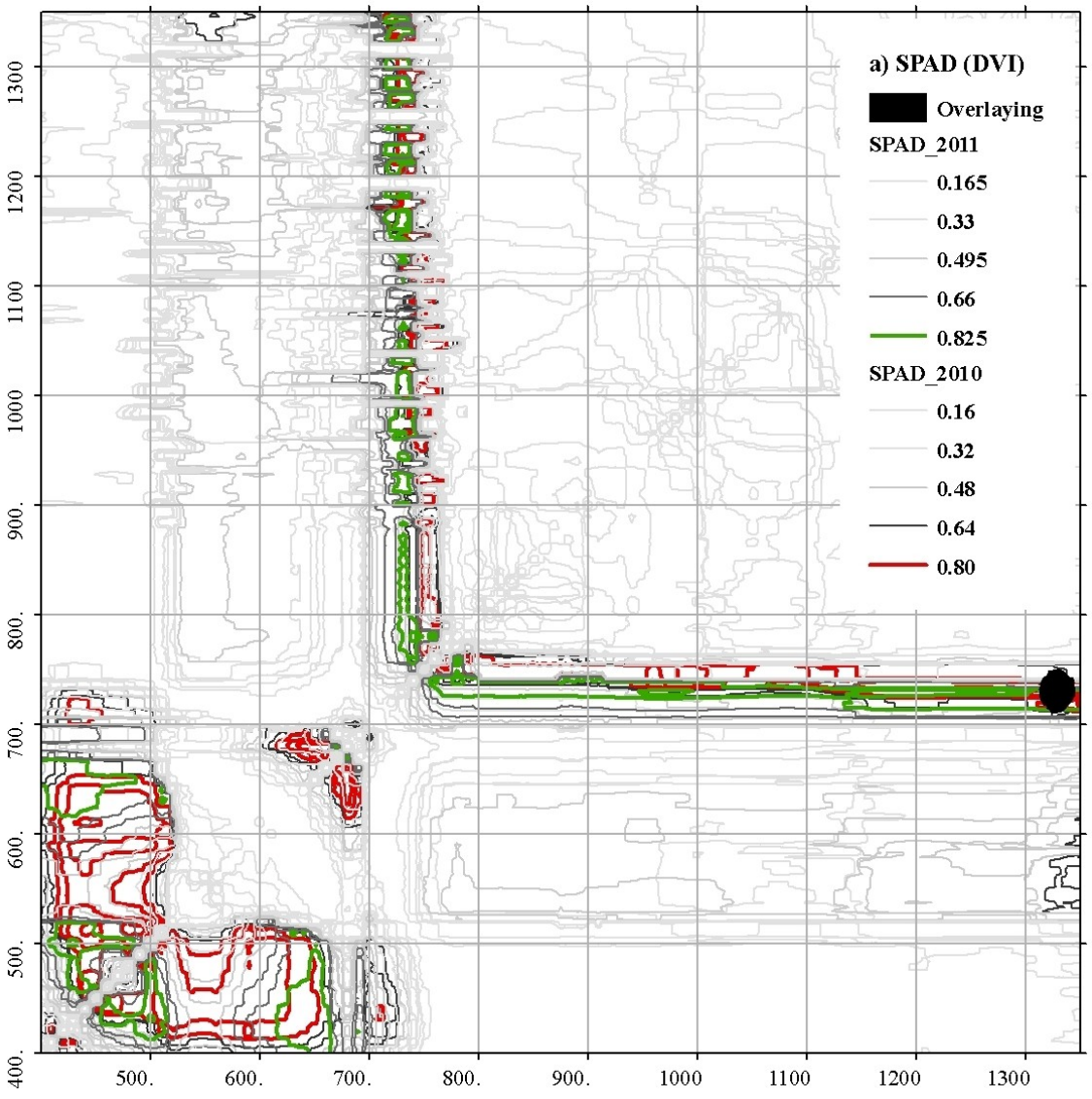

Fig. 6.2 (a, b and c) as contour plots show the correlation (R^2) between crop variables and two-band spectral vegetation indices by using overlaying method in ArcMap 9.3; (d, e and f) three dimensions scatter plot shows "hot spots" as highest relationship (R^2) between crop variables and three-band vegetation indices.

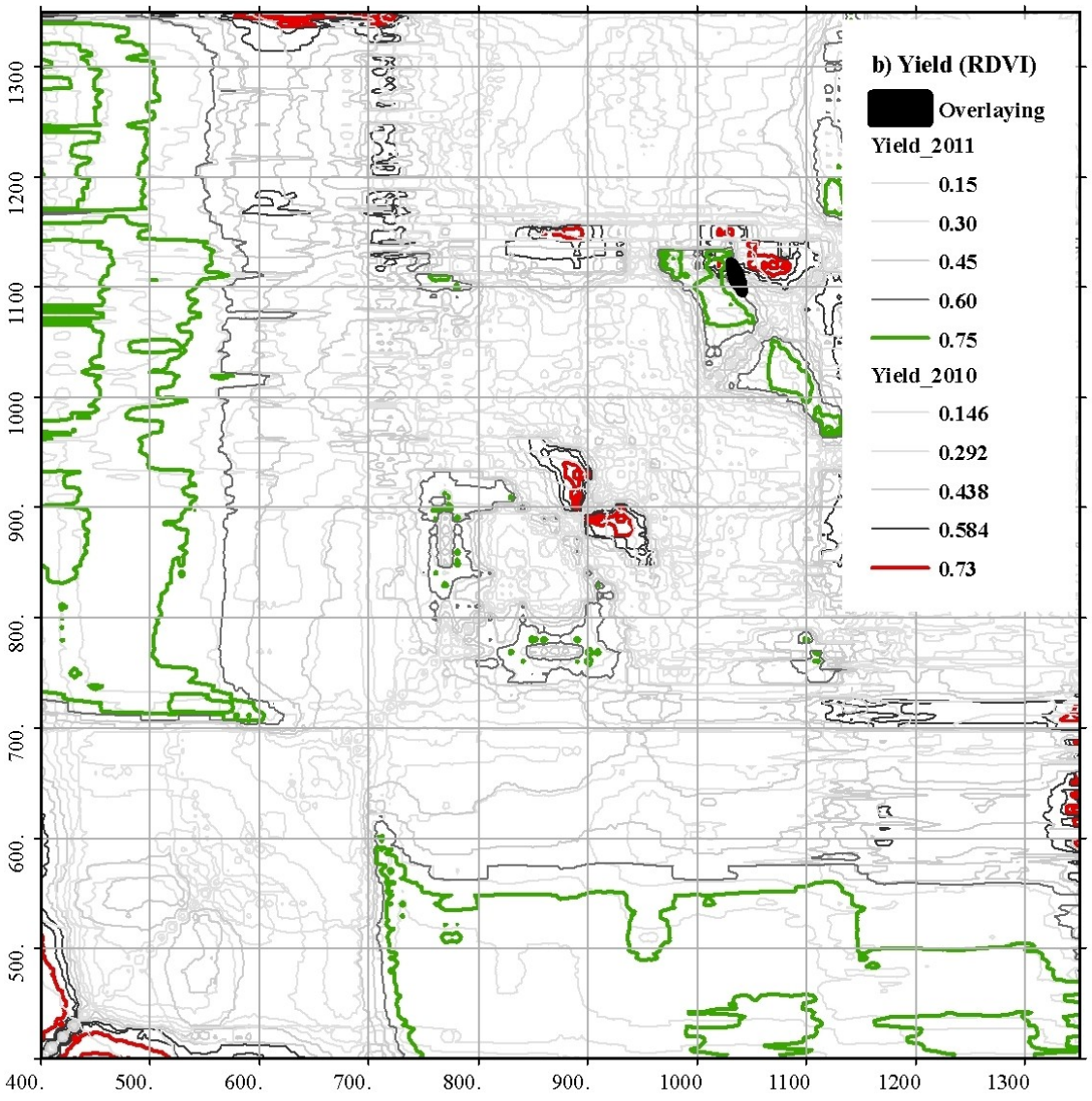

Fig. 6.2 continued

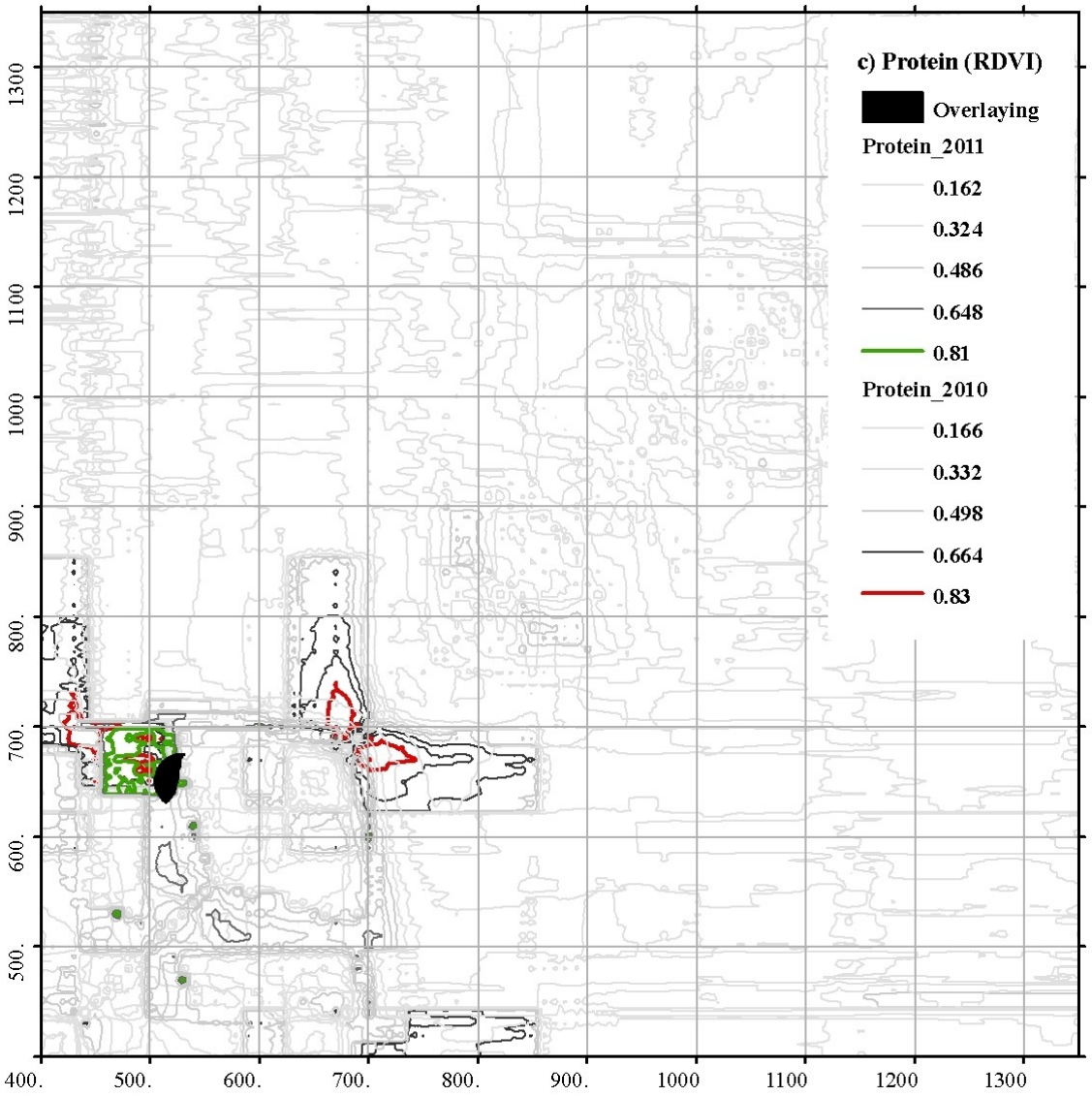

Fig. 6.2 continued

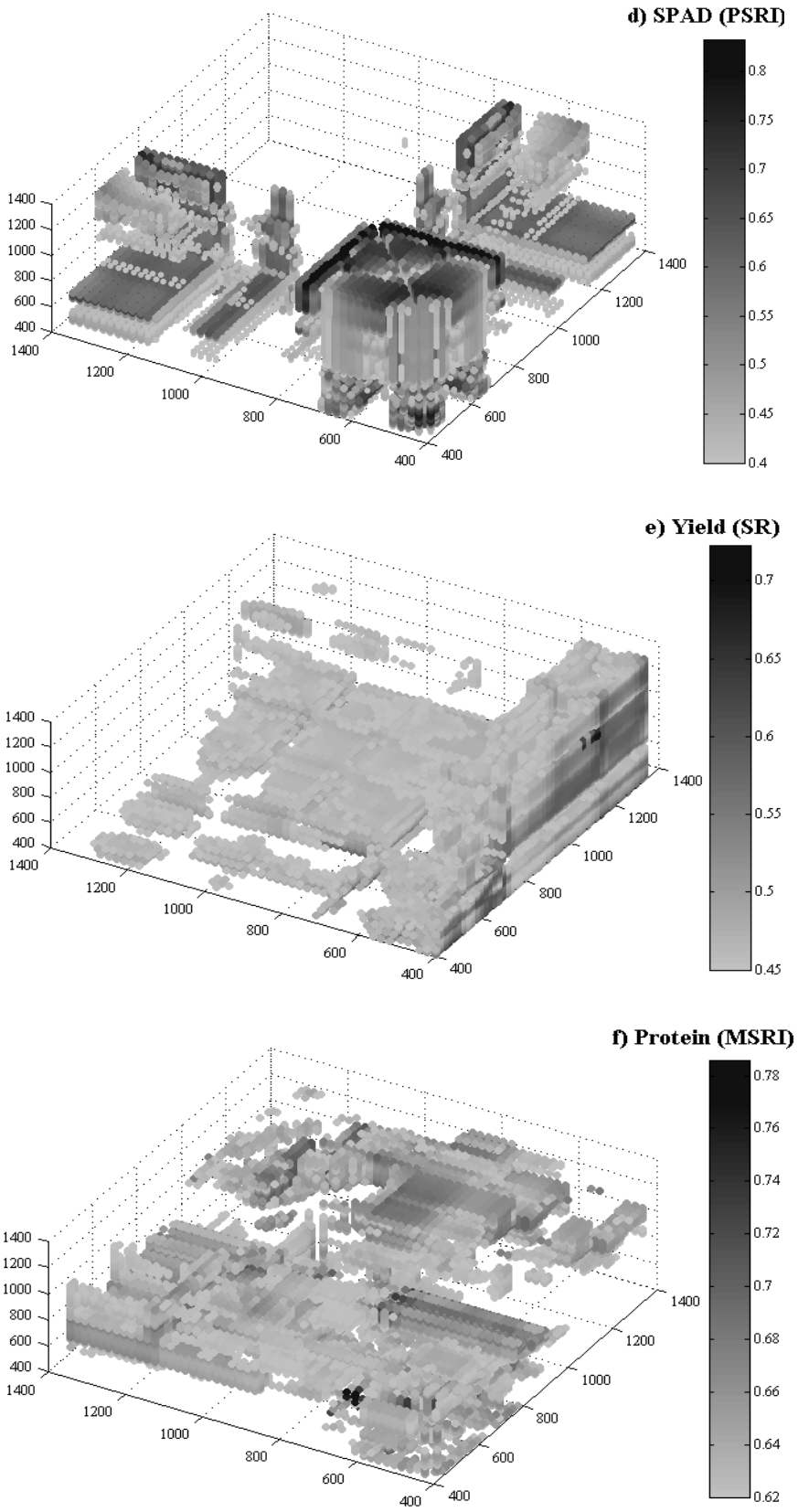

Fig. 6.2 continued

After plotting contours for each year dataset, the next step was determination of common wavebands in datasets for two years (2010 and 2011). Therefore, both the contour plot of 2010 and contour plot of 2011 were used as discrete layers in the ArcMap environment for overlaying. As shown in Fig. 6.2 (a, b and c), the area with a dark black color is a result of intersects overlaying which remarkably shows highest common R^2 value in two years. By the use of coordinates X and Y as λ_1 and λ_2, the band centers and bandwidths visually were measured (Table 6.3). A similar procedure was adopted for determining λ_1, λ_2, $\Delta\lambda_1$ and $\Delta\lambda_2$ for other indices and for the pooled data of all crop variables (not shown). When visually inspecting the contour plots of R^2 values, it must be noted that more precise bandwidths are possible with a smaller range of contour interval plots of R^2 values than shown in Fig. 6.2 (which has a >0.15 R^2 value contour interval).

Table 6.3 Band centers derivative from wavelengths combination in the two and three bands different vegetation indices according to highest R^2 (‘‘hot spots’’)

Crop Variables	Band center and width (nm)	Band centers (λ_1, λ_2 and λ_3) and bandwidths ($\Delta\lambda_1$, $\Delta\lambda_2$ and $\Delta\lambda_3$) for two and three vegetation indices						
		Index 1	Index 2	Index 3	Index 4	Index 5	Index 6	Index 7
SPAD	λ_1	735	730	730	730	660	405	705
	$\Delta\lambda_1$	8	6	7	5	15	15	15
	λ_2	1325	1330	1315	1330	720	550	425
	$\Delta\lambda_2$	10	5	9	5	15	15	15
	λ_3	-	-	-	-	1325	425	1325
	$\Delta\lambda_3$	-	-	-	-	15	15	15
Yield	λ_1	530	525	1030	530	1245	405	1125
	$\Delta\lambda_1$	5	7	5	5	15	15	15
	λ_2	1125	1125	1120	1125	1125	1265	405
	$\Delta\lambda_2$	14	12	10	9	15	15	15
	λ_3	-	-	-	-	405	1245	1080
	$\Delta\lambda_3$	-	-	-	-	15	15	15
Protein	λ_1	635	935	510	635	745	505	665
	$\Delta\lambda_1$	7	7	5	5	15	15	15
	λ_2	700	700	665	700	665	665	885
	$\Delta\lambda_2$	12	10	8	8	15	15	15
	λ_3	-	-	-	-	765	705	765
	$\Delta\lambda_3$	-	-	-	-	15	15	15

Using the same methods for three-band vegetation indices because of 3-D matrix were not possible. Therefore, we applied scatter3 command in MATLAB to generate 3-D scatter plots. Fig. 6.2 (d, e, and f) shows the most effective three-band vegetation indices that have stronger correlations with crop variables.

A number of ‘‘hot spots’’ with high R^2 values were revealed by linear regression analysis of the individual crop variables against different vegetation indices that were calculated according to equations shown in Table 6.1 for all possible two and three combinations of reflectance measured at 400 to 1350 nm wavelengths, which centered with 5 nm (Fig. 6.2). Analysis of the center wavelength and bandwidth in both directions revealed from one to seven indices depending on crop variables (Table 6.3). Bands with center wavelengths in the red and NIR spectral regions from 600 to 750 nm were represented in almost 50% of all selected bands for all crop variables in total. The bands (λ_1, λ_2 and λ_3) were often paired so that these bands were closely spaced in the steep linear shift between green, red, NIR, MS-NIR and shortwave infrared (SWIR) reflection (Table 6.3). The most effective two-band combination (index 1) to estimate the SPAD value was provided by λ_1 at 735±8 nm combined with λ_2 at 1325±10 nm (R^2 =0.764, Table 6.4). However, the other two-band indices were in almost the same wavebands as index 1, but prediction power (R^2) was lower than index 1. Although previous studies showed a stronger relationship between SPAD value and NDVI, however, may be in case of the wavebands used in the NDVI are usually in red and NIR regions, whereas in our study, one of the two wavebands was in the red-edge region and the other was in the SWIR region (Table 6.3), thus causing a weaker relationship (R^2=0.654, Table 6.4) between SPAD value and NDVI. Moreover other factors such as environmental conditions, soil background, type of crops and sunlight can affect spectral reflectance. For indices with three-band combination, index 5 by 600±15 nm in the red region, 720±15 nm in the red edge area and 1325±15 nm at SWIR region (Table 6.3), the SPAD value could be estimated with R^2 =0.832 and R^2 = 0.838 in the calibration and validation datasets, respectively. Two of the three wavelengths of index 5 were similar to index 1. This means that adding another wavelength in the red band in equation 5 could improve the SPAD value estimation by 8% (Table 6.4). A relatively broad band (λ_1) in the green region at 525~530 nm with a narrow band (λ_2) at the

MS-NIR shift (1125 nm) was different (indices 1, 2 and 4 in Table 6.3) for grain yield estimation compared to index 3 (R^2 =0.717) with λ_1=1030±5 nm and λ_2=1120±10 nm. Furthermore the blue region with λ_2=405±15 nm and the MS-NIR region with λ_1=1125±15 nm and λ_3=1080±15 nm appeared in index 7 to estimate grain yield by three-band combination as a strong relation (R^2=0.725). The red (665 nm) and red edge (745~765 nm) regions were the most effective bands in the indices for protein prediction, but there were other bands such as the green region at 510 nm in index 3 and the NIR (885 nm) region in index 7 for estimation of protein content.

To avoid models being over-fit hence the relationships need to be validated using independent datasets (2012 dataset). On the other hand, most relationships between crop

Table 6.4 Coefficients of determination (R^2) between various vegetation indices (VIs) and specific crop variables in both calibration and validation datasets

Crop variables	Indices	Calibration dataset		Validation dataset	
		R^2		R^2	
		Linear	Exponential	Linear	Exponential
SPAD	**Index 1**	**0.764**	0.773	0.761	0.776
	Index 2	0.654	0.698	0.642	0.724
	Index 3	0.706	0.747	0.726	0.753
	Index 4	0.701	0.726	0.675	0.677
	Index 5	**0.832**	0.841	0.838	0.841
	Index 6	0.801	0.807	0.812	0.819
	Index 7	0.612	0.613	0.64	0.658
Yield	Index 1	0.609	0.613	0.624	0.654
	Index 2	0.559	0.603	0.558	0.528
	Index 3	**0.717**	0.744	0.722	0.782
	Index 4	0.622	0.631	0.631	0.611
	Index 5	0.617	0.618	0.582	0.612
	Index 6	0.606	0.607	0.733	0.713
	Index 7	**0.725**	0.748	0.719	0.739
Protein	Index 1	0.652	0.693	0.652	0.676
	Index 2	0.631	0.677	0.662	0.683
	Index 3	**0.792**	0.801	0.788	0.798
	Index 4	0.673	0.703	0.696	0.676
	Index 5	0.739	0.748	0.751	0.771
	Index 6	**0.786**	0.799	0.807	0.812
	Index 7	0.682	0.736	0.688	0.648

physiological variables and spectral indices are nonlinear. It was noticed in this study that overwhelming proportions of the best nonlinear models between three different applied regression models (logarithmic, exponential and polynomial) were exponential models (Table 6.4). The relationship between broad band and short-band vegetation indices for the crop physiological variables was investigated and the performance was compared to the selected wavelengths. The best coefficients of determination (R^2) using linear and exponential regression were obtained for estimates of SPAD value, grain yield and protein content. There was a high degree of coincidence between the selected broad and narrow bands for the best vegetation index and the size of the partial least squares (PLS) regression coefficients reported by Rasooli *et al.,* (2013b). According to Table 6.5, the PLS procedure for full-spectrum analysis due to its ability to compress data has high potential to predict crop growth conditions; however, difficulties with the PLS method include a complex algorithm, which could be difficult to understand, and a large number of wavelengths that were used for the calibration model. While it is necessary to combine this large number of wavelengths in appropriate vegetation indices related to crop growth properties. Table 6.5 shows a comparison between the results of PLS models and the best two-band and three-band vegetation indices. Regarding to Table 6.5, between 7 vegetation indices in Table 6.1, index 1 for SPAD value and index 3 for both grain yield

and protein content with a two-band wavelength were fitted in the same ranges of spectral wavebands that had already been determined with PLS models. Indices 5, 7 and 6 as three-band indices were placed in the same ranges with PLS model could estimate accurately SPAD value, grain yield and protein content respectively. This means that the same wavelengths were important in both methods.

Table 6.5 The results of R^2 and RMSE were compared to PLS modelling and the best broad and narrow-bands vegetation indices with linear and exponential fit, respectively for investigated crop biophysical variables; SPAD value, grain yield and protein

Crop Variables	PLS			The best two-band Indices			The best three-band Indices		
	factors	R^2	RMSE	Index	R^2	RMSE	Index	R^2	RMSE
SPAD (-)	5	0.774	1.28	1	0.764	1.35	5	0.832	1.08
Yield ($kg^{-1}Ha$)	5	0.763	677	3	0.717	732	7	0.725	709
Protein (%)	5	0.767	0.62	3	0.792	0.58	6	0.786	0.59

These results suggest that the optimal information on crops is not necessarily concentrated in the red and NIR wavelengths. The waveband combinations providing optimal information are dependent on a host of variables, such as crop growth stage, crop condition, and cultural practices. An interesting result in Table 6.3 is the frequent appearance of narrow bands from the visible portion (400 nm to 700 nm) apart from the longer wavelength portion of NIR, MS-NIR and SWIR. The visible spectrum is very sensitive to loss of chlorophyll, browning, ripening, and senescing variations in carotenoid (Blackburn, 1998) and soil background effects. The visible spectrum is highly sensitive to crop senescence rates and is generally an excellent predictor of protein content and grain yield (Idso *et al.,* 1980). This study showed that the most sensitive portions of bands to predict senescing grain yield were predominantly in the MS-NIR broad band (centered at 1030 nm to 1130 nm) and visible green narrow bands (520 nm to 530 nm).

6.4 Conclusions

Vegetation indices are potentially useful for early estimation of crop physiological variables. However, selection of the correct wavelengths and bandwidths are important. In this study, the optimum number of hyper-spectral bands, centers, and widths in the visible (VIS), near infrared (NIR), moisture-sensitive near infrared (MS-NIR) and shortwave infrared (SWIR) spectra were investigated for establishing relationships with agricultural crop physiological characteristics (winter wheat). This recommendation is based on the study of field experiments for three years, two growth stages, and wide ranging crop growth conditions. A remarkably strong relationship with crop variables is located in specific narrow bands in the shorter wavelength portion of the red and red edge, 650 nm to 750 nm, with secondary concentrations in the longer wavelength portion of MS-NIR, 1030 nm to 1130 nm, in one particular section of SWIR, 1315 nm to 1330nm, and in the blue and green ranges at 405 nm to 530 nm. An overwhelming proportion of these channels had bandwidths that were classified as (1) very narrow (5 nm to 9 nm wide) or (2) narrow (10 nm to 15 nm wide). Index 1 with two wavelengths and index 5 with three wavelengths were appropriate for estimating the SPAD value up to R^2 =0.764 and R^2 =0.832, respectively. Index as a two-band vegetation index had a

high linear fit for early prediction of both grain yield (R^2 =0.717) and protein content *(*R^2 =0.792). Index 7 as a three-wavelength combination had a strong relationship (R^2 =0.725) with grain yield, while index 6 worked well to estimate protein content (R^2 =0.786) with three wavelengths. Selection of the optimal waveband combination in several kinds of vegetation indices improves the relation to the investigated crop using a linear regression method. On the other hand, due to the ability of PLS regression to reduce collinearity in spectral datasets, models using PLS can produce appropriate wave ranges to choose individual wavelengths by a strong relationship with crop variables. In other words, PLS models can further improve this relation to specify important wave bands that are related to crop variables. The results of this study could be used to help develop an in-field growth condition monitoring system such as an N sensor and yield estimation sensor for winter wheat.

CHAPTER 7

CONCLUSION

7.1 Introduction

Precision farming (site-specific management, prescription farming, and variable rate application technology) is an information and technology-based agricultural management system to identify, analyze, and manage site-soil spatial and temporal variability within fields for optimum profitability, sustainability, and protection of the environment. This implies the concept of using information about variability in site and climatic characteristics to manage specific sites in a field by using management practices. The main components of precision farming are global navigation satellite system (GNSS), geographic information systems (GIS), remote sensing (RS), and variable rate application (VRA). Precision agriculture requires reliable technology to acquire accurate information on crop conditions. Based on this information, the amount of fertilizers and pesticides for the site-specific crop management can be optimized. A ground-based optical sensor and instrumentation system was developed to measure real-time crop conditions.

7.2 Research background

Remote sensing has great potential for several applications because it enables wide-area, non-destructive, and real-time acquisition of information on ecophysiological plant conditions. Remotely sensed data, obtained either by satellite, aircraft or grand-based platforms, can provide a set of detailed and spatially distributed data on plant growth and development. Remote sensing can be used to delineate crop biophysical parameters, and several ground-based biophysical parameters, that can be related to the remotely sensed canopy using empirical methods. On the other hand, the growth response of vegetation in relation to measured or predicted climatic variables can be monitored by multispectral vegetation indices resulting from canopy reflectance in a relatively wide waveband. Vegetation indices such as the perpendicular vegetation index and the normalized difference have been developed to monitor vegetative growth at all stages. Vegetation indices are mostly ratios or linear combinations of signals from radiometer bands. These indices provide more highly correlated relationships than individual bands with vegetation parameters including green leaf area index, wet and dry biomass,

percent cover by vegetation, plant height, fraction of leaf chlorosis, and leaf water content.

7.3 Materials and methods

A winter wheat field of 40 m × 120 m in size was cultivated in three consecutive years in the experimental field of Hokkaido University, Japan. The field was divided into 8 areas, and four levels of fertilizer (ammonium nitrate), 0, 30, 60 and 90 kg ha^{-1} with two repetitions were applied to create a range of crop growth variations. Field in-season measurements including SPAD value, canopy reflectance using an active N-sensor embedded on the tractor as a ground-based platform with an RTK-GPS and solar sensor, spectral reflectance data using a portable spectroradiometer, height of the crop, nitrogen content of leaves, protein content of grain and grain yield were done after the stem elongation and anthesis stages.

7.4 Evaluation of plant nutrition sensor

The performance of a ground-based remote sensing system, CropSpec, for measuring wheat growth parameters was evaluated. The results showed that CropSpec has the potential to estimate growth status in winter wheat. We observed linear relationships of CropSpec values with SPAD value, height of the crop, nitrogen content, and protein content of grain. The results indicated that CropSpec can be used to determine crop health status and make an appropriate topdressing decision. CropSpec allowed better relationships for SPAD, nitrogen, and protein at the GS 39 growth stage. This suggests that the optimum time to take S1 value readings in Sapporo may be the GS 39 to GS 45 growth stages. Green NDVI had the best correlations with INSE S1 value and other measured parameters, indicating that use of other optimal wavelengths may improve the capability of CropSpec for prediction of crop conditions rather than the present wavelengths.

7.5 Individual wavelength selection by multivariate analysis

A correlation coefficient spectrum, partial least squares regression (PLSR), and stepwise multi-linear regression (SMLR) procedures were used to determine important wavelengths. Both SMLR and PLS regression procedures yielded good results. Three ranges of wavelengths were selected by considering the PLS B-coefficient and VIP plotted with spectral measurements in each crop variable (SPAD value, grain yield and protein content). The accuracy of PLSR performance (R^2) was improved from 0.77 to 0.84, 0.76 to 0.87 and 0.76 to 0.8 in SPAD, grain yield and protein content, respectively, in the validation results. Some wavelengths [(435, 550, 665, 705, 730, 1315 and 1325 nm), (410, 520, 535, 1025, 1080, 1125, 1130, 1235, 1265 and 1305 nm) and (445, 505, 640, 665, 670, 700, 760, 890 and 930 nm)] were identified by both PLSR and SMLR as significant individual wavelengths for SPAD value, grain yield and protein content, respectively, which have already been recognized in two steps of modelling and validation PLSR.

7.6 Optimal vegetation indices for monitoring winter wheat growth status

The optimum number of hyper-spectral bands, centers, and widths in the visible (VIS), near infrared (NIR), moisture-sensitive near infrared (MS-NIR) and shortwave infrared (SWIR) spectra for establishing relationships with agricultural crop physiological characteristics (winter wheat) were determined. A remarkably strong relationship with crop variables is located in specific narrow bands in the shorter wavelength portion of the red and red edge, 650 nm to 750 nm, with secondary concentrations in the longer wavelength portion of the MS-NIR, 1030 nm to 1130 nm, in one particular section of the SWIR, 1315 nm to 1330nm, and in the blue and green ranges at 405 nm to 530 nm. The difference vegetation index 1 (VDI) with two wavelengths and plant senescence reflectance index 5 (PSRI) with three wavelengths were appropriate for estimating SPAD value up to R^2 =0.764 and R^2 =0.832, respectively. The root difference vegetation index (RDVI) as a two-band vegetation index showed a high linear fit for early prediction of both grain yield (R^2 =0.717) and protein content *(*R^2 =0.792). Index 7 (SR) as a three-wavelength combination had a

strong relationship (R^2 =0.725) with grain yield, while index 6 (MSRI) worked very well to estimate protein content (R^2 =0.786) with three wavelengths.

REFERENCES

Adamchuk, V.I., Hummel, J.W., Morgan, M.T. and Upadhyaya, S.S. 2004. On-the-go soil sensors for precision agriculture. Computers and Electronics in Agriculture, 44, 71–91.

Bannari, A., D. Morin, and F. Bonn, 1995. A review of vegetation indices. Remote Sensing Reviews, 13:95-120.

Baret and Guyot, 1991. Potentials and limits of vegetation indices for LAI and PAR assessment. Remote Sensing of Environment, 35:161-173.

Barnes, J. D., Ollerenshaw, J. H., and Whitfield, C. P. 1995. Effects of Elevated Co2 And/or O3 on Growth, Development and Physiology of Wheat (triticum Aestivum L.). Global Change Biology, 1(2), 129-142.

Bartholomé, E., and Belward, A. S. 2005. GLC2000: a new approach to global land cover mapping from Earth observation data. International Journal of Remote Sensing, 26, 1959-1977.

Batte, M.T., 2000. Factors Influencing the Profitability of Precision Farming Systems. Journal of Soil and Water Conservation. 55(1): 12-18.

Bausch, W. C., and Diker, K. 2001. Innovative Remote Sensing Techniques to Increase Nitrogen Use Efficiency of Corn. Communications in Soil Science and Plant Analysis, 32(7 & 8), 1371–1390.

Beebe, K. R., and B. R. Kowalski. 1987. An introduction to multivariate calibration and analysis. Analytical Chem. 59(1): 1007A-1017A.

Bertholdsson, N. O. 1999. Characterization of malting barley cultivars with more or less stable grain protein content under varying environmental conditions. European Journal of Agronomy 10, 1–8.

Bertholdsson, N.O. and Stoy, V. 1995. Yields of dry matter and nitrogen in highly diverging genotypes of winter wheat in relation to N-uptake and N-utilization. Journal of Agronomy and CropScience – Zeitschrift fu_ rAcker und Pflanzenbau 175, 285–295.

Birch, C. J., Fukai, S. and Broad, I. J. 1997. Estimation of responses of yield and grain protein concentration of malting barley to nitrogen fertilizer using plant nitrogen uptake. Australian Journal of Agricultural Research 48, 635–648.

Blackburn, G. A. 1998. Spectral indices for estimating pho- tosynthetic pigment concentrations: A test using senescent tree leaves. Int. J. Remote Sens., 19:657–675.

Blanco, M., & Villarroya, I. 2002. NIR spectroscopy: a rapid- response analytical tool. Trends in Analytical Chemistry, 21, 240e250.

Bondeau, A., Kicklighter, D. W., Kaduk, J., and the participants of the Postdam NPP Intercomparison Project. (1999). Comparing Global Models of Terrestrial Net Primary Productivity (NPP): Importance of Vegetation Structure on Seasonal Npp Estimates. Global Change Biology, 5(s1), 35-45.

Bongiovanni, R. and Lowenberg-Deboer, J. 2004. Precision agriculture and sustainability. Precision Agriculture, 5, 359–387.

Boochs F., Kupfer G., Dockter K., and Ku¨ hbauch W. 1990. Shape of the red edge as vitality indicator for plants. International Journal of Remote Sensing, 11(10), 1741–1753.

Booker, F. L., Prior, S. A., Torbert, H. A., Fiscus, E. L., Pursley, W. A., and Hu, S. 2005. Decomposition of Soybean Grown Under Elevated Concentrations of Co2 and O3. Global Change Biology, 11(4), 685-698.

Brisco, B., R.J. Brown, T. Hirose, H. McNairn and K. Staenz, 1998. Precision Agriculture and the Role of Remote Sensing: A Review. Canadian Journal of Remote Sensing. 24(3): 315-327.

Brisson, N., Mary, B., Ripoche, D., Jeuffroy, M. H., Ruget, F., Nicoullaud, B., *et al.,* 1998. STICS: a generic model for the simulation of crops and their water and nitrogen balances. I. Theory and parameterization applied to wheat and corn. Agronomie, 18(5-6), 311-346.

Brklacich, M., C. Bryant, C , B. Veenhof, and A. Beauchesne, 1998. Implications of global climatic change for Canadian Agriculture: a review and appraisal of research

from 1984 to 1997. In Responding to Global Climate Change: National Sectoral Issue (eds) G. Koshida and W. Avis, Environment Canada, Canada Country Study: Climate Impacts and Adaptation, v. VII, p. 219-256.

Brklacich, M., C.R. Bryant, and B. Smit, 1991. FORUM: Review and Appraisal of Concept of Sustainable Food Production Systems. Environmental Management. 15(1): 1-14.

Broge, N.H. and E. Leblanc, 2000. Comparing the prediction power and stability of broadband and hyperspectral vegetation indices for estimation of green leaf area index and canopy chlorophyll density. Remote Sensing of Environment, 76: 156- 172.

Bruinsma, J. 2003. World Agriculture: Towards 2015/2030: an FAO Perspective. Ed. Earthscan.

Bullock, D. G., and D. S. Anderson. 1998. Evaluation of the Minolta SPAD-520 Chlorophyll Meter for Nitrogen Management. Journal of Plant Nutrition. 21(4), 741-755.

Bullock, P., B. Brisco, and T. Hirose, 2000. Remote Sensing for Improving Crop Management. Proceedings, First International Conf. on Geospatial Information in Agriculture and Forestry. Lake Buena Vista, Florida, USA. June 1-3/98. ERIM International. Vol II: 487-494.

Buschman, C. and E. Nagel, 1993. In vivo spectroscopy and internal optics of leavses as basis for sensing of vegetation. International Journal of Remote Sensing, 14(4): 711-722.

Campbell, J.B., 1996. Introduction to Remote Sensing. Guilford Press, New York.

Card, D. H., D. L. Peterson, P. A. Matson, and J. D. Aber. 1988. Prediction of leaf chemistry by the use of visible and near infrared reflectance spectroscopy. Remote Sens. Environ. 26(2): 123-147.

Carlson, T.B., and D.A. Ripley, 1997. On the relationship between NDVI, Fractional 164 Vegetation Cover, and Leaf Area Index. Remote Sensing of Environment, 62:241-252.

Carter, G. A., and A. K. Knapp. 2001. Leaf optical properties in higher plants: Linking spectral characteristics to stress and chlorophyll concentration. American J. Botany 88(4): 677-684.

Carter, G.A., 1992. Responses of Leaf Spectral Reflectance to Plant Stress. American Journal of Botany. 80(3): 239-143.

Cen, H., and He, Y. 2007. Theory and application of near infrared reflectance spectroscopy in determination of food quality. Trends in Food Science & Technology, 18, 72e83.

Chaerle, L., & Straeten, D. V. D. 2000. Imaging techniques and the early detection of plant stress. Trends in Plant Science, 5, 495–501.

Chen, J.M. and J. Cihlar, 1995. Plant canopy gap size anlaysis theory for improving optical measurements of leaf area index. Applied Optics, 34: 6211-6222.

Chen, J.M., 1996. Evaluation of vegetation indices and a modified simple ratio for boreal applications. Canadian Journal of Remote Sensing. 22(3):229-242.

Cihlar, J., L. St-Laurent, and J.A. Dyer, 1991. Relation between the Normalized Vegetation Indices and Ecological Variables. Remote Sensing of Environment, 35: 279-298.

Clevers, J., and van Leeuwen, H. J. C. 1996. Combined Use of Optical and Microwave Remote Sensing Data for Crop Growth Monitoring. Remote Sensing of Environment, 56, 42-51.

Combal, B., Baret, F., and Weiss, M. 2002a. Improving canopy variables estimation from remote sensing data by exploiting ancillary information. Case study on sugar beet canopies. Agronomie, 22, 205-215.

Combal, B., Baret, F., Weiss, M., Trubuil, A., Macé, D., Pragnère, A., Myneni, R., Knyazikhih, Y., and Wang, L. 2002b. Retrieval of canopy biophysical variables from bidirectional reflectance: Using prior information to solve the ill-posed inverse problem. Remote Sensing of Environment, 84(1), 1-15.

Dampney, P M R., R. Bryson., W. Clark., *et al.,* 1998. The Use of Sensor Technologies in Agricultural Cropping Systems. ADAS Contract Report, Review Report to MAFF, Project Code CE 0140.

Dash, J., & Curran, P. J. 2004. The MERIS terrestrial chlorophyll index. International Journal of Remote Sensing, 25, 5403–5413.

Datt, B. 1998. Remote sensing of chlorophyll a, chlorophyll b, chlorophyll a+b and total carotenoid content in eucalyptus leaves. Remote Sensing of Environment, 66, 111–121.

Daughtry, C.S.T., 1990. Direct Measurements of Canopy Structure. Remote Sensing Reviews. 5(1): 45-60.

Daughtry, C.S.T., C.L. Walthall, M.S. Kim, E. Brown de colstoun, and J.E. McMurtrey III, 2000. Estimating corn leaf chlorophyll concetration from leaf and canopy reflectance. Remote Sensing of Environment, 74: 229-239.

Deguise, J.C., K. Staenz, and J. Lefebrvre, 1999. Agricultural applications of airborne hyerpspectral data: Weed Detection. Proceedings, 4th International Airborne Remote Sensing Conference and 21st Canadian Symposium on Remote Sensing: Ottawa, Canada, June 20-24, 1999. Vol. II: 352-358.

DeHaan, K.R., G.T. Vessey, D.A. Holmstrom, J.A. MacLeod, J.B. Sanderson, and M.R. Carter, 1999. Relating potato yield to the level of soil degradation using a bulk yield monitor and differential global positioning systems. Computers and Electronics in Agriculture, 23: 133-143.

Demetriades-shah, T.H., Steven, M.D. and Clark, J.A. 1990. High resolution derivative spectra in remote sensing. Remote Sens. Environ. 33, 55–64.

Doerge, T.A., 1999. Site Specific Agriculture. Journal of Production Agriculture, 12(1): 54-61.

Doraiswamy, P., McCarty, G., Hunt, J., Yost, R., Doumbia, M., and Franzluebbers, A. 2007. Modeling soil carbon sequestration in agricultural lands of Mali. Agricultural Systems, 94(1), 63-74.

Duchemin, B., Hadria, R., Erraki, S., Boulet, G., Maisongrande, P., Chehbouni, A., *et al.,* 2006. Monitoring wheat phenology and irrigation in Central Morocco: On the use of relationships between evapotranspiration, crops coefficients, leaf area index and remotely-sensed vegetation indices. Agricultural Water Management, 79(1), 1-27.

Dwyer, L. M., D. W. Stewart., L. Carrigan., *et al.,* 1999. Guidelines for Comparisons Among Different Maize Maturity Rating Systems. Agronomy Journal, 91, 946–949.

Ehsani, M. R., Upadhyaya, S. K., Slaughter, D., Shafii, S. and Pelletier, M. 1999. A NIR technique for rapid determination of soil mineral nitrogen. Precision Agriculture, 1, 217–234.

EISENBEISS, H. 2004. A mini Unmanned Aerial Vehicle (UAV): System overview and image acquisition. In International Workshop on "Processing and Visualization Using High-Resolution Imagery", November 18-20, 2004, Pitsanulok, Thailand.

El-Shikha, D. M., P. M. Waller, D. Hunsaker, T. R. Clarke and E. M. Barnes. 2007, Ground-based remote sensing for assessing water and nitrogen status of broccoli. Agricultural Water Management, 92, pp. 183-193.

ESRI (Earth Systems Research Institute), 1995. Understanding GIS - The Arclnfo Method (Version 7 for Unix and Open VMS). New York: John Wiley and Sons, PPl-HFranklin,

Fageria, N. K. 2009. The use of nutrients in crop plants. Boca Raton, Florida, USA: CRC Press, Taylor & Francis Group, LLC.

Fava, F., Colombo, R., Bocchi, S., Meroni, M., Sitzia, M., Fois, N., *et al.,* 2009. Identification of hyper-spectral vegetation indices for Mediterranean pasture characterization. International Journal of Applied Earth Observation and Geoinformation, 11, 233–243.

Feng, W., Yao, X., Zhu, Y., Tian, Y. C., & Cao, W. X. 2008. Monitoring leaf nitrogen status with hyper-spectral reflectance in wheat. Europe Journal of Agronomy, 28, 394–404.

Ferrazzoli, P., Guerriero, L., and Schiavon, G. (1999). Experimental and model investigation on radar classification capability. IEEE Transactions on Geoscience and Remote Sensing, 37(2), 960-968.

Gebbers, R. and Adamchuk, V.I. 2010. Precision agriculture and food security. Science, 327, 828–831.

Gerhards, R. and Oebel, H. 2006. Practical experiences with a system for site specific weed control in arable crops using real-time image analysis and GPS-controlled patch spraying. Weed Research, 46, 185–193.

Giorgi, F., and Lionello, P. 2008. Climate change projections for the Mediterranean region. Global and Planetary Change, (In Press, Corrected Proof).

Gitelson, A. A., Vin˜a, A., Ciganda, V., Rundquist, D. C., & Arkebauer, T. J. 2005. Remote estimation of canopy chlorophyll content in crops. Geophysical Research Letters, 32, L08403.

Gitelson, A., Y. Kaufman., and M. Merzlyak. 1996. Use of a Green Channel in Remote Sensing of Global Vegetation from EOS-MODIS. Remote Sens. Environ. 58:289–298.

Haboudane, D., Tremblay, N., Miller, J. R., & Vigneault, P. 2008. Remote estimation of crop chlorophyll content using spectral indices derived from hyper-spectral data. IEEE Transactions on Geoscience and Remote Sensing, 46, 423–437.

Hammond, M.W., 1992. Cost analysis of variable fertility management of phosphorus and potassium for potato production in central Washington. Proceedings, Soil Specific Crop Management, pp. 213-228.

Hansen P. M. and Schjoerring J. K. 2003. Reflectance measurement of canopy biomass and nitrogen status in wheat crops using normalized difference vegetation indices and partial least squares regression. Remote Sensing of Environment, 86(4), 542–553.

Hansen P. M., J. R. Jorgensen and A. Thomsen 2002. Predicting grain yield and protein content in winter wheat and spring barley using repeated canopy reflectance measurements and partial least squares regression. The Journal of Agricultural Science, 139, pp 307-318

Hatfield, J. L., Gitelson, A. A., Schepers, J. S., & Walthall, C. L. 2008. Application of spectral remote sensing for agronomic decisions. Agronomy Journal, 100, 117–131.

Hoogenboom, G., Jones, J. W., and Boote, K. J. 1992. Modeling growth, development, and yield of grain legumes using soygro, pnuogro, and beangro: a review. Transactions of the ASAE, 35(6), 2043-2056.

Horler, D.N.H., M. Dockray, and J. Barber, 1983. The red edge of plant leaf reflectance. International Journal Remote Sensing, 4(2):273-288.

Huete, A.R., 1988. A Soil-Adjusted Vegetation Index. Remote Sensing of Environment, 25:295-309.

Hunt Jr., E. Raymond, M. Cavigelli, C. S. Daughtry, J. E. McMurtrey and C. L. Walthall. 2005. Evaluation of digital photography from model aircraft for remote sensing of crop biomass and nitrogen status. Precision Agriculture, 6, 359-378.

Ilbery, B.W., and I.R. Bowler, 1998. From Agricultural Productivism to Post Productivism. In B.W. Ilbery (ed) The Geography of Rural Change. Harlow, Essex, England : Longman, pp. 57-84.

Inman, D., R. Khosla., R. M. Reich., *et al.,* 2007. Active Remote Sensing and Grain Yield in Irrigated Maize. Precision Agric, 8:241–252.

Inman, D., R. Khosla., R. M. Reich., *et al.,* 2008. Normalized Difference Vegetation Index and Soil Color-Based Management Zones in Irrigated Maize. Agronomy Journal, 100:60–66.

Inoue Y. 2003. Synergy of remote sensing and modeling for estimating ecophysiological processes in plant production. Plant Production Science, 6(1), 3–16.

Jan Nausˇ. Jitka Prokopova´. Jirˇı´ Rˇebı´cˇek. Martina S ˇpundova. 2010. SPAD chlorophyll meter reading can be pronouncedly affected by chloroplast movement. Photosynth Res.105:265–271.

Jenner, C. F., Ugalde, T.D. and AspinallL, D. 1991. The physiology of starch and protein deposition in the endosperm of wheat. Australian Journal of Agricultural Research 18, 211–226.

Jensen, J. R. 1996. Introductory digital image processing: A remote sensing perspective, Saddle River: Prentice-Hall, 318, 379 P.

Johnson, L. F., S. R. Herwitz, B. M. Lobitz and S. Dunagan. 2002. Feasibility of monitoring coffee field ripeness with airborne multispectral imagery. Applied Engineering in Agriculture, 20, 845- 849.

Johnsson, E., Prieto-linde M. L. and Jonsson J. O. 2001. Effects of wheat cultivar and nitrogen application on storage protein composition and breadmaking quality. Cereal Chemistry 78, 19–25.

Jones, C. A., and Kiniry, J. R. 1986. CERES-Maize: A Simulation Model of Maize Growth and Development. Texas AandM University Press College Station (USA).

Jones, J. W., Hoogenboom, G., Porter, C. H., Boote, K. J., Batchelor, W. D., Hunt, L. A., *et al.,* 2003. The DSSAT cropping system model. European Journal of Agronomy, 18(3-4), 235-265.

Kalubarme, M. H., Potdar, M. B., Manjunath, K. R., Mahey, R. K., and Siddhu, S. S. 2003. Growth profile based crop yield models: a case study of large area wheat yield modelling and its extendibility using atmospheric corrected NOAA - AVHRR - data. International Journal of Remote Sensing, 24(10), 2037.

Karl, T. R., and Easterling, D. R. 1999. Climate Extremes: Selected Review and Future Research Directions. Climatic Change, 42(1), 309-325.

Khush, G.S., 1999. Green Revolution: preparing for the 21s t century. Genome, 42(4): 645-655.

Khush, G.S., 2001. Green Revolution: the way forward. Nature Reviews, 2: 815-822.

Kimura, R., Okada, S., Miura, H. and Kamichika, M. 2004. Relationships among the leaf area index, moisture availability, and spectral reflectance in an upland rife field. Agric. Water Manage. 69, 83–100.

Knipling, B.E. 1970. Physical and physiological basis for reflectance of visble and near-infrared radiation from vegetation. Remote Sensing of Environment, 1, 155–159.

Large, E. C. 1954. Growth stage in cereals. Plant Pathology, 3, 128–129.

Launay, M., and Guerif, M. 2005. Assimilating remote sensing data into a crop model to improve predictive performance for spatial applications. Agriculture, Ecosystems and Environment, 111(1-4), 321-339.

Le Toan, T., Laur, H., Mougin, E., and Lopes, A. 1989. Multitemporal and dual-polarization observations of agricultural vegetation covers by X-band SAR images. Geoscience and Remote Sensing, IEEE Transactions on, 27(6), 709-718.

Le Toan, T., Lopes, A., and Huet, M. 1984. On the relationships between radar backscattering Coefficient and Vegetation Canopy Characteristics. Proceedings of the International Geoscience and Remote Sensing Symposium, 155-160.

Leblanc, S.G., J.M. Chen, J.R. Miller, and J. Freemantle, 1999. Compact Airborne Spectrographic Imager (CASI) Used for Mapping LAI of Cropland. Proceedings, 4' International Airborne Remote Sensing Conference and Exhibition/21st Canadian Symposium on Remoste Sensing, Ottawa, Ontario, Canada 21-24 June. Vol I.: 297-303.

Lee K. S., D. H. Lee, K. A. Sudduth, S. O. Chung, N. R. Kitchen, S. T. Drummond. 2009. Wavelength Identification and Diffuse Reflectance Estimation for Surface and Profile Soil Properties. Transactions of the ASABE. Vol. 52(3): 683-695.

Leica Geosystems. 2005. ERDAS Field Guide. Leica Geosystems Geospatial Imaging, LLC, LO, C. P. 1986. Applied remote sensing. pp. 393 (New York: John Wiley and Sons Inc.)

Lemaire, G., Jeuffroy, M. H., & Gastal, F. 2008. Diagnosis tool for plant and crop N status in vegetative stage. Theory and practices for crop N management. European Journal of Agronomy, 28, 614–624.

Li, F., Gnyp, M. L., Jia, L., Miao, Y., Yu, Z., Koppe, W., *et al.,* 2008. Estimating N status of winter wheat using a handheld spectrometer in the North China Plain. Field Crops Research, 106, 77–85.

Li, Fei., Yuxin Miao., Simon D Hennig., *et al.,* 2010. Evaluating hyperspectral vegetation indices for estimating nitrogen concentration of winter wheat at different growth stages. Precision Agric.11:335–357.

Long, S. P., Ainsworth, E. A., Leakey, A. D., and Morgan, P. B. 2005. Global food insecurity. Treatment of major food crops with elevated carbon dioxide or ozone under large-scale fully open-air conditions suggests recent models may have overestimated future yields. Philosophical Transactions of the Royal Society B: Biological Sciences, 360(1463).

Loveland, T. R., Reed, B. C., Brown, J. F., Ohlen, D. O., Zhu, Z., Yang, L., *et al.,* 2000. Development of a global land cover characteristics database and IGBP - DISCover from 1 km AVHRR - data. International Journal of Remote Sensing, 21(6), 1303.

Lu, Yoa-Chi, C. Daughtry, G. Hart and B. Watkins, 1997. The current state of precision farming. Food Reviews International, 13(2): 141-162.

Lukina, E. V., Freeman, K. W., Wynn, K. J., *et al.,* 2001. Nitrogen Fertilization Optimization Algorithm Based on In-season Estimates of Yield and Plant Nitrogen Uptake. Journal of Plant Nutrition, 24, 885–898.

Maas, S.J. and J.R. Dunlap, 1989. Reflectance, Transmittance, and Absorptance of Light by Normal, Etiolated, and Albino Corn Leaves. Agronomy Journal, 81:105-110.

Mack, A.R., R.L. Desjardins, J.I. MacPherson, and P.H. Schuepp, 1990. Relative photosynthetic activity of agricultural lands from airborne and satellite data. International Journal of Remtoe Sensing, 11(2):237-251.

Major, D.J., F. Baret, and G. Guyot, 1990. A ratio index adjusted for soil brightness. International Journal of Remote Sensing, ll(5):727-740.

Mannion, A.M., 1998. Can biotechnology contribute to sustainable agriculture. Journal of Sustainable Agriculture, 11 (4):51-75.

Marriotti, M., L. Ercoli, L., and A. Masoni, 1996. Spectral Properties of Iron-Deficient corn and sunflower leaves. Remote Sensing Environment, 58: 282-288.

Masoni, A. L. Ercoli, and M. Mariotti, 1996. Agroclimatology: Spectral properties of leaves deficient in Iron, Sulfur, Magnesium and manganese. Agronomy Journal, 88:937-943.

Mattia, F., Dente, L., Satalino, G., and Le Toan, T. 2005. Sensitivity of ASAR AP data to wheat crop parameters. In Proceedings of the 2004 Envisat & ERS Symposium, Salzburg, Austria, 6-10 September 2004, ESA SP-572, CDROM. Ed. H. Lacoste and L. Ouwehand.

Mattia, F., Le Toan, T., Picard, G., Posa, F., D'Alessio, A., Notarnicola, C., *et al.,* 2003. Multitemporal C-band radar measurements on wheat fields. IEEE Transactions on Geoscience and Remote Sensing, 41(7), 1551-1560.

McCown, R. L., Hammer, G. L., Hargreaves, J. N. G., Holzworth, D. P., and Freebairn, D. M. 1986. APSIM: a novel software system for model development, model testing and simulation in agricultural systems research. Agricultural Systems, 50(3), 255-271.

McNairn, H. and R.J. Brown, 1999. Remote sensing in support of crop management. Proceedings, United Nations/China/European Space Agency (ESA) Conference on Space Applications for Promoting Sustainable Agriculture. Bejiing, China, Sept. 14-17, 7p.

McNairn, H., J.C. Deguise, A. Pacheco, J. Shang, and N. Rabe, 2001b. Estimation of Crop Cover and Chlorophyll from Hyperspectral Remote Sensing. 23r d Canadian Remote Sensing Symposium, Sainte-Foy, Quebec, Canada, August 21-24.

McNairn, H., J.C. Deguise, J.Seeker, and J.Shang, 2001a. Development of remote sensing image products for use in precision farming. In Proc. 3 r d European Conference on Precision Farming, Montpellier, France, June 18-20, 5p.

Milton, N.M., B.A. Eiswerth, and CM. Ager, 1991. Effect of Phosphorus Deficiency on Spectral Reflectance and Morphology of Soybean Plants. Remote Sensing Environement, 36:121-127.

Mkhabela, M. S., Mkhabela, M. S., and Mashinini, N. N. 2005. Early maize yield forecasting in the four agro-ecological regions of Swaziland using NDVI data derived from NOAA's-AVHRR. Agricultural and Forest Meteorology, 129(1-2), 1-9.

Moghimi Ali, Aghkhani Mohammad, Sazgarnia Ameneh and Sarmad Majid. 2010. Vis/NIR spectroscopy and chemometrics for the prediction of soluble solids content and acidity (pH) of kiwifruit. Biosyst. Eng. 106, 295-302.

Moran, M.S., Y. Inoue, and E.M. Barnes, 1997. Opportunities and limitations for image based remote sensing in precision crop management. Remote Sensing of Environment. 61: 319-346.

MORAN, S. M. 1994. Irrigation management in Arizona using satellites and airplanes. Irrigation Science, 15, 35-44.

Moran, S. M., Y. Inoue and E. M. Barnes. 1997. Opportunities and limitations for image-based remote sensing in precision crop management. Remote Sensing of Environment, 61, 319-346.

Moulin, S., Bondeau, A., and Delecolle, R. 1998. Combining agricultural crop models and satellite observations: from field to regional scales. International Journal of Remote Sensing, 19(6), 1021.

Mulla, D.J., 1991. Using geostatistics and GIS to manage spatial patterson in soil fertility. In Automated Agriculture for the 21s t Century. Proc. of the 1991 Symp., 336-345. St. Joseph, Mich.:ASAE.

Nash, E., Dreger, F., Schwarz, J., Bill, R. and Werner, A. 2009. Development of a model of datt-flows for precision agriculture base on a collaborative research project. Computers and Electronics in Agriculture, 66, 25–37.

Norman, J.M. and G.S. Campbell. 1989. Canopy Stucture. In: R.W. Pearcy, J. Ehleringer, H.A. Mooney, and P.W. Rundel. Plant Physiological Ecology: Field Methods and Instrumentation. Chapman and Hall. London, pp 301-326.

Oliver, C., and Quegan, S. 1998. Understanding Synthetic Aperture Radar Images Boston. MA: Artech House.

Oliver, M.A. 1990. Kriging: A Method of Interpolation for Geographical Information Systems. International Journal of Geographic Information Systems 4: 313-332.

Oppelt, N., & Mauser, W. 2004. Hyper-spectral monitoring of physiological parameters of wheat during a vegetation period using AVIS data. International Journal of Remote Sensing, 25, 145–159.

Pacheco A., A. Bannari, J-C. Deguise , H. McNairn, and K. Staenz, 2001. Application of Hyperspectral Remote Sensing for LAI Estimation in Precision Farming.

Peddle, D.R., H. P. White, R.J. Soffer J.R. Miller and E.F. LeDrew, 2001. Reflectance processing of remote sensing spectroradiometer data. Computers and Geosciences, 27: 203-213.

Penuelas, J. and Filella, I. 1998. Visible and near infrared reflectance techniques for diagnosing plant physiological status. Trends in Plant Science, 3(4), 151–156.

Perez-Munoz, F. and T.S. Colvin, 1996. Continuous Grain Yield Monitoring. Transactions of the ASAE, 39(3): 775-783.

Petrzelka, P., S. Padgitt, and K. Connelly, 1997. Crop Management - Teaching old dogs survival tricks: A case study in promoting integrated crop management. Journal of Production Agriculture, 10(4): 596-602.

Picard, G. 2002. Modélisation radar des couverts végétaux, application à la télédétection de couverts forestiers et agricoles. Thèse. Université Paul Sabatier, Toulouse, France.

Picard, G., Le Toan, T., and Mattia, F. 2003. Understanding C-band radar backscatter from wheat canopy using a multiple-scattering coherent model. IEEE Transactions on Geoscience and Remote Sensing, 41(7), 1583-1591.

Pierce, F.J. and P.Nowak, 1999. Aspects of Precision Agriculture. Advances in Agronomy, 67: 1-85.

Plant R. E., Munk D. S., Roberts B. R., Vargas R Land *et al.,* 2000. Relationships between remotely sensed reflectance data and cotton growth and yield. Transaction of the ASAEB, 43(3), 535–546.

Purevdorj, T., R. Tateishi, T. Ishiyama, and Y. Honda., 1998. Relationships between percent vegetation cover and vegetation indices. International Journal of Remote Sensing. 19(18): 3519-3535.

Qaim, M., and Zilberman, D. 2003. Yield Effects of Genetically Modified Crops in Developing Countries. Science, 299(5608), 900-902.

Räisänen, J. 2007. How Reliable Are Climate Models? Tellus A, 59(1), 2-29.

Rango, A., A. Laliberte, C. Steele, J. E. Herrick, B. Bestelmeyer, T. Schmugge, A. Roanhorse and J. Jenkins. 2006. Using unmanned aerial vehicles for rangelands: current applications and future potentials. Environmental Practice, 8, 159-168.

Rascher, U., Liebig, M. and Lüttge, U. 2000. Evaluation of instant lightresponse curves of chlorophyll fluorescence fluorometer on site in the field. Plant, Cell and Environment, 23, 1397–1405.

Rasooli Sharabian. V., Noboru Noguchi, Issei Han-ya, Kazunobu Ishi. 2013a. Evaluation of an Active Remote Sensor for Monitoring Winter Wheat Growth Status. Engineering in Agriculture, Environment and Food (EAEF) 6(3): 118-127.

Rasooli Sharabian. V., Noboru Noguchi, Kazunobu Ishi. 2013b. Optimal Vegetation Indices for Winter Wheat Growth Status Based on Multi-Spectral Reflectance. Environmental Control in Biology (ECB), *Accepted 2013/06/15*.

Rasooli Sharabian. V., Noboru Noguchi, Kazunobu Ishi. 2013c. Significant Wavelengths for Prediction of Winter Wheat Growth Status and Grain Yield Using Multivariate Analysis. Engineering in Agriculture, Environment and Food (EAEF), *Submitted*.

Raun, W. R., Solie, J. B., Johnson, G. V., *et al.,* 2001. In-season Prediction of Potential Grain Yield in Winter Wheat Using Canopy Reflectance. Agronomy Journal, 93, 131-138.

Reujean, J., & Breon, F. 1995. Estimating PAR absorbed by vegetation from bidirectional reflectance measurements. Remote Sensing of Environment, 51, 375–384.

Rigby, D., Woodhouse, P., Young, T., and M. Burton, 2001. Constructing a farm level indicator of sustainable agricultural practice. Ecoclogical Economics, 29: 463-478.

Ritchie, J. T., and Otter-Nacke, S. 1985. CERES-Wheat. A simulation model of wheat growth and development, ARS(1985). (págs. 159-175). US Department of Agriculture.

Roanhorse A., D. El Shikha, F. Szidarovszky, P. Waller. 2009. Selecting the Best Remote Sensing Platform for Agricultural Assessment Using Multi-objective Analysis. Misr J. Ag. Eng., 26(1): 11-43.

Rondeaux, G, 1995. Vegetation Monitoring by Remote Sensing: A review of Biophyscial Indices. Photo-Interpretation, 3:197-213.

Rondeaux,G., M. Steven, and F. Baret, 1996. Optimization of Soil-Adjusted Vegetation Indices. Remote Sensing Environment, 55:95- 107.

Rouse, J. W., Haas, R. H., Schell, J. A., Deering, D. W., & Harlan, J. C. 1974. Monitoring the vernal advancement of retrogradation of natural vegetation. NASA/GSFC, Type III, Final Report, Greenbelt, MD, USA. pp. 1 – 371.

Royo, C., Aparicio, N., Villegas, D., Casadesus, J., Monneveux, P., and Araus, J. (2003). Usefulness of spectral reflectance indices as durum wheat yield predictors under contrasting Mediterranean conditions. International Journal of Remote Sensing, 17, 4403-4419.

Ruget, F., Brisson, N., Delécolle, R., and Faivre, R. (2002). Sensitivity analysis of a crop simulation model (STICS) in order to determine the accuracy needed for the parameters. Agronomie, 22, 133-158.

Ryu, C.S., Suguri, M. and Umeda, M., 2009. A model for predicting the nitrogen content of rice at panicle initiation stage using data from airborne hyperspectral remote sensing. Biosyst. Eng. 104, 465–475.

Ryu, C.S., Suguri, M. and Umeda, M., 2011. Multivariate analysis of nitrogen content for rice at the heading stage using reflectance of airborne hyperspectral remote sensing. Field Crops Research 122, 214–224

Saich, P., and Borgeaud, M. 2000. Interpreting ERS SAR signatures of agricultural crops in Flevoland, 1993-1996. IEEE Transactions on Geoscience and Remote Sensing, 38(2), 651-657.

Schellberg, J., Hill, M., Gerhards, R., Rothmund, M. and Braun, M. 2008. Precision agriculture on grassland: applications, perspectives and constraints. European Journal of Agronomy, 29, 59–71.

Schilfgaarde, J.V., 1999. Is precision agriculture sustainable? American Journal of Alternative Agriculture. 14(1): 43-46.

Schotten, C. G. J., Van Rooy, W. W. L., and Janssen, L. L. F. 1995. Assessment of the capabilities of multi-temporal ERS-1 SAR data to discriminate between agricultural crops. International Journal of Remote Sensing, 16(14), 2619-2637.

Schröter, D., Cramer, W., Leemans, R., Prentice, I. C., Araujo, M. B., Arnell, N. W., *et al.,* 2005. Ecosystem Service Supply and Vulnerability to Global Change in Europe. Science, 310(5752), 1333-1337.

Shanahan, J.F., N.R. Kitchen., W.R. Raun., *et al.,* 2008. Responsive In-season Nitrogen Management for Cereals. Comput. Electron. Agric. 61:51–62.

Shaver, T. M., R. Khosla., D. G. Westfall. 2011. Evaluation of Two Crop Canopy Sensors for Nitrogen Variability Determination in Irrigated Maize. Precision Agric, OI :10.1007/s11119-011-9229-2.

Simonneaux, V., Duchemin, B., Helson, D., Er-Raki, S., Olioso, A., and Chehbouni, A. G. 2008. The use of high-resolution image time series for crop classification and evapotranspiration estimate over an irrigated area in central Morocco. International Journal of Remote Sensing, 29(1), 95.

Sims, D. A., & Gamon, J. A. 2002. Relationships between leaf pigment content and spectral reflectance across a wide range of species, leaf structures and developmental stages. Remote Sensing of Environment, 81, 337–354.

Sivakumar, M.V.K., Gommes, R., and W. Baier, 2000. Agrometerology and sustainable agriculture. Agricultural and Forest Meteorology, 103: 11-26.

Smith, A.M., D.R. Peddle, and T.C. Foster, 1999. Detection of Moisture Stress in Potatoes using multispectral remote sensing. Proceedings, 4th International Airborne Remote Sensing Conference and 21st Canadian Symposium on Remote Sensing, Ottawa, Canada, June. Vol. II, pp. 283-289.

Solari, Fernando., John Shanahan., Richard Ferguson., *et al.,* 2008. Active Sensor Reflectance Measurements of Corn Nitrogen Status and Yield Potential. Agron. J. 100:571–579.

Solomon, S., Qin, D., Manning, M., and Marquis, M. 2007. Climate change 2007: the physical science basis contribution of Working Group I to the fourth assessment report of the Intergovermental Panel on Climate Change. Cambridge University Press, Cambridge.

Spitters, C. J. T., van Keulen, H., and van Kraalingen, D. W. G. 1989. A simple and universal crop growth simulator: SUCROS87. Simulation and Systems Management in Crop Protection, 147-181.

Staenz, K., J.C. Deguise, J.M. Chen, H. McNairn, and T. Szeredi, 1999. Estimation of Leaf Area Index (LAI) from Crop Fraction Using Hyperspectral Data, Commission VII, Working Group I, 31pp.

Stafford, J.V. 2000. Implementing precision agriculture in the 21st Century. Journal of Agricultural Engineering Research, 76, 267–275.

Stafford, J.V., B. Ambler and M.P. Smith, 1991. Sensing and mapping grain yield variation. In Automated Agriculture for the 21s t century. Proc. Of the 1991 Symp., 356-365. St. Joseph, Mich.: ASAE.

Stamatiadis, Stamatis., Christos Tsadilas., James S. Schepers. 2010 b. Ground-based Canopy Sensing for Detecting Effect of Water Stress in Cotton. Plan Soil , 331: 277-287.

Stamatiadis, Stamatis., Dimitris Taskos ., Eleftheria Tsadila., *et al.,* 2010 a. Comparison of Passive and Active Canopy Sensors for the Estimation of Vine Biomass Production. Precision Agric , DOI: 10.1007/s11119-009-9131-3

Steven, M.D., 1998. The sensitivity of the OSAVI Vegetation Index to Observational Parameters. Remote Sensing of Environment. 63:49-60.

Stone, M. L., Soile, J. B., Raun, W. R., Whitney, *et al.,* 1996. Use of Spectral Radiance for Correcting In-season Fertilizer Nitrogen Deficiencies in Winter Wheat. Transactions of the American Society of Agricultural Engineers, 39(5), 1623–1631.

Stoskopf, N.C., 1981. Leaf area and plant architecture. In: Stoskopf, N.C. Understanding Crop Production, Reston Publishing Company inc., Reston, Virginia, pp 93-111.

Strahler, A., Muchoney, D., Borak, J., Friedl, M., Gopal, S., Lambin, E., *et al.,* 1999. MODIS land cover product, algorithm theoretical basis document (ATBD), version 5.0.

Stroppiana, D., Boschetti, M., Brivio, P. A., & Bocchi, S. 2009. Plant nitrogen concentration in paddy rice from field canopy hyper-spectral radiometry. Field Crops Research, 111, 119–129.

Su B. 2013. Monitoring and Assessment for Water Quality of Lake and Marsh Based on Remote Sensing Technique and GIS. Doctoral thesis, Hokkaido University, Japan.

Thenkabail PS, Smith RJ3, De Pauw E, 2000. Hyperspectral vegetation indices and their relationships with agricultural crop characteristics. Remote Sensing of Environment, 71(2): 158-182.

Thenkabail, P. S., R. B. Smith., E. DePauw. 2000. Hyperspectral Vegetation Indicies and their relationships with agricultural crop characteristics. Remote Sensing of Environment, 71, 158–182.

Thenkabail, P.S., A.D. Ward, and J.G. Lyon, 1994. Landsat-5 Thematic Mapper models of soybean and corn crop characteristics. International Journal of Remote Sensing, 15(1) 49-61.

Thomas, J.R. and H.W. Gausman, 1977. Leaf Reflectance vs. Leaf Chlorophyll and Cartonoid Concentration for Eight Crops. Agronomy Journal, 69: 799-802.

Thomason, W. E., S. B. Phillips., P. H. Davis., *et al.,* 2011. Variable Nitrogen Rate Determination from Plant Spectral Reflectance in Soft Red Winter Wheat. Precision Agric , 12: 666-681.

Thomasson, J. A., R. Sui, M. S. Cox, and A. Al-Rajehy. 2001. Soil reflectance sensing for determining soil properties in precision agriculture. Trans. ASAE 44(6): 1445-1453.

Thomson, S. J., P. V. Zimpa, C. T. Bryson and V. Alarcon. 2005. Potential for remote sensing from agricultural aircraft using digital video. Applied Engineering in Agriculture, 21, 531-537.

Trietz, P.M. and P.J. Howarth, 1999. Hyperspectral remote sensing for estimating biophysical parameters of forest ecosystems. Progress in Physical Geography 23 (3): 359-390.

Tso, B., and Mather, P. M. 1999. Crop discrimination using multi-temporal SAR - imagery. International Journal of Remote Sensing, 20(12), 2443.

Tumbo, S. D., D. G. Wagner, and P. H. Heinemann. 2002. Hyperspectral-based neural network for predicting chlorophyll status in corn. Trans. ASAE 45(3): 825-832.

Turner, D. P., Cohen, W. B., Kennedy, R. E., Fassnacht, K. S., and Briggs, J. M. 1999. Relationships between Leaf Area Index and Landsat TM Spectral Vegetation Indices across Three Temperate Zone Sites. Remote Sensing of Environment, 70(1), 52-68.

Turner, D.P., W.B. Cohen, R.E. Kennedy, K.S. Fassnacht, and J.M Briggs, 1999. Relationships between Leaf Are Index and Landsat TM Spectral Vegetation Indices across Three Temperate Zone Sites. Remote Sensing of Environment, 70:52-68.

Tyler, D.A., D.W. Roberts and G.A. Nielson, 1997. Location and Guidence for Site Specific Management. In The State of Site Specific Management for Agriculture, F.J. Pierce and E.J. Sadler (Eds.), Madison, Wl, Amercian Society of Agronomy, ppl61-181.

Vasques, G. M., S. Grunwald, and J. O. Sickman. 2009. Modeling of soil organic carbon fractions using visible/near infrared spectroscopy. SSSA J. 73(1): 176-184.

Vicente-Serrano, S. 2007. Evaluating the Impact of Drought Using Remote Sensing in a Mediterranean, Semi-arid Region. Natural Hazards, 40(1), 173-208.

Vicente-Serrano, S., Cuadrat-Prats, J., and Romo, A. 2006. Early prediction of crop production using drought indices at different timescales and remote sensing data: application in the Ebro Valley (northeast Spain). International Journal of Remote Sensing, 27, 511-518.

Walter-Shea, E.A., J.M. Norman, B.L. Blad, and B.F. Robinson, 1991. Leaf Reflectance and Transmittance in Soybean and Corn. Agronomy Journal, 83:631-636.

Weiss, M., Myneni, R. B., Pragnère, A., and Knyazikhin, Y. 2000. Investigation of a model inversion technique to estimate canopy biophysical variables from spectral and directional reflectance data. Agronomie, 20, 3-22.

Wiegand, C.L. and A.J. Richardson, 1977. Distinguishing Vegetation from Soil Background Information. Photogrammetric Engineering and Remote Sensing, 43(12): 1541-1552.

Wiegand, C.L. and A.J. Richardson, 1984. Leaf area, light interception, and yield estimates from spectral components analysis. Agronomy Journal, 76: 543-548.

Wiegand, C.L. and A.J. Richardson, 1990. Use of spectral vegetation indices to infer leaf area, evapotranspiration and yield: I. Rationale. Agronomy Journal, 82: 623-629.

Wiegand, C.L., A.J. Richardson, D.E. Escobar, and A.H. Gerbermann, 1991. Vegetation Indices in crop assessments. Remote Sensing of Environment, 35:105-119.

Wold, S. 1994. "PLS for Multivariate Linear Modeling," QSAR: Chemometric Methods in Molecular Design. Methods and Principles in Medicinal Chemistry, ed. H. van de Waterbeemd, Weinheim, Germany: Verlag-Chemie.

Wollenhaupt, N.C. and D.D. Buchholz, 1992. Profitability of farming by soils. Proceedings, Soil Specific Crop Management, pp. 199-211.

Wolley, J.T., 1971. Relfectance and transmittance of light by leaves. Plant Physiology, 47: 656-662.

Wood, G. A., J. C. Taylor., R. J. Godwin. 2003. Calibration Methodology for Mapping Within-field Crop Variability Using Remote Sensing. Biosystems Engineering, 84(4), 409–423.

Yi, Q.X., Huang, J.F., Wang, F.M., Wang, X.Z. and Liu, Z.Y. 2007. Monitoring rice nitrogen status using hyperspectral reflectance and artificial neural network. Environ. Sci. Technol. 41, 6770–6775.

Yoder, B. J., & Pettigrew-Crosby, R. E. 1995. Predicting nitrogen and chlorophyll content and concentrations from reflectance spectra (400–2500 nm) at leaf and canopy scales. Remote Sensing of Environment, 53, 199–211.

Zadoks, J. C., T. T. Chang., D. F. Konzak. 1974. A Decimal Code for the Ggrowth Stages of Cereals. Weed Research, 14, 415–421.

Zhang, J. H., K. Wang and R. C. Wang. 2003. Application of chlorophyll meter SPAD in diagnosis nitrogen status and nitrogenous fertilizer in rice. Journal of Northwest A&F University (Natural Science Edition). 31(2): 177-180.

Zhang, N., Wang, M. and Wang, N. 2002. Precision agriculture – a worldwide overview. Computers and Electronics in Agriculture, 36, 113–32.

Zillmann, Erik., Simone Graeff., Johanna Link., *et al.,* 2006. Assessment of Cereal Nitrogen Requirements Derived by Optical s on Heterogeneous Soils. Agron. J. 8:682–690.